Distributed Biodynamic Response Analysis of the Hand-Arm System Exposed to Vibration along the Forearm Direction

JIANHUI DONG

A thesis

in

the Department

of

Mechanical and Industrial Engineering

Presented in Partial Fulfillment of the Requirements
for the Degree of Master of Applied Science at
Concondia University
Montreal, Quebec, Canada

March 2007

Your file Votre référence
ISBN: 978-0-494-34590-0
Our file Notre référence
ISBN: 978-0-494-34590-0

ABSTRACT

DISTRIBUTED BIODYNAMIC RESPONSE ANALYSIS OF THE HAND-ARM SYSTEM EXPOSED TO VIBRATION ALONG THE FOREARM DIRECTION

Jianhui Dong

Prolong and intensive exposure to hand-transmitted vibration could cause a series of disorders in the vascular, neurosensorial, and musculoskeletal structures, which have been collectively termed as hand-arm vibration syndrome (HAVS). From the review of literature, it is apparent that biodynamic response of the hand-arm system is one of the important foundations for understanding the causations of HAVS and for developing effective methods for exposure assessment. Although considerable efforts have been made to characterize the biodynamic responses of the hand-arm system and develop biodynamic models, only little knowledge exists on distribution of biodynamic response and power absorption for assessing health risks to the localized substructures. This dissertation research is concerned with development of an effective hand-arm vibration model that can predict distributed mechanical impedance and power absorption properties various substructures within the hand-arm system.

This dissertation research proposes a new model structure that mimics the basic structures of the hand-arm system grasping a handle. The proposed model comprises two driving-points as opposed to the single driving-point invariably considered in the reported models. The model thus permits analyses of biodynamic forces developed on the fingers and palm-sides. The model parameters are identified based on the selected experimental data using a curving fitting method. The model structure revealed reasonably good agreements with the reported experimental data acquired under selected hand actions.

The model also revealed very good agreements in terms of biodynamic responses distributed in the fingers and the palm in both the impedance magnitudes and phase.

The model was applied to predict biodynamic responses of the human hand-arm system exposed to forearm direction of vibration. These were evaluated in terms of mechanical impedance, vibration transmissibility, dynamic force and power absorption. The basic characteristics of distributed biodynamic responses are analyzed to gain insight into relative health risks of vibration posed to various substructures of the hand-arm system. The results showed that the vibration power absorption (VPA) is mainly distributed in the forearm and shoulder structures under low frequency vibration. At higher frequencies, the vibration power is mostly absorbed in the tissues close to the hand-tool contact area, which can be associated with potential disorders of the fingers caused by operation of high frequency tools. This study also suggests that the distributed power absorption may be used as an alternative vibration measure for assessing various risks of the hand-transmitted vibration exposure.

ACKNOWLEDGEMENTS

First of all, I would like to thank Dr. Subhash Rakheja for his guidance, support, and supervision throughout the course of this study.

I also want to thank Dr. R. Dong and Dr. J. Wu of National Institute for Occupational Safety and Health (NIOSH) for their contributions at different stages of the research work. I am grateful to the technical helps provided by NIOSH.

I would also like to express my profound gratitude to my parents and grandparents, for all their love and support.

TABLE OF CONTENTS

LIST OF FIGURES

LIST OF TABLES

LIST OF ABBREVIATIONS

APMS	Apparent mass
c	Damping coefficient
D	Handle diameter
DOF	Degrees-of-freedom
DPBR	Driving-point biodynamic response
DPDS	Driving-point dynamic stiffness
DPMI	Derive-point mechanical impedance
f	Frequency
F	Dynamic force at driving point
F_g	Grip force
F_p	Push force
g	Gram
G_{Fv}	Cross spectral density of force and velocity
G_{vv}	Power spectral density of velocity
HAV	Hand-arm vibration
HTV	Hand-transmitted vibration
Hz	Hertz
ISO	International Standards Organization
k	Stiffness coefficient
kg	Kilogram
N	Newton

P	Absorbed power
r^2	Correlation coefficient
rms	Root Mean Square
SD	Standard deviation
VPA	Vibration power absorption
VPAD	Vibration power absorption density
VWF	Vibration white finger
ω	Circular frequency
W	Watt
z_h	Direction of vibration

CHAPTER 1

INTRODUCTION

1.1 General

Vibrating tools such as chipping hammers, saws, drills, grinders, road breakers, rock drills are widely used in many workplaces. Exposure to hand-transmitted vibration (HTV) can be found in several industrial sectors, such as manufacturing, construction, mining, agriculture, forestry, transportation, and public services. According to the latest US Labor Statistics (BLS, 2004), more than one million workers are occupationally exposed to HTV, which is close to 1.45 millions estimated by NIOSH (1989) in 1989. In Canada, it was estimated that approximately 200,000 workers are occupationally exposed to HTV (Brammer, 1984).

Vibration exposure may cause discomfort, annoyance, interference with activities, impaired health and pain, depending on various contributory factors (Griffin, 1990). These factors include the characteristics of HTV, duration of exposure, physical characteristics and actives of the exposed individual, environment conditions, etc. The adverse effects of HTV exposure have been of concern for many years (Griffin, 1990; Pelmear and Wasserman, 1998). Many epidemiological studies have demonstrated that prolonged intensive exposure to HTV could cause a series of disorders in the vascular, neurological, and musculoskeletal structures of the hand-arm system (Griffin, 1990; Pelmear and Wasserman, 1998; NIOSH, 1997; Bovenzi, 1998), which has been collectively termed as hand-arm vibration syndrome (HAVS) (Gemne and Taylor, 1983). According to the reported studies, the prevalence of HAVS could range from 6% to 100%, with an average of approximately 50% (NIOSH, 1989).

The International Standard Organization (ISO) had set forth guidelines on measurement, evaluation, and risk assessment of HTV exposure in 1986 (ISO 5349, 1986), which were later revised on the basis of additional (ISO 5349-1, -2, 2001). Many countries have also set forth their national standards to specify the exposure limits that are not recommended in the international standard. However, the precise mechanisms of HAVS have not been sufficiently understood (ISO 5349-1, 2001). Contradictory attitudes on the mechanisms of HAVS have dominated the published studies, which range from hyperactivity of the sympathetic nervous system and 'local defects' to statements of primary central nervous system mechanisms (Sakakibara, 1998; Stoyneva et al., 2003). Effective methods for reliably diagnosing the major components of HAVS have not been sufficiently developed. The development of a better frequency weighting continues to be an important issue for further studies since its introduction in ISO-5349 (1986). The use of better tools may be an effective solution for reducing the exposure at the source, which requires improving the designs of tools and their effective assessments. Several standards have also been developed for assessing vibration expressions of various tools (e.g., ISO 8662 (1-14), 1988-1999) but some of the methods need further improvements. Several anti-vibration handles and gloves have also been developed and used to help reduce the exposure level but their effectiveness has not been sufficiently evaluated. The methods for evaluating their effectiveness also remain important issues for further studies.

To resolve these issues and to significantly advance the knowledge in this field, further systematical studies are required. Figure 1 illustrates a conceptual model of the relationships among the various factors and effects of vibration exposure (Dong et al., 2005f). Based on this model, the theoretical foundations of HTV exposure can be

classified into five groups: (i) measurement of HTV at the source; (ii) biodynamic of the hand-arm system; (iii) psycho-physiological studies of subjective perception or discomfort; (iv) physiological and pathological mechanisms of vibration-induced injuries and disorders; and (v) epidemiological studies of HAVS. Whereas the first two foundations address the issues related to vibration stimuli acting on the hand tissues and cells, the other three foundations focus on the effects or responses to vibration stimulus. These suggest that biodynamic of the hand-arm system forms an essential component in enhancing understanding of the HTV exposure studies. This thesis focuses on the investigations on some aspects of the biodynamic responses of the hand-arm system.

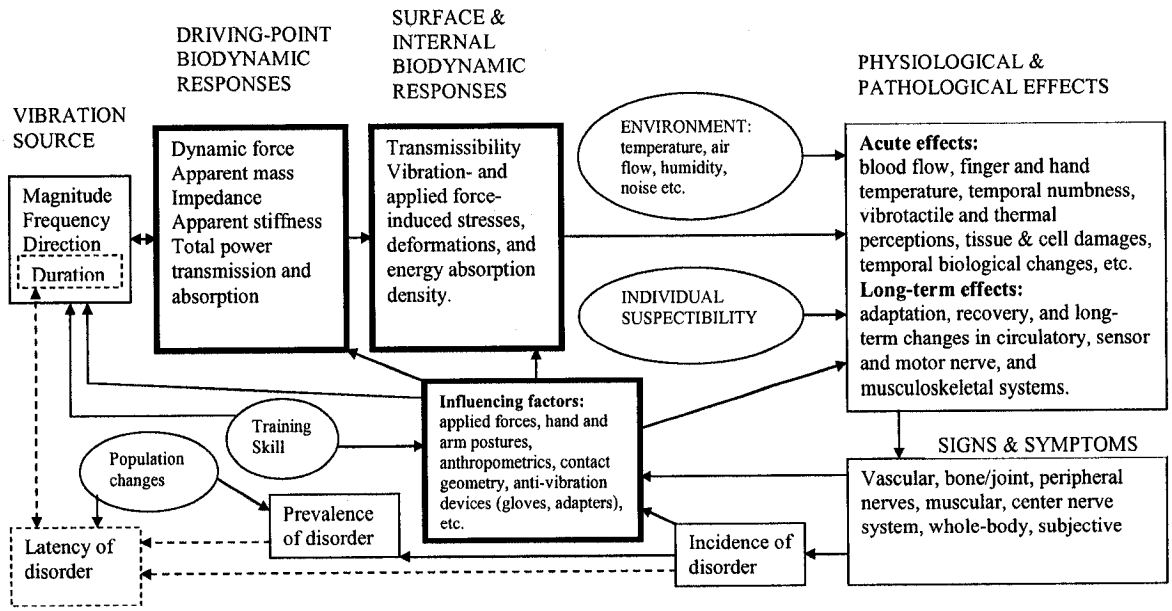

Figure 1.1: conceptual model of factors influencing cause-effect relationships for hand-transmitted vibration exposure.

This dissertation research focuses on development and analysis of a mechanical-equivalent model of the hand-arm structure to simulate for biodynamic responses to vibration. The model is constructed to facilitate analyses of vibration power absorbed

with various substructures of the hand-arm system. The model responses in terms of power flow and distribution are correlated with available epidemiology data to demonstrate its potential applications.

1.2 Symptoms and Effects of Prolonged Exposure to Hand-transmitted vibration

As shown in Figure 1.1, the safety and health effects of HTV exposure are directly linked to biodynamic responses of the hand-arm system. A comprehensive review of reported studies on biodynamic responses of the human hand-arm system to HTV is conducted to develop a better understanding of the HAVs. For this purpose, the vibration-induced disorders are outlined in this subsection on the basis of reported epidemiology and other studies. The disorders or symptoms of HAVS can be broadly classified into the following four groups: (a) vascular disorders; (b) neurological disorders; (c) bone and joint disorders; and (d) muscular disorders. These disorders are briefly described below.

1.2.1 Vascular disorders

Workers exposed to hand-transmitted vibration may complain of episodes of pale or white finger, usually triggered by cold exposure. This disorder, due to temporary abolition of blood circulation to the fingers, is called Raynaud's phenomenon (cited in Maurice Raynaud, 1862). It is believed that vibration can disturb the digital circulation making it more sensitive to vasoconstrictive action of cold. Various synonyms have been used to describe vibration-induced vascular disorders: dead or white finger, Raynaud's phenomenon of occupational origin, traumatic vasosapastic disease, and, more recently, vibration-induced white finger (VWF) (Bovenzi et al., 2000). VWF is a prescribed occupational disease in many countries. During VWF attacks, blood flow to the affected

segments of the fingers is reduced or completely shut off by contraction of the muscles, resulting in severe pain (Pyykkö, 1975). Since the late 1970s a decrease in the incidence of VWF has been reported among active forestry workers in both Europe and Japan after the introduction of anti-vibration chain saws and administrative measures curtailing the saw usage time together with endeavors to reduce exposure to other harmful work environment factors (e.g. cold and physical stress). Recovery from VWF has also been reported among retired forestry workers. Similar findings, however, have not yet been reported for other tool types (Chetter et al., 1997).

1.2.2 Neurological disorders

Workers exposed to hand-transmitted vibration may experience tingling and numbness in their fingers and hands. Under continued vibration exposure, these symptoms tend to worsen and can interfere with work capacity and life actives. In the more advanced stages, intermittently or persistently reduced sensory perception, tactile discrimination and manipulative dexterity can occur (Fridén, 2001). Vibration-exposed workers may exhibit a reduction in normal sense of touch and temperature as well as an impairment of manual dexterity (Bovenzi, 1997). It has been suggested that continuous vibration exposure can not only depress the excitability of skin receptors but also induce pathological changes in the digital nerves, such as perineural oedema, followed by fibrosis and nerve fibre loss (Bovenzi, 1990).

1.2.3 Bone and joint disorders

Many radiological investigations have also revealed a high prevalence of bone vacuoles and cysts in the hands and wrists of vibration-exposed workers (Gemne and Srarste, 1987). More recent studies, however, have shown that such prevalence rates are

comparable to those among the manual workers not exposed to vibration (Bovenzi, 1990; Gemne, 1997). Excessive occurrences of wrist and elbow osteoarthritis as well as ossifications at the sites of tendon insertion, mostly at the elbow, have been found among miners, road construction workers and metal-working operators exposed to shock and low-frequency vibration (<50 Hz) of high magnitude arising from pneumatic percussive tools (Taylor et al., 1984; Gemne and Srarste, 1987).

1.2.4 Muscular disorders

Workers with prolonged exposure to vibration may complain of muscular weakness, muscle fatigue, pain in the hands and arms, and diminished muscle force. Vibration exposure has also been found to be associated with a reduction of hand-grip strength. In some individuals muscle fatigue can cause a form of disability. Direct mechanical injury or peripheral nerve damage have been suggested as possible etiologic factors for such muscle symptoms. Other work-related disorders have been reported in vibration-exposed workers, such as tendonitis and tenosynovitis (i.e. inflammation of tendons and their sheaths) in the upper limbs, and Dupuytren's contracture, a disease of the fascia tissues of the palm of the hand. These disorders seem to be related to ergonomic stress factors arising from heavy manual work, while a definite association with hand-transmitted vibration is not be identified (Bovenzi, 1990).

1.3 Exposure Assessment

Reported studies on epidemiology together with those on vibration exposure have resulted in a HTV exposure assessment method that has been mentioned in ISO 5349 (2001), The standard defines measurement method, frequency-weighting of transmitted vibration, and risk assessment method on the basis of eight-hours equivalent energy. As

the first step, it is generally required to measure the vibration on each type of tool in real working conditions. The acceleration values in three orthogonal directions of the bascentric hand coordinate system (ISO 8727, 1997) are generally measured. ISO 5349-2 (2001) also recommends the accelerometer installation locations on many tools. The daily working hours for each type of tool is further required for risk assessment, which may be directly measured or estimated using a reliable and feasible method.

The acceleration measured in each axis is expressed by its root-mean-square (rms) value in the one-third octave band spectrum with center frequencies ranging from 6.3 Hz to 1,250 Hz. The ISO frequency weighting shown in Figure 1.2 is applied to calculate the overall rms value of the frequency-weighted acceleration due to vibration along each axis, such that:

$$a_{hw} = \sqrt{\sum_{i=1}^{24} (a_{hi} w_i)^2} \tag{1.1}$$

where a_{hi} is rms value of acceleration at the center frequency of i^{th} one-third octave band, and w_i the corresponding frequency weighting value.

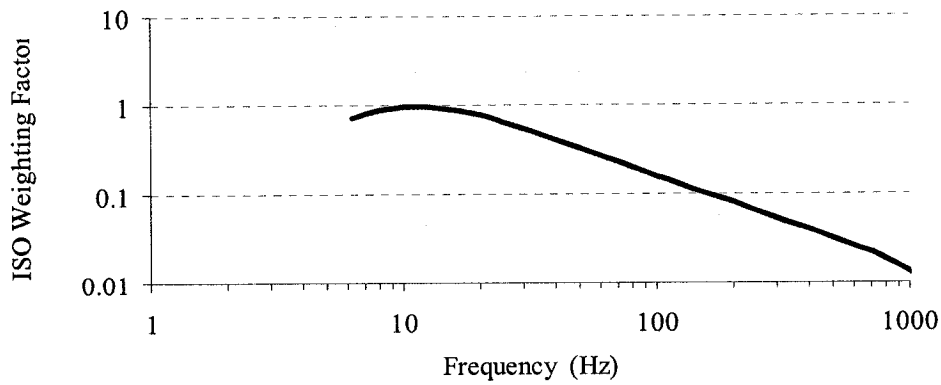

Figure 1.2: ISO frequency weighting (ISO 5349-1, 2001)

The total frequency-weighted rms acceleration due to vibration along three axes is calculated from

$$A_{hw} = \sqrt{a_{hx}^2 + a_{hy}^2 + a_{hz}^2} \tag{1.2}$$

The vibration dosage is expressed in terms of eight-hours equivalent acceleration, A(8), computed from

$$A(8) = \sqrt{\frac{1}{T}\sum_{i}^{n} A_{hwi}^2 T_i} \tag{1.3}$$

Where A_{hwi}^2 total rms acceleration due to exposure over the interval T_i, T is total exposure duration over 8 hours period and n is total number of exposure segment.

According to the EU directive (EU, 2002) and ANSI 2.70 (2006), if A(8) is greater than 5.0 m/s^2, the exposure is considered severe and it should be significantly reduced. For A(8) <2.5 m/s^2, the exposure is considered to be minor and the risk of developing HAVS is believed to be small. A control action is thus not required. If in this case A(8) lies between 2.5 and 5.0 m/s^2, some form of introduction is recommended for the employer to reduce the exposure dosage.

The standard outlines a relatively simple method for risk assessment and measurements in the field. It is also generally believed that the standardized method yield guidelines for some control of exposure levels, which can significantly reduce the incidence of HAVS. However, these limits are set largely based on consensus among investigators and scientists but not necessarily based on sufficient evidences. There are many issues that have not been satisfactorily resolved by the standardize method and the

frequency weighting. The weighting is known to be established based on limited subjective sensation data (Miwa, 1968; Louda et al., 1994). The dose-response relationship is also estimated based on limited epidemiological data on several tools (Brammer, 1986).

Furthermore only a few studies report consistent results on risk estimation using the standard (Brammer, 1986; Anttonen and Virokannas, 1992). Many other epidemiological studies have reported that the predicted prevalence of the vibration-induced white finger could be largely different from that actually observed in the field (Brubaker et al., 1986; Tominaga, 1993; Tasker, 1986; Walker et al., 1986; Griffin et al., 2003; Dandanell and Engstrom, 1986; Engstrom and Dandanell, 1986; Bovenzi et al, 1980; 1988; Bovenzi, 1998; Seppalainen et al., 1986; Starck and Pyykko, 1986; Pelmear et al., 1989). As suggested in some of these studies, the ISO weighting could significantly overestimate the low frequency effects but underestimate the high frequency effects. The dose-response relationship used in the ISO standard may not be very reliable. Moreover, the physical characteristics of the impact vibration could not be taken into account using the rms value (Starck et al., 1990). Further studies have thus been widely emphasized to improve the weighting function, dose quantification, and dose-response relationship.

However, any significant change in the current frequency weighting would require sufficient epidemiologic and dosage assessment studies and concrete evidences on health effects, since such changes could have profound impacts not only on the risk assessment method, but also on the general operation of the industries. As one of the important foundations, one of the major goals of the future biodynamic studies is to help identify the required evidences and develop a better frequency weighting (Dong et al., 2005f).

The current knowledge of the biodynamic responses of the system is far from sufficient to achieve such a goal.

1.4 Biodynamic Response of the Hand-Arm System to Vibration

The Biodynamic Response of the hand-arm system is a branch of biomechanics that applies laws of physics and engineering concepts to describe the force and motion behavior of a biological system. Hand-transmitted vibration stimulates the motion and force responses of the hand-arm system, which could be related to dynamic stresses and strains in the tissues and cells within the biological structures of the system. These stresses and strains are among the direct stimuli that are likely to be closely associated with vibration-induced disorders (Dong et al., 2005f). Therefore, the biodynamic response of the system is one of the important foundations for understanding the mechanisms of HAVS, which could facilitate further development of the risk assessment standard (Griffin, 1994).

Since the vibration stresses and strains directly act on the tissues and cells, they may be considered as the best theoretical biodynamic measures. However, the hand-arm system is a highly complex biological system. So far, a direct and reliable measure of stresses and strains of the tissues cannot be obtained. Although such measurements may be performed using a cadaver, their reliability is not yet known. Moreover, such measurements have not yet been attempted. Although attempts have been made to quantify the stresses and strains within finger tissues using a modeling approach, the quantifications of stress and strain distributions in the entire hand-arm system remain formidable research tasks.

Alternatively, the biodynamic responses of the hand-arm system have been extensively investigated in terms of vibration transmitted to various segments, and the overall driving-point biodynamic responses, such as apparent mass, mechanical impedance and power absorption. Mechanical equivalent models with lumped mass, stiffness, and damping elements have been formulated based on these convenient biodynamic measures. These approaches have greatly helped to understand the overall responses of the hand-arm system to HTV, while ample challenges remain for understanding the power flow and distribution, injury mechanisms and health risks. As also shown in Figure 1.1, many factors such as the applied hand forces, hand and arm postures, hand anthropometry, handle geometry and dimensions, and gloves properties may also affect the biodynamic responses. Systematic studies for characterizing the influences of various contributory factors on the responses are also highly desirable.

A few studies have also attempted to measure vibration transmitted to different segments of the hand-arm system (Cherian, 1994; Reynolds and Angevine, 1997; Kattel and Fernandez, 1999). These studies have shown complex contributions of various intrinsic and extrinsic factors, which are discussed in the following subsections.

1.4.1 Vibration Transmissibility

The biodynamic responses have been mostly characterized through force-motion relationships at the hand-handle interface, which are expressed in terms of mechanical impedance or apparent mass or dynamic stiffness. Vibration transmissibility is defined as a ratio of the vibration measured on a particular location of the hand-arm system and the input vibration at the hand-tool interface. It can provide significant insight into relative motions of various components of the system, apart from the resonance frequencies and

damping properties. It can also be used to assess vibration attenuation performance of anti-vibration devices, such as anti-vibration gloves. The measurement of the vibration transmissibility is mostly performed with miniature or subminiature accelerometers attached to the skin (Reynolds and Angevine, 1977; Aatola, 1989; Kattel and Fernandez, 1999; Cherian et al., 1996; Abrams and Suggs, 1969; Kihlberg, 1995). The sensor mass and the elasticity of the skin could yield contaminating effects on the measured response. Non-contact laser vibrometers have also been used in a few studies (e.g., Gurram, 1994; Sörensson and Lundström, 1992). High speed cameras have also been used for the measurement (e.g. Ksiazek, 2001).

The vibration transmission characteristics of the human hand-arm system have been derived in the laboratory under controlled grip conditions and deterministic vibration (e.g., Reynolds and Angevine, 1977; Pyykko et al., 1976). Other investigators have performed these measurements in the field during tool operation to assess the vibration performance of different tools and protective devices (Aatola, 1989; Kattel et al., 1999). The reported studies have invariably concluded that magnitudes of vibration transmitted to the hand-arm decrease with increasing frequency and the distance from the vibration source (Dong et al., 2001). Less than 10% of vibration is transmitted to the wrist and beyond at frequencies above 250 Hz. Vibration at frequencies less than 100 Hz is effectively transmitted to the forearm, while the vibration below 40 Hz can be transmitted to the forearm and upper arm without any noticeable attenuation. Vibration transmitted to the fingers and carpal bones, however, generally show amplification of handle vibration. Although the resonant-peak values for the phalanges reported in different studies differ considerably, the peak values occurred in the 80 to 200 Hz

frequency range. Increasing the hand force generally increases the resonant frequencies in a linear manner, such that (Aatola, 1989):

$$f_1(Hz) = 0.7 \cdot F_{Grip} + 10 \tag{1.4}$$

where f_1 is the resonance frequency and F_{Grip} is grip force in N.

The low frequency vibration may also be transmitted to the whole-body, depending upon the characteristics of HTV, body posture and hand posture. Sakakibara et al. (1986) measured the vibration transmitted from the operator's hand to the head and concluded that the vibration transmitted to the head was highly dependent on the elbow angle. A straight-arm posture generally transmitted more vibration to the head the bent elbow posture. The vibration transmitted to the head was shown to alter continuous manual control and oculo-manual coordination; the effect was found to be frequency dependent. Mussan et al. (1989) reported that back pain or back stiffness was the most common complaint among workers (54%) using impact power tools even though back pain is not often mentioned as a disorder of exposure to HTV. Pope et al. (1997) further investigated the transmission of HTV and/or impacts through the hand-arm system to the spine. Their study concluded that the simulated vibration and impacts could be effectively attenuated by the hand-arm system, and their transmission to lumbar spine was of little concern, at least under the conditions employed in their study. Therefore, it is questionable whether the back pain could be strongly associated with exposure to HTV.

Since the biodynamic force is directly related to acceleration, the biodynamic stresses and strains are also expected to be related to acceleration. Several investigators

have proposed using the acceleration transmissibility of an anatomical segment as a frequency weighting for assessing the risk of the vibration-induced disorders at that location of the same segment (Thomas and Beauchamp, 1998). A recent study has shown that the acceleration of the arm calculated using transmissibility-based (TAB) weighting was highly correlated with that desired using the ISO weighting (Dong et al., 2005c). Another study (Malchaire et al., 2001) reported that the wrist sensorineural disorders were reasonably correlated with the ISO-weighted acceleration. The TAB weighting method may thus have some value for assessing the risk of some of the disorders of the wrist-arm system. However, the local stresses and strains may not solely be caused by the local acceleration; it may also depend on the response of the global hand-arm system. Therefore, an understanding of the transmissibility alone may not be sufficient to determine the total dynamic behavior of the system.

An important application of vibration transmissibility is to assess the isolation performance of anti-vibration gloves and vibration mitigation devices. The ISO and CEN (European Committee for Standardization) have jointly developed a standard method to assess the vibration attenuation performance of gloves (ISO-10819, 1996). A palm-held adapter with a single-axis transducer is used to measure the vibration transmitted through a glove. The vibration attenuation performance of a glove is evaluated on the basis of vibration transmissibility through the hand, computed from accelerations measured at the palm-held adapter and the handle. Several studies have evaluated this standardized methodology and proposed several improvements (e.g., Griffin, 1998; Hewitt, 1996; Dong et al., 2002; Rakheja et al., 2002b). The effectiveness of gloves can also be evaluated using vibration transmitted to the fingers, the back of the hand, and the wrist

(e.g., Paddan and Griffin, 2001; Dong et al., 2003). The US ANSI 3.40 (1989) is based on this approach. Similar to ISO 10819, ISO 13753 (1999) is mainly designed for screening glove materials. It uses the mechanical impedance of the hand-arm system recommended in ISO 10068 (1998) for assessing the vibration isolation effectiveness of a material (Boileau and Boutin, 2001). The improvements of these standards are among various topics suggested for further biodynamic studies (Dong et al., 2005f).

1.4.2 Force-motion Based Biodynamic Responses

The force-motion relationship based driving-point biodynamic response (DPBR) may be expressed in terms of driving-point dynamic stiffness (DPDS), driving-point mechanical impedance (DPMI) or apparent mass (APMS) in the following manners (Griffin, 1990):

$$K_d(j\omega)=\frac{F_q(j\omega)}{x(j\omega)}, \qquad Z(j\omega)=\frac{F_q(j\omega)}{v(j\omega)}, \qquad M_a(j\omega)=\frac{F_q(j\omega)}{a(j\omega)} \tag{1.5}$$

where K_d, Z and M_a are complex dynamic stiffness, mechanical impedance, and apparent mass, respectively; x, v and a are the displacement, velocity and acceleration due to vibration, respectively, measured at the driving-point, F_q is driving force along the axis of the motion; ω is the circular frequency of vibration and $j = \sqrt{-1}$.

Although different measures may yield different aspects of the hand-arm response to vibration, they are directly related to each another. The most frequently reported DPBR is expressed in mechanical impedance. Both the dynamic stiffness and apparent mass can be directly related to mechanical impedance, such that:

$$K_d(j\omega) = j\omega Z\ (j\omega) \quad \text{and} \quad M_a(j\omega) = \frac{1}{j\omega} Z\ (j\omega) \tag{1.6}$$

The DPDS, DPMI and APMS functions may also be expressed by the respective displacement mobility or compliance, velocity mobility and accelerance, which are computed from inverse of the above functions (McConnell, 1995). Another important measure of the DPBR has also been expressed in terms of the power absorbed by the hand and arm. The energy absorption rate (*power*) at any time (t) is defined as:

$$P(t) = \tilde{F}(t) \cdot \tilde{V}(t) \tag{1.7}$$

where $\tilde{F}(t)$ is the driving force, and $\tilde{V}(t)$ is the corresponding driving velocity. The power can be obtained in the frequency domain from the cross-spectrum density of the force and velocity (Bendat and Piersol, 1992). Because of the phase difference between measured force and motion at the driving-point, the cross-spectrum density is normally complex, which can be generally expressed as:

$$P(j\omega) = C_{vF}(\omega) - jQ_{vF}(\omega) \tag{1.8}$$

In the above equation, $P(j\omega)$ is spectral density of vibration power in $\text{Nms}^{-1}/\text{Hz}$. $C_{vF}(\omega)$ is coincident spectral density function or the co-spectrum, and $Q_{vF}(\omega)$ is quadrature spectral density function or the quad-spectrum. The real component determines the energy absorption due to the transformation of vibration energy into heat caused by internal friction within the tissues and tissue deformations. The imaginary component relates to energy stored within the biological structure. Unlike the other two

driving point dynamic functions, the absorbed power can be used to measure a vibration 'dose', as it increases with vibration magnitude and duration.

1.4.3 Measurement Methods

All the reported studies have measured the biodynamic response of the hand-arm system under controlled laboratory test conditions using a single-degree-of-freedom vibration test system. Consequently, the possible coupling effects of the hand-arm system response to multi-axis vibration have been ignored. Although the driving-point response has been studied for many years, the measurement methods have not yet been standardized. A variety of instrumented handles, recording systems, and analyses algorithms have been employed in various studies (e.g., Miwa, 1964; Mishoe and Suggs, 1977; Reynalds and Falkenberg, 1984; Gurram et al.; Cronjager and Hesse, 1989; Hempstock, 1989; Jandak, 1989; Dong et al., 2004a; Gurram et al., 1995a; Kihlberg, 1995; Burstrom, 1990).

There are considerable differences among the reported data (Gurram et al., 1995b), which have been mostly attributed to differences in measurement systems and methods, analyses methods, test conditions, hand-arm anthropometry, etc. Furthermore, arrays of influencing factors are known to affect DPMI in a significant manner. The accuracy of measurement strongly relies upon dynamic behavior of the handle structure and nature of instrumentation. Welcome et al. (2006) has developed an instrumented handle that can be used to measure biodynamic response accurately up to 1,500 Hz. Appropriate compensation of force due to handle tare mass is also very critical for DPBR measurement, since the hand apparent mass approaches very small values at high frequencies. Earlier studies had employed mass compensation in the time-domain (e.g.,

Reynolds, 1977). This method could yield considerable errors due to strong frequency dependence of the apparent mass of the handle and dynamic behavior of the handle. Alternatively, frequency domain method has been widely used to circumvent this problem (McConnell, 1995). Furthermore, the frequency-domain method offers greater convenience of analysis (Marcotte et al., 2005; Aldien et al., 2005b).

1.4.4 Basic Characteristics of DPBR

The DPBR is generally a function of frequency. The apparent mass (APMS) generally decrease with increase in frequency. The mechanical impedance (DPMI) in the z_h- and x_h-directions (Figure 1.3) generally show a clear resonance in the 16 to 63 Hz frequency range, depending on the applied force, and hand and arm posture (Miwa, 1964; Mishoe and Suggs, 1977; Reynalds and Falkenberg, 1984; Hempstock, 1989; Jandak, 1989; Kihlberg, 1995; Aldien et al., 2005a; Marcotte et al., 2005). This frequency has been associated with palm-handle interactions (Dong et al., 2004b), which is also consistent with the reported wrist resonant frequency (Aatola, 1989; Thomas and Beauchamp, 1998; Gurram et al., 1994b). The second major resonance is usually in the 100 to 350 Hz frequency range and is made of the fingers-handle interaction, which is also consistent with the resonance observed in reported transmissibility studies (Aatola, 1989; Thomas and Beauchamp, 1998). The resonances of the hand-arm system subject to y_h-axis vibration, however, are not clearly evident from the DPBR data.

Dong et al. (2005e) have recently investigated distribution of the biodynamic responses in the hand-arm system exposed to z_h-axis vibration, the mechanical impedance is mostly distributed in the palm at low frequencies ($\leq$40 Hz) and the majority of the hand DPMI remains concentrated at the palm up to 100 Hz. At frequencies above 160

Hz, the finger DPMI is comparable to or higher than that at the palm. Moreover, among the three coupling actions (pull-only, grip-only, and combined grip and push) used in the reported study, the finger DPMI approaches lowest magnitudes under the combined grip and push action at low frequencies (<40 Hz). However, at frequencies equal to or above 100 Hz, the fingers appear to be independent of the palm-handle coupling conditions. The power absorption measured under a constant-velocity vibration also revealed similar characteristics (Dong et al., 2004b).

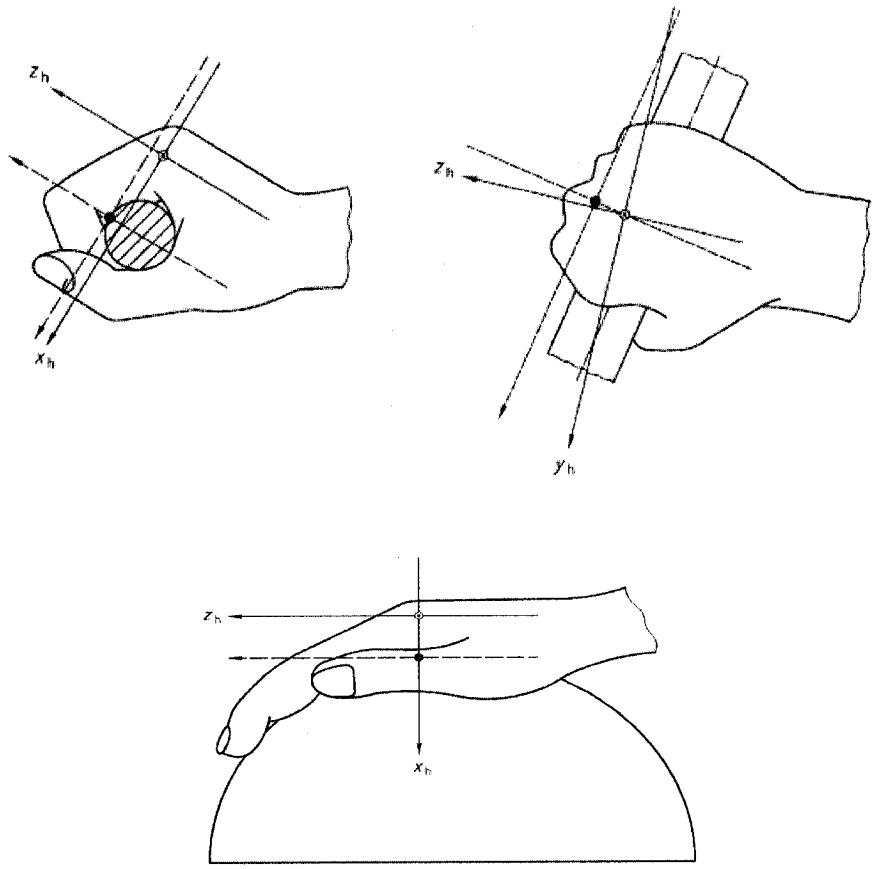

Figure 1.3: Hand coordinate system defined in ISO 5349 (2001)

Many factors could influence the biodynamic response. These factors include vibration magnitude, excitation types (e.g., discrete frequency sinusoid, impact or random), grip and feed forces, hand and arm postures anthropometric parameters or individual differences, and handle sizes (Burstrom, 1990; 1997; Rakheja et al., 2002; Gurram et al., 1995b; Burstrom and Sorensson, 1999; Dong et al., 2001). Increasing the applied hand forces generally increases the response magnitude and the resonant frequencies (Kihlberg, 1995). The resonant peak values measured under discrete sinusoidal vibration are generally higher than those observed under a broad-band random vibration (Dong et al., 2005e; 2005g; 2004a), which may be because the resonance is not fully developed under a random excitation. However, increasing the magnitude of vibration slightly reduces the resonant frequency (Kihlberg, 1995), similar to the softening effect observed in whole-body vibration response of the subjects (Griffin, 1990), which demonstrates non-linear behavior of the system.

1.4.5 Vibration Power Absorption

More than 40 years ago, several investigators (Pradko et al., 1965; Lidström, 1973; Cundiff, 1976) proposed that the vibration energy/power absorption (VPA) could serve as a significant etiological factor for assessing vibration-induced disorders. Furthermore, the VPA can also account for many influencing factors that are not adequately considered in DPMI, such as hand-tool coupling conditions, hand-arm posture, vibration direction in tool operation. Vibration magnitude and exposure duration, Lidström (1973) further hypothesized that the power dissipated in the hand-arm system could provide a better indication of vibration damage than the acceleration due to HTV. Since the introduction of this energy concept, a total energy method describing the VPA

of the entire hand-arm system has been invariably used. It has also been reported that a correlation exists between the subjective annoyance and the total VPA (Reynolds et al. 1977). There was only one reported epidemiological study that directly investigated the relationship between the VPA and vibration-induced white finger (Lidström, 1977), which is the most recognized and important component of the HAVS (ISO 5349-1, 2001). The results showed that the prevalence of finger disorders increased with total VPA but the relationship was substantially nonlinear. Although these investigations were far from sufficient to validate the energy method, some investigators concluded that the measurement of energy absorbed in the hand and arm may serve as a better and more objective method for risk assessment of HTV (e.g. Burström, 1990 Burström and Bylund, 2000; Bylund and Burström, 2003).

This total energy method, however, can not predict local disorders within the hand-arm system, such as disorders in the fingers and hand. Specifically, it ignores the distribution and frequency dependence of power absorption. Considering that HTV due to different tools differ considerably in dominant vibration magnitudes and frequencies, the frequency dependent absorbed power distribution in the hand-arm system is vital for predicting risk of disorders among different substructures. The power absorption associated with operation of a low frequency tool, such as a sand tamper is likely to be higher than that of a high frequency tool such as a high speed grinder. Only a few signs of vibration-induced white finger (VWF), however, were found among tamper users while a large prevalence was found among the grinder users (Tominaga, 1993). Tominaga (2005) recently proposed a new frequency weighting based on his epidemiological study on VWF. This weighting suggests that the ISO weighting greatly

overestimates the low frequency vibration effect but substantially underestimates the high frequency vibration exposure. Many physiological and pathological data also suggest that the substantial health effects of HTV exposure mostly occur in the middle frequency range (30-500 Hz) (Bovenzi et al., 2000; 2001; Harada and Griffin, 1991), which also disagrees with the ISO weighting. Considering that the total power absorption is well correlated with the ISO-weighted acceleration, it may have some association with the subjective sensation (Reynolds et al., 1977). Furthermore, the frequency characteristic of the total power absorption suggests that it may be related to disorders in the palm-wrist-arm system (Malchaire et al., 2001; Bovenzi et al., 1987; Gemne and Saraste, 1987)

Sörensson et al. (1997) extended the basic concept of energy transmission at the driving point to study the energy absorption at different locations of the hand and arm, specifically the knuckle, wrist and elbow. The velocities at different locations were measured to estimate the energy transmission at different locations. Since the actual forces transmitted to different locations are expected to be different from the force at the driving point in terms of both the magnitude and phase, the computed energy values may not truly describe the energy absorption at different locations. In a recent study, Dong et al (2004b) proposed vibration power absorption density (VPAD) and its distribution for quantifying the power absorption in the fingers. The study showed that VPAD depends on both the 'vibration source power density' and a 'power absorption coefficient' that depends on dynamic response of the finger-hand-arm system and effective mass of the soft tissue.

1.4.6 Other Applications of Biodynamic Responses

Biodynamic force developed at the hand-handle interface can be directly measured or estimated from the other DPBR measures. Moreover, the biodynamic force could be easily measured at the finger and palm-side driving points, which maybe applied to derive the frequency weighting (Dong et al., 2005i). Since the biodynamic force acting on the fingers is directly related to stress and strains developed in the fingers and that the force is directly related to fingers APMS, the apparent mass can be used to represent the frequency dependency of the stress and strain in the fingers. The apparent mass measured on the palm, in a similar manner, may be used to determine the frequency weighting for assessing the risk of disorders in the wrist-arm system.

Considering that the vibration transmissibility is correlated with the force-motion biodynamic response, the biodynamic response may be applied to evaluate the vibration isolation performance of anti-vibration glove materials, as recommended in ISO 13753 (1999). Dong et al. (2005b) proposed an alternative approach for evaluating vibration isolation performance of gloves on the basis of biodynamic responses of the bare- and gloved-hand-arm system. This approach eliminated the use of the palm- adapter in assessing the glove, which is known to affect the glove-hand coupling leading to overestimation of the glove effectiveness in the middle- and high-frequency ranges. Wasserman et al. (2004) proposed the use of a flexible force sensor to measure the biodynamic force for glove evaluation.

1.5 Biodynamic Modeling of the Hand-Arm System

Biodynamic models of the hand and arm can provide significant insight into the dynamic behaviors of the hand-arm system. The models have been proposed to

characterize the biodynamic responses and power flow in the coupled hand, tool and work piece system, analyze the potential performance benefits of vibration attenuation mechanisms, and to develop test rigs and hand-arm simulators for assessment of vibration transmission of different tools (e.g., Abrams and Suggs, 1977; Jahn and Hesse, 1986; Bystrom et al., 1982; Nilsson and Olsson, 1978).

Owing to extreme complexity of the hand-arm system, the theoretical modeling has been generally performed using mechanical equivalent models with lumped mass, stiffness, and damping elements or with continuous beams coupled with lumped stiffness and damping elements (e.g., Fritz, 1991; Reynolds and Falkenberg, 1984; ISO 10068, 1998). The parameters of these models are identified upon curve fitting of the measured vibration transmissibility values at several anatomical locations (e.g., Cherian et al., 1996), or the mechanical impedance measured at the driving point (e.g., Gurram et al., 1995a). While the majority of the models are derived to characterize the biodynamic response of the entire hand-arm system, only a few models focus on the biodynamic response of the fingers alone (Calada, 1985; Lundstrom, 1984). All the models assume a single-point contact relationship between the hand and the tool handle, and are thus not suited to describe the biodynamic responses distributed at the fingers and the palm of the hand.

Rakheja et al. (2002) evaluated the biodynamic response characteristics of various mechanical models of the hand and arm system in terms of their driving-point mechanical impedance modulus and phase responses, static deflections and free vibration response. It was concluded that a vast majority of these models could not be applied for development of a mechanical hand–arm simulator or for assessing dynamic behavior of the coupled

hand–tool system. Higher order models, with three- and four- degrees-of-freedom, in general, yield impedance characteristics within the range of the values recommended in ISO 10068 (1998), but exhibit excessive static deflections. Moreover, these models involve very light masses (in the order of 1-8 gram range). It is not practical to use such models to construct a test rig for testing of tools as anti-vibration devices. The majority of the lower order models yield reasonable magnitudes of static deflections but relatively poor agreement with recommended impedance values. These problems could be attributed to either in appropriate mass of impedance values recommended in ISO 10068 as inability of model to accurately predict the hand-arm system biodynamics. These observations suggest that further studies are required to evaluate the impedance data and to develop better models.

Moreover, the mechanical equivalent models do not adequately represent the biomechanical properties of the system. It is very difficult to directly use such models to understand the local dynamic behaviors in terms of stress, strain or power absorption density. Whereas a detailed biodynamic model of the entire hand-arm system has not been reported, several models of a finger or fingertip have been developed to study the stresses developed under static and dynamic loads. Srinivasan and Dandekar (1996) proposed a two-dimensional finite element (FE) fingertip model which was composed of soft tissue, bone and nail. The soft tissue was represented by homogeneous, isotropic, and incompressible elastic media, the bone was considered as linearly elastic, and the nail was represented by constrained boundaries. Dandekar et al. (2003) developed a three-dimensional fingertip model to incorporate realistic external geometries of the fingertips, while the soft tissues were considered as multi-layered elements with different elastic

moduli. Wu et al. (2002; 2003a) have proposed nonlinear, two-dimensional FE models of the fingertips to derive local biodynamic responses in the fingertip and their associations with some health effects. As a further development from their 2-D models, Wu et al. (2006) have recently reported a 3-D fingertip model and its applications.

1.6 Scope and Objectives of the Dissertation Research

Prolong and intensive exposure to hand-transmitted vibration could cause a series of disorders in the vascular, neurosensorial, and musculoskeletal structures, which have been collectively termed as hand-arm vibration syndrome. From the review of literature, it is apparent that biodynamic response of the hand-arm system is one of the important foundations for understanding the causations of HAVS and for developing effective methods for exposure assessment. Although considerable effects have been made to characterize the biodynamic responses of the hand-arm system and develop biodynamic models, only little knowledge exists on distribution of biodynamic response and power absorption for assessing localized health risk.

The biodynamic measurement and analyses, invariably, consider a single driving-point and provide overall response characteristics of the hand-arm system to HTV. This approach does not permit for analyses of distributed biodynamic responses, which could yield significant insight into concentration of biodynamic stresses within different substructures of the hand-arm system. Moreover, the consideration of a single driving-point in the models does not permit for study fingers-handle and palm-handle interactions. A hand-arm vibration model with two driving-points would thus be desirable.

Whereas the components of HAVS in the palm-wrist-arm system may be more closely related to biodynamic response measured at the palm of the hand, the finger disorders may be more closely associated with biodynamic response distributed in the fingers. It is thus important to quantify and understand the distributed biodynamic responses. Experimental methods have been developed for characterizing the biodynamic responses distributed at the fingers and the palm of the hand, while the distributed absorbed power cannot be quantified by experimental means.

Although the finite element method can provide detailed information on the biodynamic stresses and strains. The development of an FE model of the entire hand-arm system is quite complex. Alternatively, a mechanical equivalent model with two driving-points may be developed to predict distributed DPMI and power flow responses. Moreover, the lumped parameter models responses may be used as inputs to the FE model of a particular substructure for predicting the dynamic stresses and strains in the fingers or the hand. This may thus lead to a practical hybrid approach to conduct detailed analyses of vibration-induces stresses. This approach in the first-stage, however, requires the development of a model that mimics the structures of the hand-arm system.

Anti-vibration devices, such as anti-vibration gloves and handles may provide some reductions the vibration transmitted to the entire hand-arm system, while the vibration transmitted to the fingers may be amplified, when used with specific tools. An effective biodynamic model comprising the finger biodynamic responses can be vital for exposure analysis, and design and evaluations of such devices for finger protection. Therefore, apart from characterizing the distributed biodynamic responses and generating the motion and force inputs for the FE model, an effective model could also be applied to

analyze the coupled hand-tool systems dynamics, evaluations of anti-vibration devices, and design of hand-arm simulator.

1.6.1 Objectives of Thesis Research

The primary objective of this dissertation research is to contribute to development of an effective hand-arm vibration model that can predict distributed mechanical impedance and power absorption properties of the hand-arm striation. On the basis of the background gained from review of literature and scope summarized above, the specific objectives of this dissertation research are as follows:

a) Conduct a review of experimental method employed for measuring the biodynamic responses distributed at the fingers and palm of the hand and perform analyses of measured data under selected experimental conditions;

b) Identify target datasets on distributed biodynamic responses for different hand actions for model development;

c) Develop a new model structure that mimics the basic structures of the hand-arm system grabbing a handle with driving points, and identify model parameters based on the selected experimental data using a curving fitting method;

d) Investigate model validity and distributions of biodynamic responses expressed in terms of mechanical impedance, biodynamic force, vibration transmissibility and power absorption under selected hand actions.

e) Explore predictions of distributed biodynamic responses based on biodynamic response of the entire hand-arm system.

1.6.2 Thesis Organization

This thesis is presented in five chapters. The initial chapter provides a review of the reported relevant literature relevant to health effects of exposure to hand-transmitted vibration, the standardized risk assessment method, the state-of-the-art of the biodynamic responses of the hand-arm system, and scope and objectives of the thesis research.

Chapter 2 describes the experimental method employed for measuring the biodynamic responses distributed at the fingers and the palm of the hand, and analyses of

the selected data acquired from US National Institute of Occupational Safety and Health (NIOSH) for model development. The structure of hand-arm vibration model is presented together with parameter identification. Chapter 3 is devoted to the results attained on distributions of biodynamic responses expressed in terms of biodynamic forces, vibration transmissibility, and power absorption. The fundamental characteristics of the distributions are discussed, which provide significant insight into the biodynamic behaviours of the hand-arm system. The relationships among the biodynamic measures are also explored. Chapter 4 explores predictions of distributed biodynamic responses based on response of the entire hand-arm system, while the major conclusions and recommendations for future studies are summarized in Chapter 5.

CHAPTER 2

DISTRIBUTED BIODYNAMIC RESPONSES OF THE HAND-ARM SYSTEM MODEL

2.1 Introduction

Biodynamic models of the hand and arm can provide considerable insight into the dynamic behavior of the hand-arm system exposed to hand-transmitted vibration (HTV). Such models have been used to characterize the biodynamic responses and power flow in the coupled hand, tool and work piece system; to analyze the potential performance benefits of vibration attenuation mechanisms; and to develop test rigs and hand-arm simulators for assessment of vibration transmission of different tools (e.g., Abrams and Suggs, 1977; Jahn and Hesse, 1986; Bystrom et al., 1982; Nilsson and Olsson, 1978).

Complexities associated with biological properties of the hand-arm system have motivated the theoretical modeling of the hand-arm system in terms of mechanical equivalent models with lumped mass, stiffness, and damping elements or with continuous beams coupled with lumped stiffness and damping elements (e.g., Fritz, 1991). The parameters of these models are identified upon curve fitting the measured vibration transmissibility values at several anatomical locations (e.g., Cherian et al., 1996), or the mechanical impedance measured at the hand driving point (e.g., Gurram et al., 1995a). While the majority of the models are derived to characterize the biodynamic response of the entire hand-arm system, only a few models focus on the biodynamic response of the fingers alone (Calada, 1985; Lundstrom, 1984). All these models assume a single-point contact relationship between the hand and the tool handle and thereby a resultant biodynamic force of the entire hand-arm system. And the single-point hand-handle

coupling relationship, invariably assumed in these models, cannot be considered valid for simulating the responses distributed at the fingers and the palm of the hand. In order to achieve the primary goal of this thesis research, it is essential to develop a new model structure that incorporates a minimum of two driving points reposing fingers-handle and palm-handle interface. Moreover, a reliable set of experimental data is required. Although NIOSH has recently acquired biodynamic data at the fingers and palm of the hand under z_h-axis HTV, no attempts have been made in formulating a representative model. Furthermore, it needs to be expected whether such a model established from the experimental data can be used to interpret the behaviors of the hand and arm structures, and whether the effects of the hand forces can be reflected in the model parameters.

Therefore, the specific aims of the study described in this chapter are: (i) to configure a new model structure that simulates the basic structure of the hand and arm subjected to vibration along the forearm direction or the z_h-axis of the basicentric hand coordinate system defined in ISO 5349 (2001); (ii) to determine the model parameters by simulating the measured driving-point biodynamic responses (DPBRs) distributed on the fingers and the palm of the hand; (iii) to examine the sensitivity of the predicted response on the variations in each model parameter; and (iv) to evaluate the effects of applied hand forces on the parameters. The structures and responses of the proposed model are also discussed to enhance an understanding of phenomena observed in the experimental studies.

2.2 Development of Mechanical- Equivalent Biodynamic Model

Figure 2.1 illustrates the model structure formulated for simulating the biodynamic responses distributed at the fingers and the palm of the hand exposed to vibration in the

forearm direction. The hand is virtually divided into three parts: the fingers, the palm-wrist-forearm and upper arm-shoulder structure. The soft tissue is known to exhibit nonlinear force-displacement relationship (Chaffin et al., 1990). To make the modeling easily manageable, the stiffness and damping properties in this study are assumed to be linear. The non-linear behaviors observed under varying hand actions are taken into account by considering these parameters as functions of the applied hand forces. The fingers positioned on the half of the handle are represented by two effective mass elements (M_2 and M_4). The palmar-side skin of the fingers is assumed to be tightly in contact with the handle, which is known to exhibit only little relative movement up to a certain high frequency (Wu et al., 2006). The skin is represented by a lumped mass M_4, as in case of the fingers skin mass M_4. The remaining effective mass of fingers is considered as M_2, which is coupled to M_4 through the soft tissues of the fingers, represented by lumped stiffness (k_4) and damping (c_4) elements. The palm-wrist-arm structure is also represented by two mass elements (M_1 and M_3) in a similar manner, where M_3 represents the lumped palm skin mass and M_1 the remaining mass of palm-wrist-arm structures. The two masses are coupled through a linear spring-damping element (k_3 and c_3). The distributed masses due to fingers (M_2) and the wrist-palm-arm (M_1) structures are also coupled through another linear spring-damping element (k_2 and c_2), representing elastic and viscous properties of the carpals and metacarpals substructure. The mass M_0 represents the mass due to upper arm-shoulder structure, which may also include a portion of the upper body mass. The masses M_1 and M_0 are also coupled through a linear spring-damping element (k_1 and c_1). M_0 is connected to the other part of the body through another linear spring-damping element (k_0 and c_0).

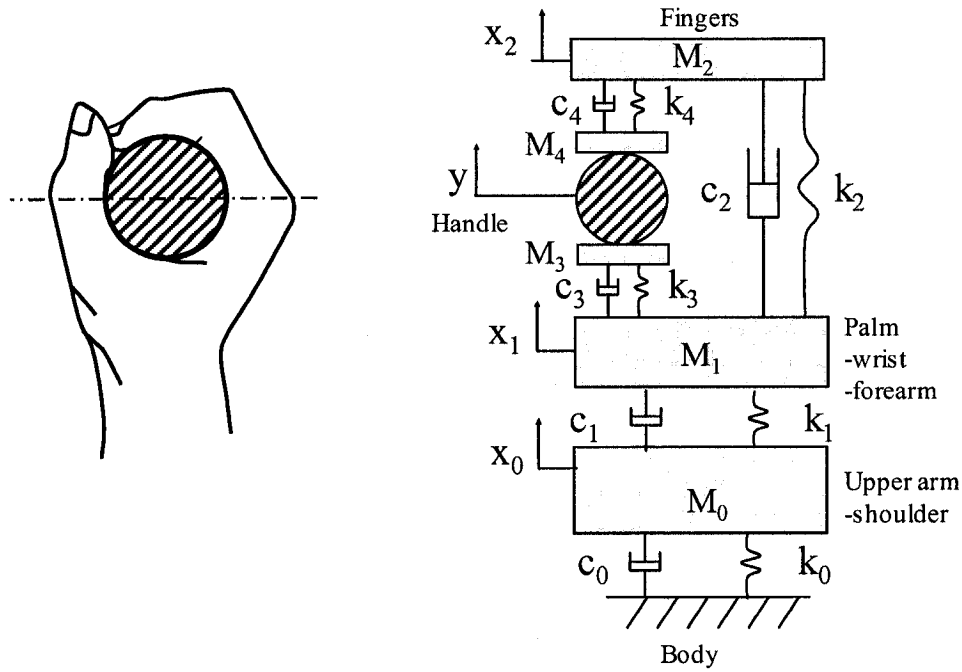

Figure 2.1: Hand grip posture and a 5-DOF model structure of the hand-arm system.

As shown in Figure 2.1, the two skin (dermis and epidermis) mass elements are rigidly attached to the handle. Therefore, this model can be considered to possess only three effective DOFs. The equations of motion for the model are thus formulated considering the effective DOF, such that:

$$\begin{bmatrix} M_0 & 0 & 0 \\ 0 & M_1 & 0 \\ 0 & 0 & M_2 \end{bmatrix}\begin{bmatrix} \ddot{x}_0 \\ \ddot{x}_1 \\ \ddot{x}_2 \end{bmatrix} + \begin{bmatrix} c_0 + c_1 & -c_1 & 0 \\ -c_1 & c_1 + c_2 + c_3 & -c_2 \\ 0 & -c_2 & c_2 + c_4 \end{bmatrix}\begin{bmatrix} \dot{x}_0 \\ \dot{x}_1 \\ \dot{x}_2 \end{bmatrix} + \begin{bmatrix} k_0 + k_1 & -k_1 & 0 \\ -k_1 & k_1 + k_2 + k_3 & -k_2 \\ 0 & -k_2 & k_2 + k_4 \end{bmatrix}\begin{bmatrix} x_0 \\ x_1 \\ x_2 \end{bmatrix} = \begin{bmatrix} 0 & 0 \\ k_3 & c_3 \\ k_4 & c_4 \end{bmatrix}\begin{bmatrix} y \\ \dot{y} \end{bmatrix} \tag{2.1}$$

Where $y(t)$ and $\dot{y}(t)$ are the displacement and velocity due to handle vibration, x_0, x_1 and x_2 are the displacements of mass M_0 due to upper arm-shoulder, mass M_0 due to palm-wrist-forearm and mass M_2 due to fingers substructures, respectively. The dynamic force acting on the palm, F_P, can be computed from:

$$F_P = k_3(y - x_1) + c_3(\dot{y} - \dot{x}_1) + M_3\ddot{y} \tag{2.2}$$

The dynamic force acting on the fingers, F_F in a similar manner is derived from::

$$F_F = k_4(y - x_2) + c_4(\dot{y} - \dot{x}_2) + M_4\ddot{y} \tag{2.3}$$

The total biodynamic force developed at the handle interface, F_H, can thus be calculated from

$$F_H = F_F + F_P \tag{2.4}$$

2.3 Driving-Point Mechanical Impedance Analysis

The driving-point biodynamic response of the hand-arm system is often characterized by the force-motion relationship at the driving-point in terms of mechanical impedance, apparent mass or dynamic stiffness. These measurements are not independent and can be related to each other through excitation frequency as described in equation (1.5). The mechanical impedance (Z) is used to represent the DPBR in this study. Assuming excitation of the form, $y = Ye^{j\omega t}$, where Y is the magnitude of the excitation displacement, the DPBR can be derived from the steady-state solution of equations of motion EQS (2.1) to (2.4), such that:

$$Z(j\omega)=\frac{F(j\omega)}{V(j\omega)} \tag{2.5}$$

where F is the dynamic force developed at the driving-point interface considered and $V(j\omega)$ is the handle vibration velocity corresponding to excitation frequency ω. $Z(j\omega)$ is the complex DPBR in terms of mechanical impedance. The biodynamic driving-point force may be expressed in terms of finger force $F_F(j\omega)$, palm-side force $F_P(j\omega)$, and total force $F_H(j\omega)$ to derive mechanical impedance of the fingers, palm-wrist-forearm structure or the total hand, respectively.

The proposed model structures comprise two driving-points for analyses of DPBR distributed at the fingers and the palm. The dynamic forces developed at the finger-handle and palm-handle driving-points are designated as F_F and F_P respectively, while the total hand-handle dynamic force is represented by F_H.

Equations (2.1) to (2.4) can be solved to determine the DPBR in terms of impedance distributed at the fingers (Z_F) and the palm (Z_p) in the following manner:

$$Z_F(j\omega)=\frac{F_F(j\omega)}{V(j\omega)}=\frac{(k_4+j\omega c_4)(Y-X_2)}{j\omega Y}+j\omega M_4 \tag{2.6}$$

$$Z_P(j\omega)=\frac{F_P(j\omega)}{V(j\omega)}=\frac{(k_3+j\omega c_3)(Y-X_1)}{j\omega Y}+j\omega M_3 \tag{2.7}$$

where X_1 and X_2 are the magnitude of displacement response of M_1 and M_2, respectively. The DPBR of the entire fingers-hand-arm system can be evaluated from the sum of Z_F and Z_P, such that:

$$Z_H(j\omega)=\frac{F_H(j\omega)}{V(j\omega)}=\frac{F_F(j\omega)+F_P(j\omega)}{V(j\omega)}=Z_F(j\omega)+Z_P(j\omega) \tag{2.8}$$

2.4 Measurement of Biodynamic Responses

The driving-point mechanical impedance of the fingers and the palm-wrist-forearm structures were measured in the laboratory under z_h-axis vibration and different hand actions. The experiments were performed at the US National Institute for Occupational Safety and Health (NIOSH) laboratory using a specially designed instrumented handle, which permitted for measurement of biodynamic responses distributed at the fingers and the palm of the hand. The experimental data under selected hand actions were acquired from NIOSH and subsequently analyzed for constructing the model presented in this thesis. In order to obtain a comprehensive understanding of the experimental data and the test conditions, the methodology employed and the experimental data are briefly described in this section.

2.4.1 Experimental Setup

The experiments were performed using a specially designed instrumented handle mounted on an electro-dynamic vibration exciter along the z_h-axis. Figure 2.2 illustrates the design schematic of the instrumented handle used in the experiment (Dong et al, 2004a; 2005a). The handle structure comprised an aluminum handle base and a magnesium measuring cap. Two piezoelectric single-axis force sensors (Kistler 9212) were sandwiched between the two parts along the centerline of the handle to measure the static and dynamic hand-handle coupling forces. An accelerometer (PCB 356A12) was fixed on the measuring cap at the center point of the handle with an adhesive. The handle was installed on a vibration exciter fixture. During measurements, each subject was advised to place fingers on the measuring cap when assessing the response at the fingers in a power grip situation, as shown in Figure 2.3. To assess the response at the palm, the

handle shown in the figure is rotated 180° within the fixture about the longitudinal axis of the handle so that the palm is positioned on the measuring cap.

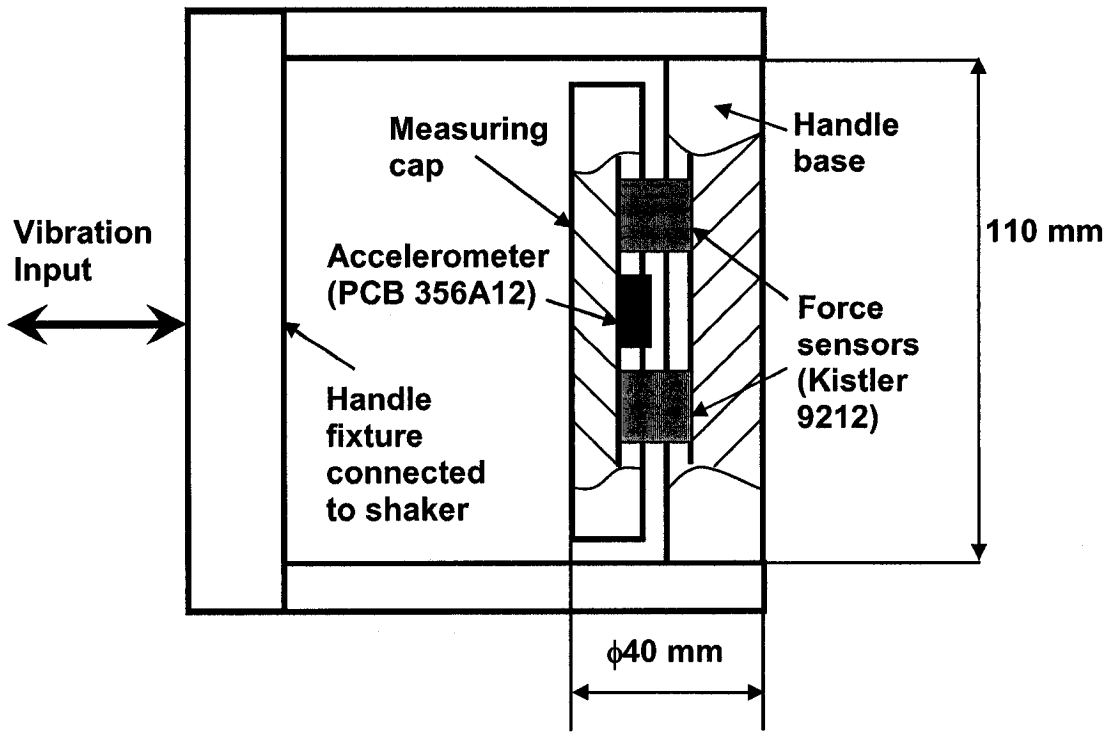

Figure 2.2: A sketch of the instrumented handle used for measurements of the finger and palm responses. With the measuring cap orientation in this figure, the finger response can be measured.

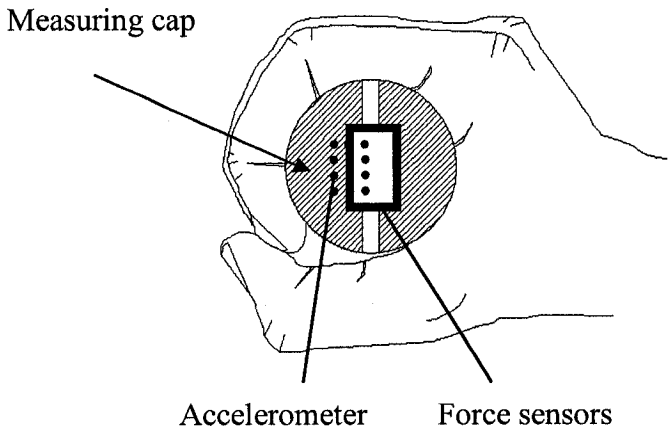

Figure 2.3: Orientation of the measuring cap for measuring the finger response

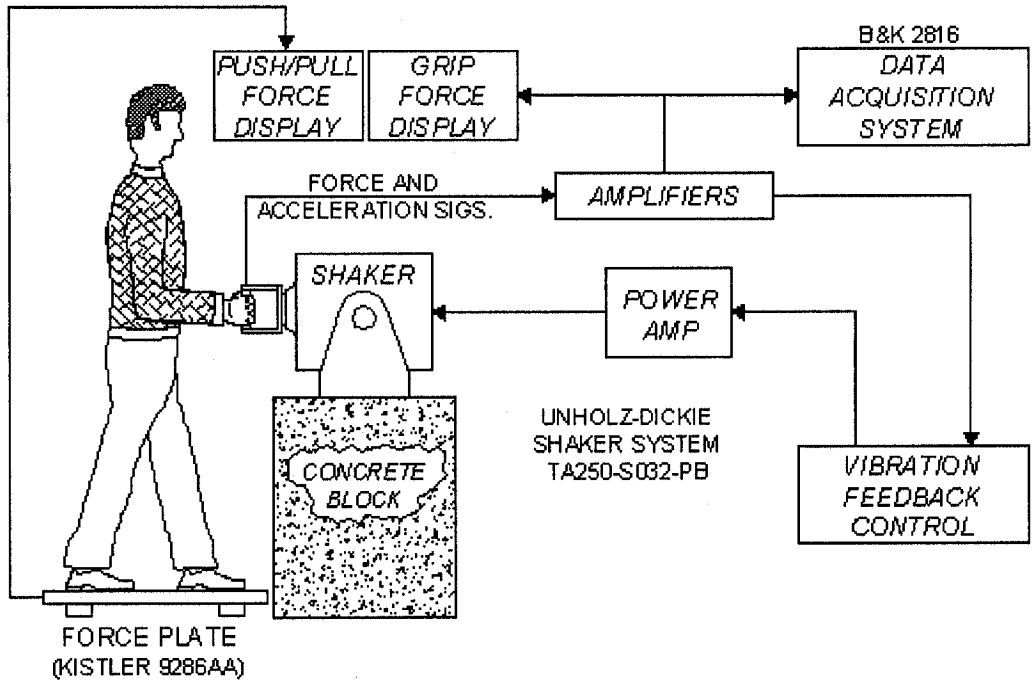

Figure 2.4: Subject posture and measurement set-up that includes a closed-loop controlled vibration exciter, vibration measurement system, a grip force measurement and display system, and a feed force measurement and display system.

The experimental set-up used in this study is illustrated in Figure 2.4. The vibration was delivered to the hand along the forearm axis or in the z_h-direction (ISO 8727, 1998; ISO 5349-1, 2001). As conventionally defined by ISO-10819 (1996), the grip force measured using the handle shown in Figure 2.2 is actually the quasi-static component of the force measured with two force sensors depicted in the figure. The measured force signal was thus branched to a low-pass filter with a 4 Hz cut-off frequency to derive the grip force. A custom program was developed using LabVIEW™ software (National Instruments, version 5.0) to display the grip force. The grip force was displayed on a computer monitor as a strip chart, which served as feedback for the test

subject and allowed him to control the force to a derived level. The pull or push force acting on the handle was measured using a force plate (Kistler 9286A) and displayed as a strip chart on a separate computer monitor. The force plate measurements were verified using the instrumented handle when a pull-only or push-only action was required.

2.4.2 Test Conditions and Methodology

Ten male volunteers from a local university participated in the measurement. The right hand was used for the test. The hand arm dimensions of each participant were measured and the individual hand-arm anthropometry is summarized in Table 2.1. The finger and hand volumes were measured using a water immersion method (Chaffin et al., 1990). To determine the volume of the fingers with the hand positioned in a power grip, the subject gripped an aluminum pipe with diameter identical to that of the handle (40 mm) as using the same grip posture as that used in the biodynamic measurement. In the measurement, the fingers were submerged in water up to the handle centerline, as shown in Figure 2.5. The finger volume was obtained by subtracting half of the pipe volume from the total volume.

The subjects wore normal office clothes without jackets during the experiment. After going through the test explanation and consent-form-signing procedures, a short section of first-aid bandage was placed on the back of the index finger of the right hand of a subject. A line was marked on the bandage in line with the crease at the base of the subject's third proximal phalange, which served as a reference for aligning the hand with the handle in the subsequent tests. Each subject was advised to stand on the force plate adjusted to an appropriate height, and to grip the vibrating handle with the alignment mark in line with the handle-splitting line, which assured that the hand gripped the handle

at the same location during each exposure. Once the grip posture and position were set, an investigator advised the subject to perform a specific hand-handle coupling action.

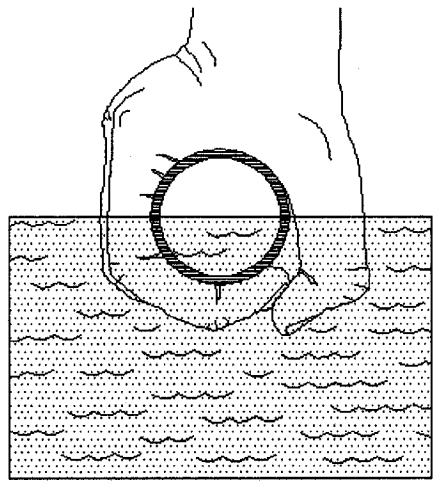

Figure 2.5: Hand posture used for measurement of finger grip volume. The subject grasps a section of a 40 mm and the pipe. Hand is immersed to a level marked on the index finger that is in-line with the crease at the base of the subject's third proximal phalange.

Table 2.1: Subject anthropometry (hand length = tip of middle finger to crease at wrist; hand breadth = the width measured at metacarpal of the hand; hand circumference = the circumference measured at metacarpal of the hand; hand volume = water displaced by hand submerged to crease at wrist; finger grip volume = water displaced by fingers submerged to centerline of a 40mm handle(Figure 2.5); and hand & forearm volume = water displaced by hand-forearm submerged to crease at elbow) (Dong et al., 2004a).

Subject	Height (cm)	Weight (kg)	Hand Length (mm)	Hand Breadth (mm)	Hand Volume (ml)	Finger Grip Volume (ml)	Hand/ Fore-arm Volume (ml)
1	162.6	61.2	180	80	295	95	1075
2	185.4	66.2	197	93	350	110	1290
3	175.3	69.5	185	88	360	115	1370
4	175.3	77.1	190	85	375	125	1510
5	177.8	83	197	93	406	132	1648
6	185.4	90.7	192	97	440	147	1723
7	185.4	96.6	200	101	445	119	2210
8	175.3	100.2	184	103	445	145	1830
9	175.3	132.5	207	101	550	183	2352
10	198.1	152.4	205	107	550	195	2550
Mean	179.6	92.9	194	95	422	137	1755.8
SD	9.5	29.4	9	9	83	32	

Table 2.2 shows coupling actions and hand forces used in measurement of finger responses. Table 2.3 shows the coupling actions and hand forces employed for measurement of palm responses. In four treatments (50 N grip, 15 N grip + 35 N push, 30 N grip + 45 N push, and 50 N grip + 50 N push), the responses were measured at both the fingers and the palm. For the purpose of this study, both responses are required to form the hand total response. Hence, only the data acquired under these hand actions were used for model development.

Table 2.2: Coupling actions and hand forces used for finger response measurements

Coupling Action	Total Effective Forces Acting at the Palm (N)		
Grip-only	15 N	30 N	50 N
Combined grip and push	50 N (15 N grip + 35 N push)	75 N (30 N grip + 45 N push)	100 N (50 N grip + 50 N push)

Table 2.3: Coupling actions and hand forces used for palm response measurements

Coupling Action	Total Effective Forces Acting at the Palm (N)		
Grip-only	15 N	30 N	50 N
Combined grip and push	50 N (15 N grip + 35 N push)	75 N (30 N grip + 45 N push)	100 N (50 N grip + 50 N push)

Measurements were performed under a broad band random vibration in the 10-1000 Hz frequency range under a constant acceleration spectral density. The overall rms acceleration due to vibration was computed as 10 m/s^2. When the subject attained the desired coupling action the acceleration due to excitation and resulting biodynamic force were acquired for a period of 30 seconds in a multi-channel signal analyzer. The subject was then advised to relax for 3 minutes before performing the next trial. Two trials were performed for each treatment. The sequence of the treatments was independently randomized among the subject. Also on a random basis, one-half of the subjects

performed all finger response measurements first, and others conducted the palm response measurements first. After completing the first series of experiments (finger or palm response), the instrumented handle was rotated 180° conduct the second series of measurement involving either fingers or palm responses. Prior to the second series of experiments, each subject was re-instructed to maintain the desired hand actions, alignment and hand-arm posture.

2.4.3 Data Analysis

The measured force and acceleration data were analyzed to derive transfer function in terms of real and imaginary components of mechanical impedance in one-third octave bands with center frequency ranging from 10 Hz to 1,000 Hz. The impedance responses distributed at the fingers and the palm were subsequently derived in terms of magnitude and phase for the hand actions considered. The total responses of the entire hand-arm system were obtained by summing the complex fingers and palm impedances as in EQ (2.8). The data acquired over two trials were averaged to determine mean responses corresponding to each hand action. The mean data sets obtained for ten subjects were further analyzed to determine the mean responses together with standard deviation of the mean.

2.5 Determinations of Model Parameters

The parameters of mechanical-equivalent models of the hand-arm system are invariably identified through curve-fitting of the experimental data (Rakheja et al., 2002). This approach was also adopted in this thesis, using the four sets of data attained for different hand actions.

In the parameter identification process, an initial value of the parameter vector was assumed. The initial values for the fingers mass, palm-wrist-arm mass, upper arm-shoulder mass and their contact stiffness were estimated based on the resonance frequencies observed in the experimental data. Each of the parameters was varied sequentially so that the rms difference (Δ) between the predicted DPBR and the experimental data corresponding to each hand action. The mean data were considered as the target datasets for identification of model parameters reaches a minimum value. Each parameter, however, was constrained to assume a positive value. Both the real and imaginary components of the DPBR were considered in the error minimization in order to achieve good agreements in magnitude and the phase. A error minimization function was formulated as:

$$E(\chi) = \mathrm{Re}[\Delta Z_F] + \mathrm{Im}ag[\Delta Z_F] + \mathrm{Re}[\Delta Z_P] + \mathrm{Im}ag[\Delta Z_P] \tag{2.9}$$

$$\text{Subject to:} \quad 0 < \sum_{i=0}^{4} M_i < 10kg.; \sum_{i=0}^{4} k_i > 0.; and \sum_{i=0}^{4} c_i > 0$$

where $E(\chi)$ is the error function of DPBR, and 'Re' and 'Imag' designate the real and imaginary components, respectively. ΔZ_F and ΔZ_P are the rms deviations between the predicted and measured DPBR distributed at the fingers and the palm, respectively, corresponding to excitation frequency ω, which are calculated from

$$\Delta Z_F = \sqrt{\frac{1}{n}\sum_{i=1}^{n}[Z_F(j\omega_i) - Z_E(j\omega_i)]_F^2}$$

$$\Delta Z_P = \sqrt{\frac{1}{n}\sum_{i=1}^{n}[Z_P(j\omega_i) - Z_E(j\omega_i)]_P^2} \tag{2.10}$$

where n the number of one-third octave band frequencies considered for error analysis 10 to 1,000 Hz frequency range. $Z_E(j\omega_i)$ is the target (measured) impedance value corresponding to a selected hand action and center frequency ω_i of the i th frequency band. Subscripts 'P' and 'F' refer to palm and finger functions, respectively.

The above equations are applied for both the real and imaginary components to compute the error function in Eq. (2.9), where χ is the parameter vector, which is given by:

$$\chi = [M_0, M_1, M_2, M_3, M_4, k_0, k_1, k_2, k_3, k_4, c_0, c_1, c_2, c_3, c_4]$$

Each set of the experimental data used in error minimizations included 84 independent points corresponding to a total of 21 frequency bands.

The parameter identification process was initiated by assuming an initial value of the parameter vector. Each of the parameters was gradually varied sequentially subject to limit constraints, until the error function $E(\chi)$ approached a minimum value, while all other parameters were held as their last updated values. An iteration cycle is completed when all the parameter values are updated. The iteration cycles were repeated until the difference between the error values of the last two consecutive cycles approached less than 0.01 N·s/m. This error value was considered as very small considering that peak impedance magnitude approach as high as 300 N.s/m. The minimization process was repeated assuming alternate values of initial parameter vector, which was attached by randomly varying each parameter within a ±20% range. The process was performed by considering more than five different initial vectors. The resulting model parameters

corresponding to these searches converged to very similar values. However, only slight in parameters of elements close to the support (M_0, k_0, k_1, c_0, c_1) were observed.

2.6 Model validation

The identified model parameters were used to examine validity of the models corresponding to different hand actions by comparing the model responses with the target measured data. Figure 2.6 illustrate comparisons of target data and the predicted responses distributed at the fingers and the palm of hand acquired under the 50 N grip-only actions. The response of the entire hand-arm system is also presented in this figure. The mechanical impedance is expressed in terms of its magnitude and phase. Figures 2.7 to 2.9, in a similar manner, show comparisons of target data and predicted responses under three combined grip and push actions (15 N grip and 35 N push, 30 N grip and 45 N push, and 50 N grip and 50 N push). Figures show impedance magnitude and phase together with the correlation coefficient (r) values.

The model responses generally show very good agreements with the experimental data in both the magnitude and phase in respective of the component and hand action. Some deviations, however, can be observed in the impedance phase responses of the fingers at low frequencies (< 25 Hz) under hand actions involving both grip and push forces. The proposed model structure can thus be considered valid for predicting biodynamic responses distributed at the fingers and the palm of the hand and that of the total hand response.

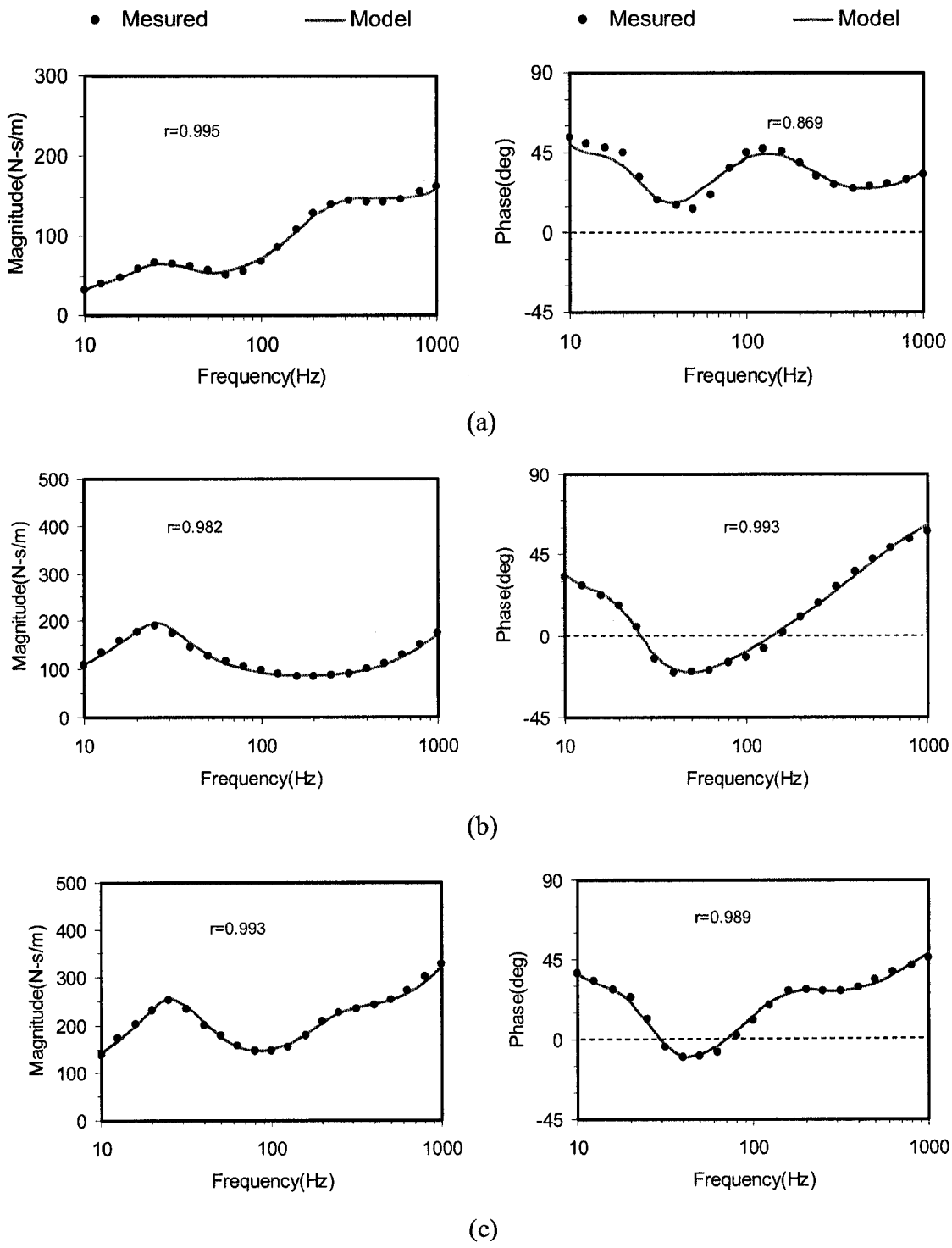

Figure 2.6: Comparisons of model responses and measured values of mechanical impedance components distributed at the fingers and the palm of the hand together with that of the total hand-arm system under a 50 N grip-only action: (a) Fingers; (b) Palm; and (c) Hand-arm.

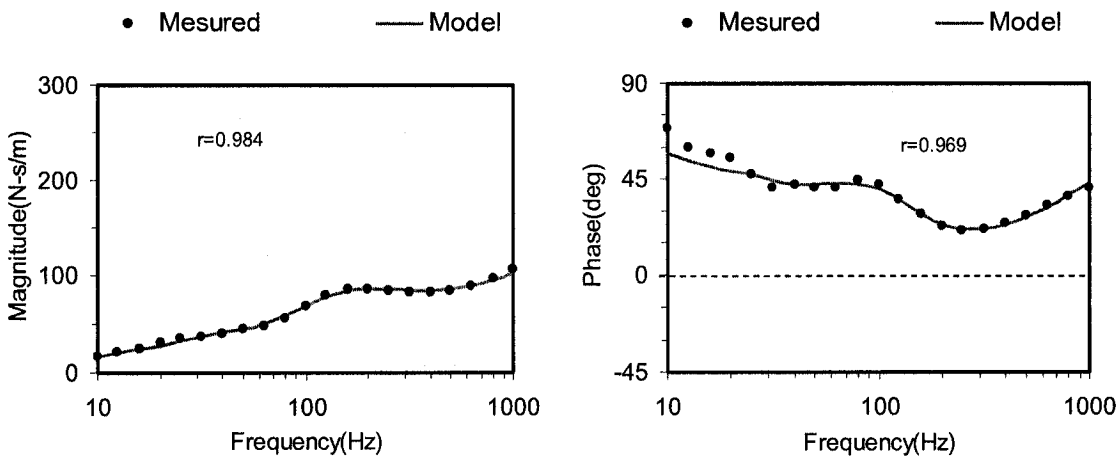

(a)

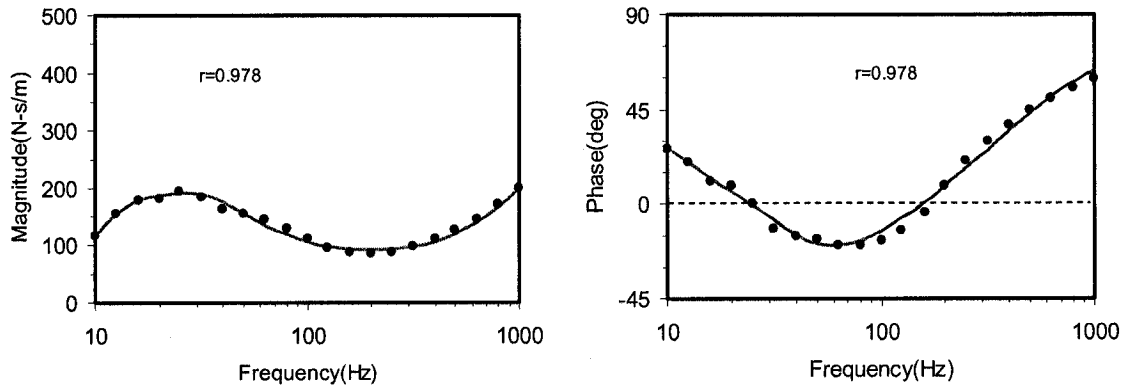

(b)

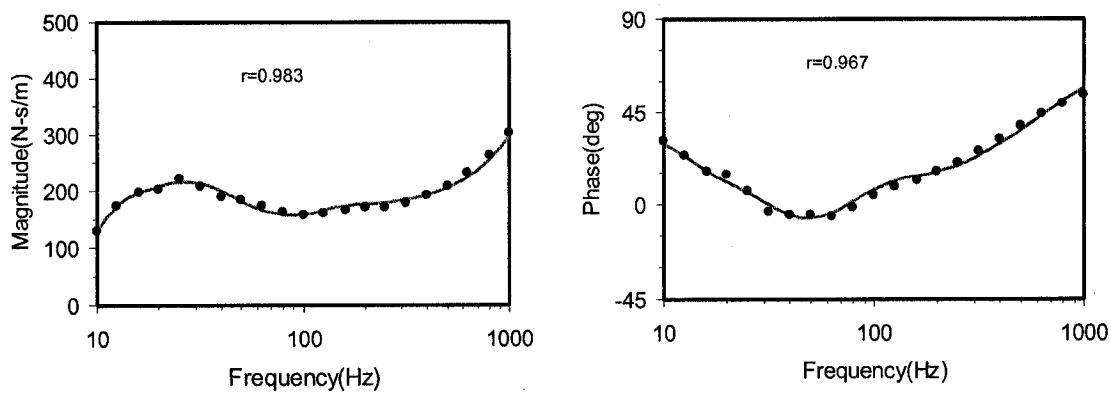

(c)

Figure 2.7: Comparisons of model responses and measured values of mechanical impedance components distributed at the fingers and the palm of the hand together with that of the total hand-arm system under 15 N grip and 35 N push force: (a) Fingers; (b) Palm; and (c) Hand-arm.

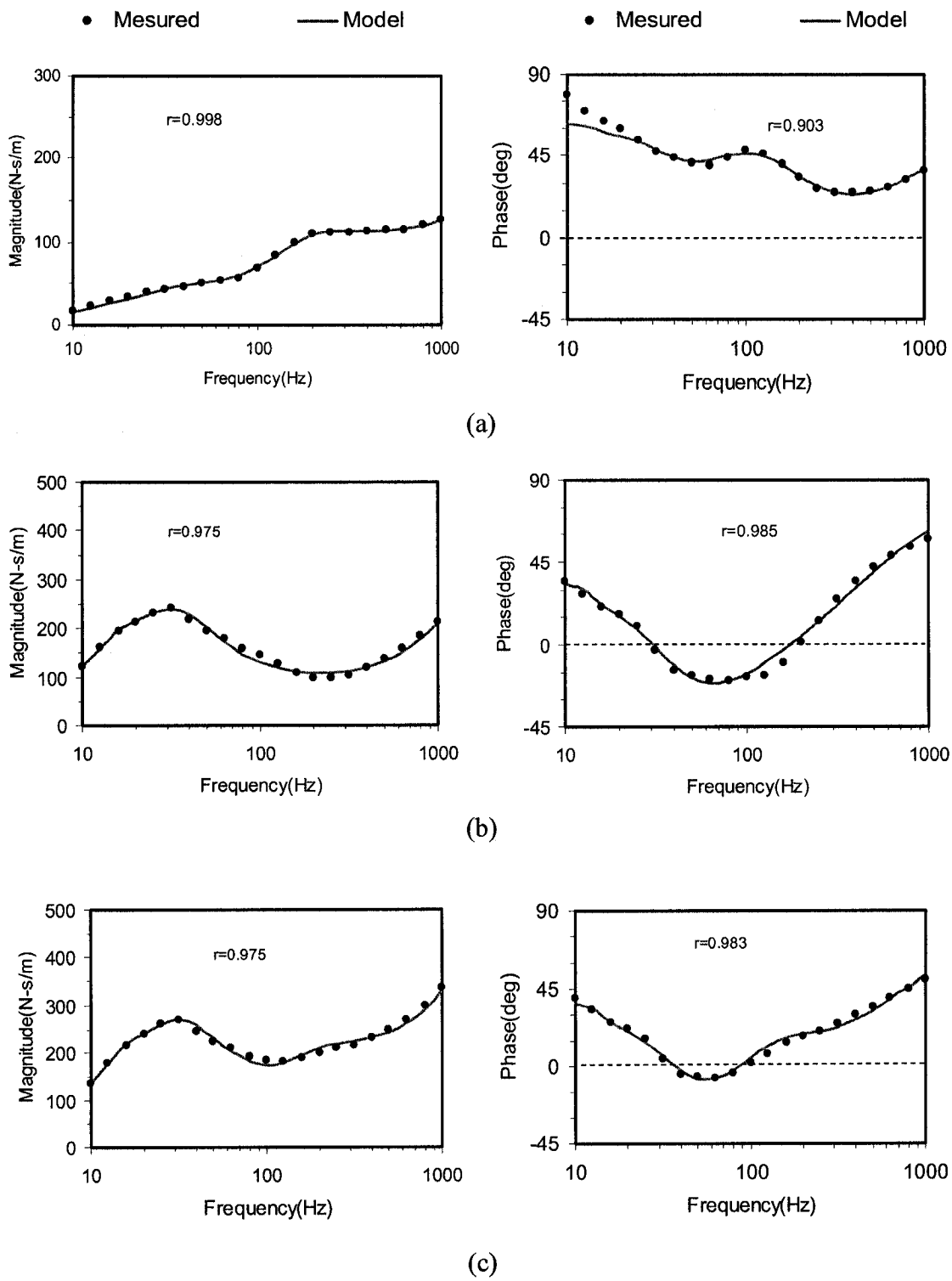

Figure 2.8: Comparisons of model responses and measured values of mechanical impedance components distributed at the fingers and the palm of the hand together with that of the total hand-arm system under 30 N grip and 45 N push force: (a) Fingers; (b) Palm; and (c) Hand-arm.

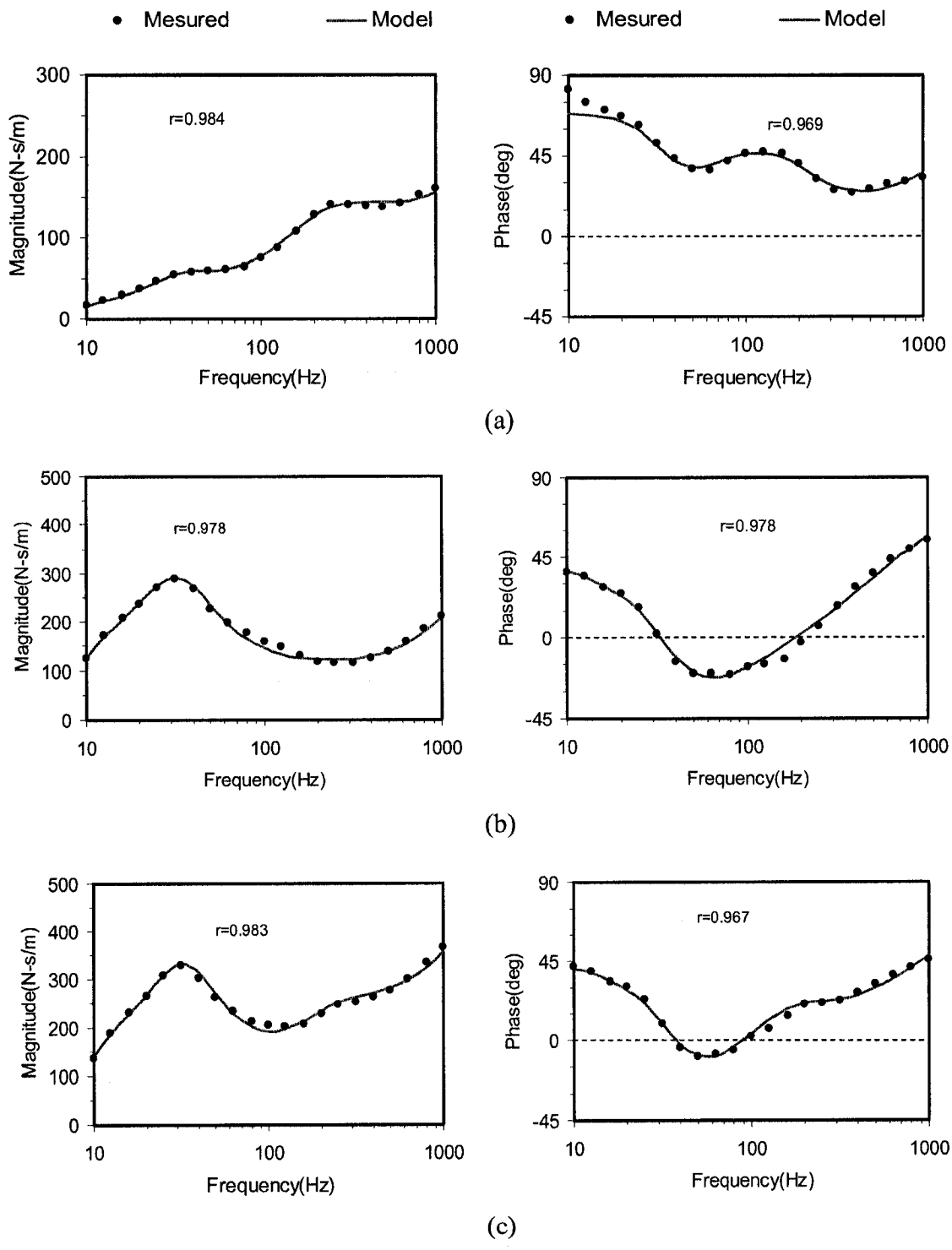

Figure 2.9: Comparisons of model responses and measured values of mechanical impedance components distributed at the fingers and the palm of the hand together with that of the total hand-arm system under 50 N grip and 50 N push force: (a) Fingers; (b) Palm; and (c) Hand-arm.

The measured data sets clearly revealed strong influences of the hand forces on DPBR, which have also been demonstrated in a few studies. Both the peak magnitudes and corresponding frequencies tend to vary with variations in hand forces, suggesting nonlinear behavior of the hand-arm system. The validity of the proposed linear model structure for varying hand forces is thus further evaluated through examination of model parameters. Table 2.4 lists identified model parameters under the four hand actions considered in this study. The results show that effective mass of finger skin (M_4) varies in the 11.2 to 13.2 g for the hand forces considered. It remains almost identical for cases involving 50 N grip-only 13.1 g and combined 50 N grip and 50 N push force (13.2 g). Lowering the grip force yields slightly lower mass due to fingers skin. The finger effective mass (M_2) under the 50 N grip force (82.8 g) is also almost identical that under 50 N grip and 50 N push action (82.5 g). Under the other two finger force levels (15 N and 30 N), this mass value is only slightly different. These results suggest consistent fingers structure masses under different hand actions. Under the three combined hand actions, the palm skin effective mass (M_3) are also quite similar (28.7 – 30.5 g), while it tends to be lower under the grip action alone. The value of effective mass of palm-wrist-forearm structure (M_1) is affected by both the hand action and the palm effective force. Increasing the palm push force increases the M_1 value, suggesting stronger coupling of the hand with the handle. The M_0 values also vary in a fairly small range (5.8-6.5 kg) for the hand action considered for each hand action, palm-side skin mass M_3 is about two times of finger-side skin mass M_4, and M_1 is more than 10 times of M_2.

Table 2. 4: Model parameters identified under four different hand actions

Parameter	Hand actions				
	Grip Force (N)	50	15	30	50
	Push Force (N)	---	35	45	50
M_0 (Kg)		5.8543	6.0987	6.5050	5.8626
M_1 (Kg)		1.3242	0.8495	0.9774	1.2482
M_2 (Kg)		0.0828	0.0841	0.0800	0.0825
M_3 (Kg)		0.0247	0.0292	0.0305	0.0287
M_4 (Kg)		0.0131	0.0110	0.0115	0.0132
k_0 (N/m)		13740.3	17272.1	18826.0	16903.3
k_1 (N/m)		2462.0	2416.1	1017.6	1697.9
k_2 (N/m)		6788.1	3445.4	4026.1	4035.4
k_3 (N/m)		26191.7	38684.4	48930.4	52492.0
k_4 (N/m)		157119.0	56152.8	96313.9	143915.8
c_0 (N s/m)		107.07	152.87	163.76	169.70
c_1 (N s/m)		97.80	159.20	158.94	140.53
c_2 (N s/m)		39.03	25.26	28.97	35.47
c_3 (N s/m)		81.79	86.53	101.31	114.83
c_4 (N s/m)		127.98	74.73	99.87	124.59
$^*f_0$ (Hz)		8.3	9.0	8.8	9.0
$^*f_1$ (Hz)		25.9	36.4	37.3	34.3
$^*f_2$ (Hz)		223.9	134.0	178.2	213.1
ξ_0		0.3528	0.4730	0.4574	0.4813
ξ_1		0.4920	0.6844	0.6236	0.5330
ξ_2		0.7175	0.7079	0.7198	0.7249

2.7 Analysis of identified stiffness and damping parameters

Although the variations in hand forces yield only slightly changes in mass parameters, the visco-elestic properties of the model vary considerably, as observed from Table 2.4. The variations in these parameters could be related to applied force, which influence the impedance responses. Figure 2.10 illustrates variations in finger contact stiffness (k_4) and damping (c_4) constants obtained under three different finger forces considered in this study (15, 30 and 50 N). Results suggest that increasing the finger force increases the finger stiffness and damping constants. An eigenvalue problem is formulated and solved to compute the undamped natural frequencies (f_0, f_1 and f_2) and damping ratios (ξ_0, ξ_1, and ξ_2) of the model, which are also listed in Table 2.4. The natural frequencies of the uncoupled finger substructure are further estimated from the finger mass (M_2) and stiffness (k_4) corresponding to the hand actions considered. This resulted in estimates of finger frequencies of 219 Hz, 130 Hz, 175 Hz and 210 Hz under 50 N grip, 15 N grip +35 N push, 30 N grip +50 N push and 50 N grip +50 N push conditions, respectively. These estimated frequencies are only marginally less than the highest frequencies (f_2) derived from eigen analysis, as evident in Table 2.4. This suggests that frequency f_2 is the finger resonance frequency. An increase in the finger force also yields an increase in the finger resonance frequency, which is shown in Figure 2.11. The parameters further showed only negligible effect of finger force on the associated damping ratio (ξ_2), which is most likely attributed to comparable increases in c_4 and f_2.

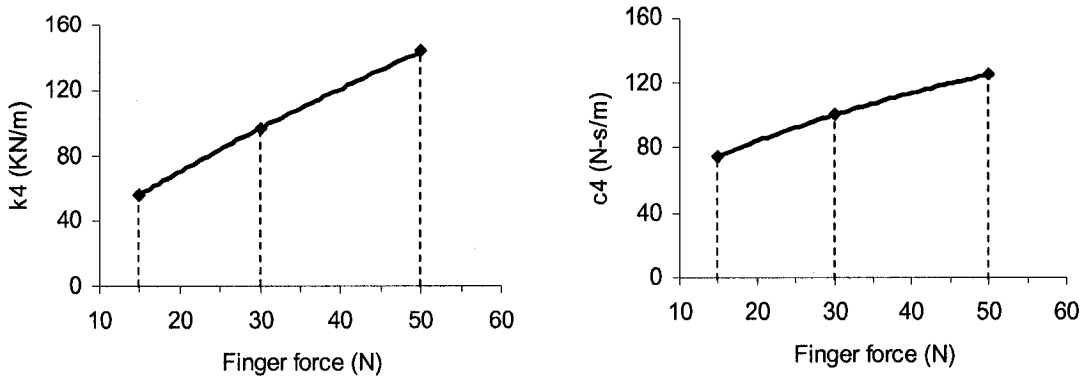

Figure 2.10: Influence of finger force on finger contact stiffness (k_4) and damping (c_4) constants

The Influence of variations in palm force on the palm contact stiffness (k_3) and damping (c_3) constants can also be examined by considering the parameters corresponding to different push or palm force conditions. Figure 2.12 illustrates variations in k_3 and c_3 due to different palm forces considered. It is evident that an increase in palm force causes an increase in the palm contact stiffness and damping constants. The influence of palm force on palm resonance frequency (f_1) and damping ratio (ξ_1), however, did not produce a clear pattern. The primary resonance frequencies of the entire hand-arm system can be roughly estimated from $\sqrt{k_3/M_1}$ (grip-only: 22 Hz; 15 N grip+35 N push: 34 Hz; 30 N grip+45 N push: 36 Hz; and 50 N grip+50 N push: 33 Hz), which are only marginally lower less than those (grip-only: 26 Hz; 15 N grip+35 N push: 36 Hz; 30 N grip+45 N push: 37 Hz; and 50 N grip+50 N push: 34 Hz) derived from the eigenvalue analyses of the coupled hand-arm model. This reveals that the primary frequency of the hand-arm system mostly depends on the palm contact stiffness and the effective mass of the palm-wrist-arm system. The lowest resonance frequency of the entire hand-arm system was further observed to primarily depend on the upper arm-

shoulder effective mass (M_0) and the body-arm coupling stiffness (k_0). It does not vary greatly with the hand action and the applied hand forces. The damping ratios associated with higher modes generally tend to be higher. The presence of push force yields higher modal damping, while an increase in grip force tends to reduce modal damping.

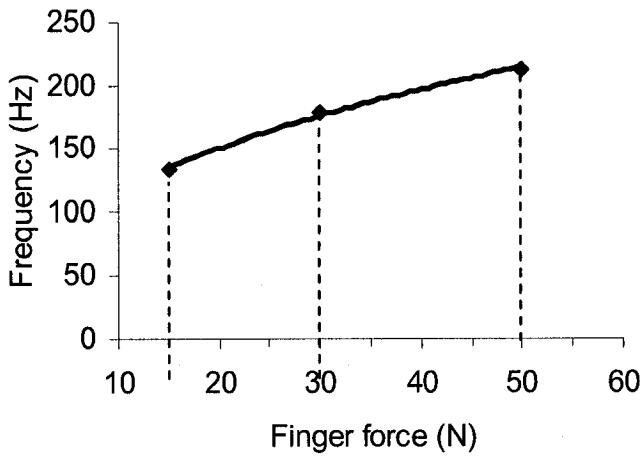

Figure 2.11: Influence of finger force on finger resonant frequency

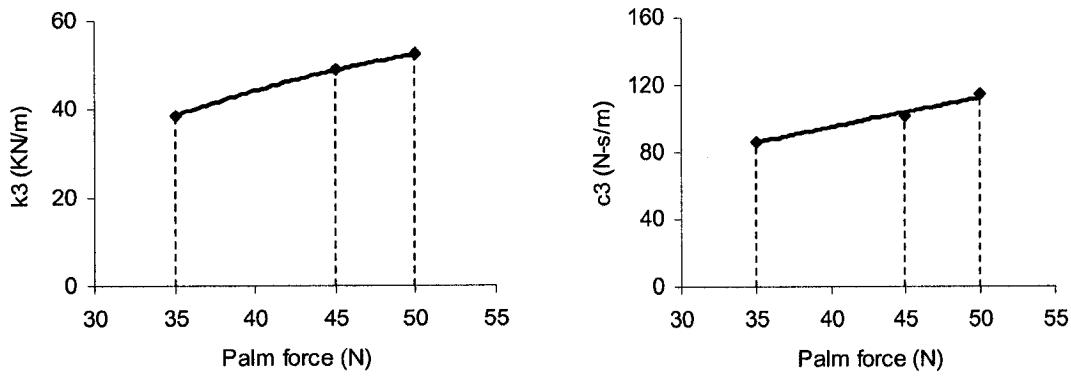

Figure 2.12: Influence of the palm force on palm contact stiffness (k_3) and damping (c_3) constants

An increase in the palm force yields only slightly higher effective mass due to the palm skin (M_3) in contact with the handle. This feature may facilitate evaluation of effect

of applied force on the biodynamic responses. The identified model parameters further indicate that effective mass due to the palm skin is larger than that of the fingers' skin in contact with the handle, which can also be attributed to considerably higher contact area on the palm side (Aldien et al., 2005; Welcome et al, 2004).

2.8 Parametric Sensitivity Analysis

A parametric study was further performed to examine the sensitivity of predicted response to variations in each model parameter. The model parameters attained for combined 30 N grip and 45 N push action were considered as the baseline parameters (Table 2.4). Each parameter was varied from 80% to 120% of its base value, while the other parameters were held as their base values. The rms error values of the corresponding responses distributed at the fingers and the palm were calculated with respect to impedance values of the base model together with r^2 values as measures of sensitivity of the parameters. The results are also used to further demonstrate validity of the identified parameters. The rms deviation in impedance response and change in r^2 value caused by a parameter change are computed from:

$$S_Z = \frac{\overline{Z_m}(q^* + \Delta q) - \overline{Z_m}(q^*)}{\overline{Z_m}(q^*)} \times 100\%$$

$$S_r = \frac{r^2(q^* + \Delta q) - r^2(q^*)}{r^2(q^*)} \times 100\% \qquad (2.11)$$

Where S_Z defines the percent change in overall rms value of impedance response measured either on the fingers or palm-side, and S_r defines the percent change in correlation coefficient caused by a variation in a model parameter Δq about the baseline value q^*. $\overline{Z_m}(q^*)$ is the overall rms impedance response of the baseline model and

$\overline{Z_m}(q^* + \Delta q)$ is the overall rms value of impedance response derived upon considering perturbation Δq of a given parameter. The overall impedance value is computed from:

$$\overline{Z_m} = \sqrt{\frac{1}{n}\sum_{i=1}^{n} | Z(j\omega_i) |^2} \tag{2.12}$$

In Eq.(2.11) $r^2(q^*)$ and $r^2(q^* + \Delta q)$, in a similar manner, are the correlation coefficients of baseline model response and perturbed $(q^* + \Delta q)$ model parameters, evaluated with respect to the target (measured) data.

The results generally showed that parameters M_2, M_4, k_4 and c_4 are strongly associated with responses of the fingers. Figure 2.13 and Table 2.5 show the effects of variations in these parameters on percent deviations of impedance and r^2 values of finger responses. Results suggest that variations in fingers mass (M_2) and damping coefficient (c_4) produce most significant effects on the deviations. A more detailed examination of impedance responses of the model revealed that variations in damping coefficient c_4 mostly affect the response in the high frequency range (200 to 1,000 Hz), as shown in Table 2.6. The response deviations due to variations in M_2 mostly occurred in the middle frequency range (63 to 400 Hz). The model responses revealed relatively lower sensitivity to variations in finger skin mass M_4, which mostly influenced the fingers response in the high frequency range (250-1,000 Hz). The effects of k_2 and c_2 on the finger response are relatively small as shown in Figure 2.10; the effects are mostly seen in the finger response from 40 to 315 Hz and from 80 to 200 Hz, respectively.

Table 2.5: Effects of variations in model parameters (M_2, M_4, k_2, k_4, c_2, c_4) on deviations in (a) r^2 -values; and (b) rms values of finger impedance

Percent change	% Percent change in r-value					
	M_2	M_4	k_2	k_4	c_2	c_4
80%	-1.23102	-0.08905	-0.09289	-0.28495	-0.27177	-2.35521
90%	-0.30129	-0.02524	-0.04102	-0.07015	-0.06722	-0.44883
100%	0	0	0	0	0	0
110%	-0.2942	-0.01853	0.028304	-0.0689	-0.08399	-0.35928
120%	-1.14741	-0.08376	0.042024	-0.2655	-0.33314	-1.13853

Percent change	% Percent change in impedance rms value					
	M_2	M_4	k_2	k_4	c_2	c_4
80%	372.0145	87.99084	39.48078	152.1394	100.9872	480.5453
90%	149.022	30.82295	18.81426	54.50303	32.18249	195.1284
100%	0	0	0	0	0	0
110%	137.5971	27.96862	-14.9059	53.14868	31.52225	195.1226
120%	339.1133	96.23817	-22.7847	155.7034	96.68864	448.8486

Table 2.6: Important frequency ranges of parametric sensitivity

Parameters	Frequency range (Hz)	
	Lower limit	Upper limit
M_0	10	25
M_1	10	200
M_2	63	400
M_3	80	1000
M_4	250	1000
k_0	40	315
k_1	25	50
k_2	40	315
k_3	12.5	80
k_4	100	630
c_0	10	25
c_1	10	100
c_2	80	200
c_3	80	1000
c_4	200	1000

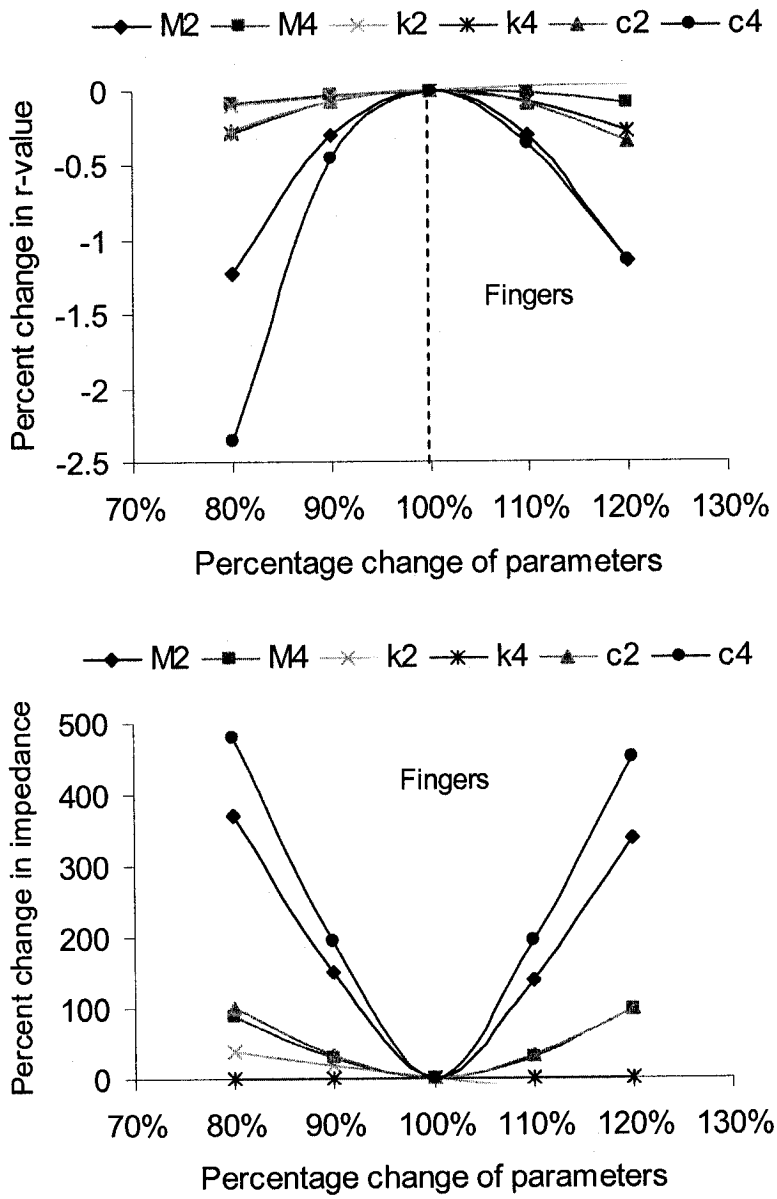

Figure 2.13: Effects of variations in model parameters (M_2, M_4, k_2, k_4, c_2, c_4) in terms of (a) Percent change in r^2 -values; and (b) Percent change in impedance error rms values

Figure 2.14 and Table 2.7 show the effects of the variations in selected model parameters (M_1, M_3, k_3, c_3) on the palm side response. These parameters are directly associated with the palm-hand-wrist-forearm structures. Clearly, the variations of the palm contact stiffness (k_3) and damping (c_3) constants have the greatest effect on the palm response. However, these two parameters show influences in different frequency

ranges variations in k_3 tend to affect the palm-side response in the 12.5 to 80 Hz and range, while those in c_3 were observed in the 80 to 1,000 Hz range, as shown in Table 2.7. The variations in masses M_1 and M_3 also affect the response considerably in the 10 to 200 Hz and 80 to 1,000 Hz, respectively.

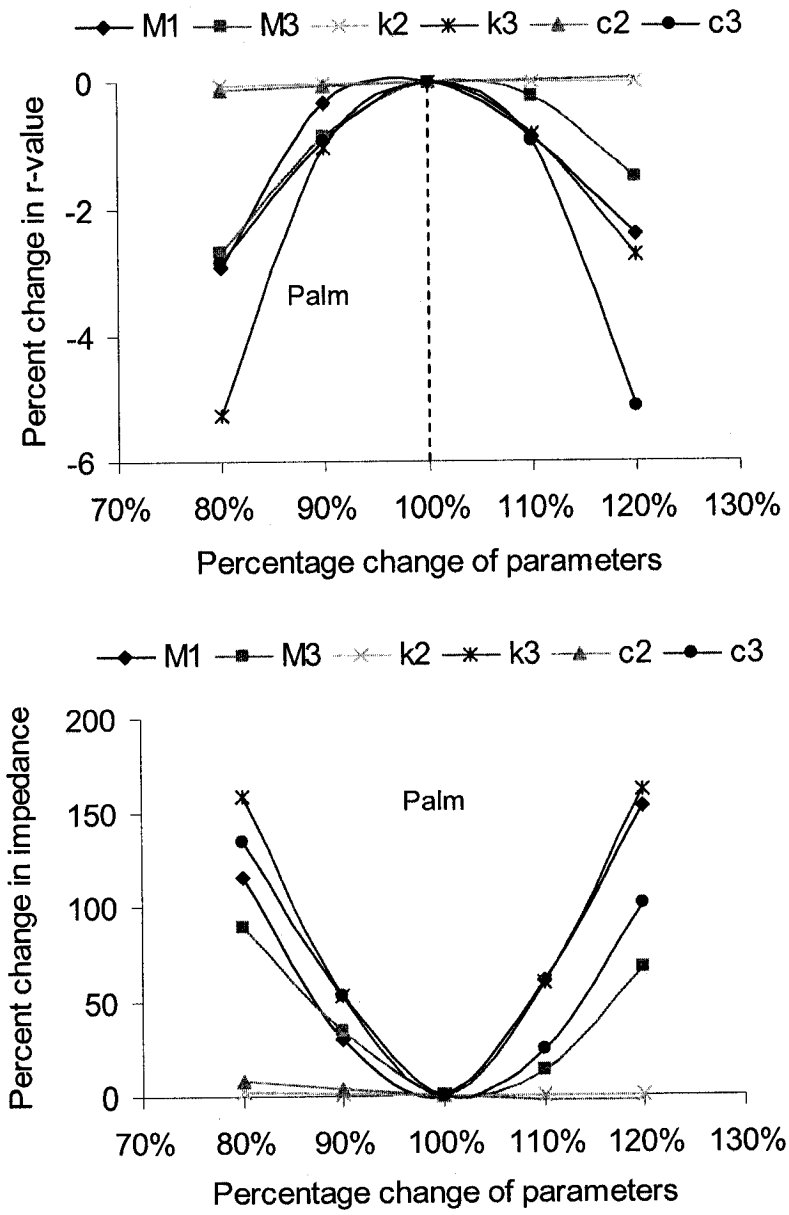

Figure 2.14: the effect of the variation of the major parameters (M_1, M_3, k_2, k_3, c_2, c_3) on the percentage change of *r*-values and rms of the palm: (a) Percentage change of *r*-value; (b) Percentage change of error rms value.

Table 2.7: Effects of variations in model parameters (M_1, M_3, k_2, k_3, c_2, c_3) on deviations in (a) r^2-values; and (b) rms values of palm impedance

Percent change	% Percent change in r-value					
	M_1	M_3	k_2	k_3	c_2	c_3
80%	-2.90341	-2.67246	-0.0603	-0.28495	-0.12541	-2.86672
90%	-0.32214	-0.85445	-0.02427	-0.07015	-0.05467	-0.92661
100%	0	0	0	0	0	0
110%	-0.87665	-0.21636	0.012875	-0.0689	0.038157	-0.92107
120%	-2.38507	-1.49583	0.014735	-0.2655	0.059352	-5.12707

Percent change r	% Percent change in impedance rms value					
	M_1	M_3	k_2	k_3	c_2	c_3
80%	115.8816	89.33544	2.57855	158.2443	8.153715	134.1327
90%	30.0063	34.58901	1.031058	52.34899	3.398763	52.61737
100%	0	0	0	0	0	0
110%	60.46628	13.45022	-0.52088	59.87064	-1.98863	24.57386
120%	152.9148	66.84143	-0.54501	161.6671	-2.564	100.6379

The influences of variations in the carpal and meta-carpal parameters (k_2 and c_2) on the palm response are considerably less than those observed on the finger response. The stiffness k_2 and damping c_2 constants mostly influence the finger response from 40 to 315 Hz and from 80 to 200 Hz, respectively. The influences of variations in the remaining model parameters on the palm response were observed to be relatively small with the exception of c_1, as shown Figure 2.15, mass M_0 mostly influence the palm response at frequencies less than 25 Hz while the corresponding stiffness k_0 affected the palm response mostly in the 40 to 315 Hz range. The results further showed that variations in stiffness k_1 affect the palm response mainly in the 80 to 200 Hz range, while the damping constant c_1 affects the response at frequencies less than 100 Hz.

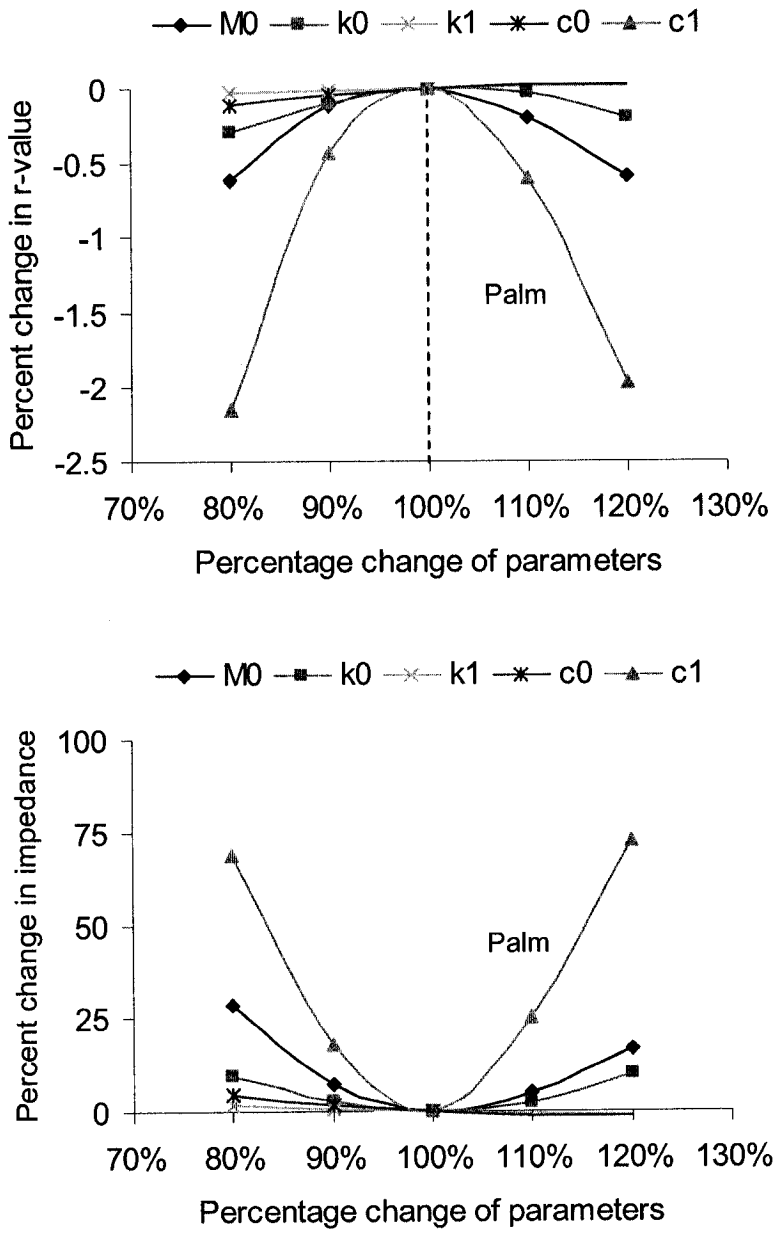

Figure 2.15: the effect of the variation of the major parameters (M_0, k_0, k_1, c_0, c_1) on the percentage change of *r*-values and rms of the palm: (a) Percentage change of *r*-value; (b) Percentage change of error rms value

2.9 Discussions

The proposed model structure provides vital information related to distribution of biodynamic forces and responses in the fingers and the palm-wrist-hand structure, which have not been attempted thus far. Moreover, the proposed model is structured to mimic

the biomechanical structure of the hand, which unlike the reported mechanical-equivalent models permits for interpretations of the responses in light of the biological system behaviors. Moreover, the model responses show very good agreements with the measured data for the fingers, palm-wrist-hand and the total hand-arm structures, in terms of both the impedance magnitude and phase. Only a few of the reported DPBR models exhibit such good agreements between the model predictions and the experimental data for the total hand-arm system (Rakheja et al., 2002), while none is capable of predicting the distributed DPBR. The results thus suggest that the proposed model reasonably reflects the fundamental dynamic features of the system. The parameters of the model are also considered to be reasonable for the physical construction of a hand-arm simulator that may be applied for vibration assessment of power tools. More importantly, this model can serve as an effective tool for further studies on hand-transmitted vibration exposure, and design and analyses of vibration isolation concepts for power tools. This study also theoretically confirms the validity of the superposition method for calculating the total hand-arm system response from the distributed responses, which was originally proposed by Dong et al. (2005b).

As it is evident in Figures 2.6-2.9, the model results agree well the measured responses distributed at the fingers, the palm, and the entire hand in terms of both the impedance magnitude and phase for all the four hand actions considered. Many of the model parameter values listed in Table 2.5 can also be reasonably explained. For example, the total finger effective mass (M_2+M_4=94 g) is less than the actual mass (158 g) of the fingers positioned on half of the handle, which was estimated from the measured volume (137 ml) of the fingers and the hand mass density of 1.16 g/ml (Chaffin et al.,

1999; Gibson and Ashby, 1997). This is considered to be reasonable since not all of fingers mass are involved in any specific vibration modal of the fingers. This principle also applies to the total hand-forearm effective mass (M_1+M_3= 1.13 kg), which is less than the mass estimated from measured volume of 1,800 ml (Dong et al., 2005b). Furthermore, the predicted palm skin average effective mass (28 g) is greater than that (12 g) for the fingers, since the palm contact area is much greater than the fingers contact area (Welcome et al., 2004; Yasser et al., 2005). M_0 represents a part of the upper arm and body mass subject to low frequency vibration. This mass is thus greater than the other masses of the model. Increasing the hand forces resulted in increases in the finger and palm contact stiffness values due to collapse and hardening property of the soft tissue with the applied force (Wu et al., 2004). This study also found that increasing the hand forces increases the system damping and thus the vibration power absorption of the system. These observations suggest that the model used in this study can not only provide a reasonably good agreement with the distributed experimental data but also representative model parameters of the hand-arm structure.

The identified parameters also yield reasonable deflections of the fingers and palm masses. The application of an additional 50 N force by the fingers would yield static deformation of nearly 0.25 mm of the fingers mass, as determined from the contact stiffness k_4. Application of an additional 50 N force by the palm would yield a relative deformation of the palm in the order of 0.85 mm under combined grip/push action and 1.67 mm under a grip-only action. These palm-side deformations are directly determined from the contact stiffness k_3. The lower values of k_2, particularly under combined push and grip, would also lead to considerable static deformation between the fingers and

palm-wrist-arm system, which may also be attributed to the flexibility of the finger joints. The lower value of the support stiffness also suggests relatively large deflections of the entire hand-arm system relative to the body, which may be partly due to rotational flexibility of the upper arm about the shoulder joint. This rotational stiffness, however, would depend on the loading and activities of muscles and tendons, which would be highest under combined grip and push action. These interpretations can also be derived from the identified values of k_1 corresponding to different hand actions (Table 2.5).

The mass M_0 in the model can be excited only at low frequencies ($\leq$25 Hz) (Reynolds, 1977), while the experimental data used in this study were attained at frequencies above 10 Hz. This explains why M_0 could take different values in the curve fitting process. Its uncertainty could also affect the parameters of the elements connected to M_0. Further experimental studies are thus required to generate lower frequency data to verify these parameters.

This study confirms that the three resonance frequencies identified for the model are closely associated with different substructures a modes biological system. Considering that the finger resonance frequency depends on the finger contact stiffness and the palm contact stiffness determines the palm resonance frequency, it is impossible to use a single-point contact model to simulate the hand structure appropriately. Hence, this study further proved that it is essential to use at least two parallel connections for modeling the hand-handle coupling relationship.

The developments in biomechanical and mechanical-equivalent models of the hand-arm systems have been faced with highly complex challenges primarily associated with parameter identifications, particularly due to nonlinear biodynamic responses. It is

clearly evident that the vast majority of the model parameters, could not be directly measured, even if a cadaver hand-arm was to be used. For example, the measurement of finger skin deformation or force while grasping a curved surface is quite complex, particularly when the magnitudes of deflections and dynamic forces are very small. The finger contact stiffness of about 200 kN/m would yield deformation in the order of only 0.5 mm under the application of an extreme force of 100 N. The curving fitting technique used in this study thus provides a convenient approach for estimating the model parameters.

Compared with the models recommended in ISO-10068 (1998), the proposed model offers a rather simple clamp-like structure for developing a hand-arm simulator for laboratory evaluations of tools and vibration mitigation devices. Moreover, the resulting simulator could simulate for different hand actions in the laboratory. The model structure proposed in this study is quite simple for fabrication of a hand-arm simulator, where the M_3 and M_4 are rigidly attached to the handle through a clamp-like mechanism with adjustable tension.

The biodynamic responses of the upper arm, shoulders, and upper body generally dominate in the low frequency range. The magnitude of the impedance tends to be considerably lower at lower frequencies. The biodynamic responses measured at the driving points in the vicinity of the fingers and the palm surface may not be very sensitive to the properties of the forearm, upper-arm and the upper body, particularly at higher frequencies when the vibration becomes localized to the hand. The biodynamic model predictions would perhaps yield inadequate inputs to a detailed FE biomechanical model for estimating the stresses and strains in these structures. However, the model developed

in this study can provide the relative motions and dynamic forces between the fingers and the handle, which can serve as an important input for a FE finger model for estimating the vibration-induced stress and strain under different contact conditions. The stresses and strains in the wrist may also be simulated using the relative motion and dynamic force between the handle and the palm-wrist-arm structures, which can also be generated from the models. An understanding of these detailed mechanical stimuli may yield considerable insight into the mechanisms of HAVS and help create more reliable exposure dose formulas for the disorders at different locations.

Finally, it should be noted that the model parameters listed in Tables 2.4 were determined using the mean experimental data provided by NIOSH, which may not describe the dynamic properties of a specific individual and should not be used to predict the individual-specific biodynamic responses. However, the model configurations and methodology proposed in this study would be applicable for deriving parameters for the individual-specific models.

2.10 Summary

This study developed the new lumped parameter model of the human hand-arm system for deriving the biodynamic responses distributed at the fingers and the palm of the hand. The model structure revealed reasonably good agreements with the reported experimental data acquired under four different hand actions, namely grip only, combined 15 N grip and 35 N push, combined 30 N grip and 45 N push, and combined 50 N grip and 50 N push. The model also revealed very good agreements in terms of biodynamic responses distributed in the fingers and the palm in both the impedance magnitudes and phase. The model revealed realistic magnitudes of static deformations of

the fingers, which in-part verified the validity of the identified model parameters. It is thus concluded that the model can be effectively used to conduct further investigations on the distributed vibration transmission, energy absorption, and vibration isolation concepts. The outputs from this model may also be used as inputs to a finite element biomechanical model for estimating the dynamic stresses and strains in the fingers and the palm-wrist-arm structures under hand-transmitted vibration and different types of hand-handle interactions.

CHAPTER 3

DISTRIBUTED BIODYNAMIC RESPONSE ANALYSES

3.1 Introduction

As stated earlier in Chapter 1, the biodynamic responses of the human hand-arm system exposure to vibration have been invariably reported at a single driving-point. The reported mechanical equivalent models also characterize the total response at the driving-point, while the model parameters generally do not relate to anthropometry of the hand-arm system. The reported model and data do not yield information related to local concentrations of biodynamic forces and dissipated energy, and thus the stresses imposed due to HTV. While the measurement of distributed biodynamic response is extremely complex, the mechanical-equivalent model could be effectively applied to determine the distributed biodynamic responses, when the model adequately represents the human hand-arm structure.

In the present study, proposed model structure is applied to investigate the biodynamic response (BR) of human hand-arm distributed at the fingers, palm and the arm related vibration power transmission (VPT) to each segment of the hand-arm system. Vibration transmissibility and VPT of each segment can provide useful information for a more comprehensive understanding of dynamic characteristics of the human hand-arm system to HTV and of mechanisms of vibration-induced injuries or disorders. The distributed responses can also be applied to develop more effective prevention strategies through selection of appropriate tools and work durations, and anti-vibration devices, particularly for finger protection. Therefore, this study investigates the distributions of the biodynamic responses expressed in mechanical impedance, biodynamic force,

vibration transmissibility, power absorption using the developed model, and the predictions of the distributed biodynamic responses based on the response of the entire hand-arm system.

3.2 Analysis Method

The hand-arm system model formulated in Chapter 2 is used to simulate for distributed biodynamic responses under vibration along the forearm direction. Considering that effective mass due the finger skin (M_4) and the palm skin (M_3) were assumed to be fixed to the handle, the five-DOF model could be reduced to only three-DOF. The equation of motion of the system in three independent coordinates is expressed in the following form:

$$[M]\{\ddot{x}\}+[C]\{\dot{x}\}+[K]\{x\}=\{F\} \tag{3.1}$$

where *[M]*, *[C]* and *[K]* are (3x3) mass, damping and stiffness matrix, *{F}* is forcing vector and $\{x\}$ is vector of independent displacement coordinates (x_0, x_1, x_2).

The mechanical impedance responses distributed at the palm and fingers-sides are computed from the resulted biodynamic forces at the respective driving-points, using equations (2.6) and (2.7). The total driving-point impedance of the hand-arm system is then derived upon summing $Z_F(j\omega)$ and $Z_P(j\omega)$, such that:

$$Z_H(j\omega) = Z_F(j\omega) + Z_P(j\omega) \tag{3.2}$$

3.2.1 Vibration transmissibility

Apart from the distributed and total DPMI, the model is analyzed to determine the nature of vibration transmitted to various substructures of hand-arm system. A few

studies have reported measured values of vibration transmitted to the metacarpals, wrist, and elbow and shoulder joints under vibration along z_h-axis. These measurements were performed by attaching miniature accelerometers to the skin using double-faced tape, Velcro bands, etc. The reported measured data generally show reasonably good agreements in terms of frequencies of dominant peaks (often referred to as resonance frequencies) but very little agreements in terms of transmissibility magnitudes. These discrepancies may be attributed to several contributory factors, including relative movement of skin-mounted accelerometers, and variation in postures, test conditions, and individuals' anthropometry. The proposed mechanical-equivalent model of the hand-arm system may also be employed to obtain estimates of vibration transmitted to the fingers (mass M_2), palm-wrist-forearm substructure (mass M_1), and upper arm and body substructure (mass M_0).

The equations of motion, Eq.(3.1), are solved to determine vibration transmissibility of different substructures considered in the model. The vibration transmissibility of a substructure is defined as a ratio of vibration measured on the substructure mass to the input vibration at the hand-tool interface. This response function thus determines the frequency dependence of the transmitted vibration at an anatomical location on the hand-arm system. The transfer function or vibration transmissibility, $TR(\omega)$, is a complex function, given by

$$TR_m(\omega) = \frac{X_m(j\omega)}{Y(j\omega)}; \quad \text{for } m = 0, 1, 2 \tag{3.3}$$

where $Y(j\omega)$ is the handle displacement, $X_m(j\omega)$ is the displacement response of the m^{th} mass element of model, computed from Eq.(3.1), as:

$$\{X_m(j\omega)\} = [[K] - \omega^2[M] + j\omega[C]]^{-1}\{F(j\omega)\} \tag{3.4}$$

Where the forcing vector $F(j\omega) = \{0, (k_3 - \omega c_3)Y(j\omega), (k_4 - \omega c_4)Y(j\omega)\}^T$ and 'T' designates transpose

3.2.2 Biodynamic force distribution

It is common knowledge that the dynamic force acting on the hand-tool interface is associated with the stress and strain within the biological system. It may thus be used as an alternate measure of vibration exposure. The biodynamic force is an essential factor for evaluating the driving-point biodynamic parameters such as apparent mass, mechanical impedance, and total power absorption. The biodynamic force comprises two components: a static and a dynamic force component. In the operation of a powered hand tool, the worker must apply forces on the tool to control, guide, and/or lift the tool, in order to achieve a desired task. Such forces may be expressed by static push/pull and grip forces, which not only result in quasi-static stress and strain, but may also influence tool vibration, vibration transmission, and biodynamic responses by altering the visco-elastic properties of the biological system.

Most tool handles can be approximated by a circular cross-section. Figure 3.1 illustrates a circular cross-section handle subject to hand forces. The handle is evenly split into two parts at the centerline to illustrate the hand forces and to obtain a relationship between the forces. In a power grip situation, both the fingers and the palm contact the tool handle. The force imparted by the finger is generally compensated by the

palm force; the resulting force is termed as the grip force. The total fingers and palm forces, however comprise static as well as dynamic components. The total force acting on the hand, F_T, can be considered as the sum of the resulting fingers and palm forces acting on the surfaces of the two parts of the handle, such that:

$$F_T = (F_p - F_f) + (\tilde{F}_p + \tilde{F}_f) \tag{3.5}$$

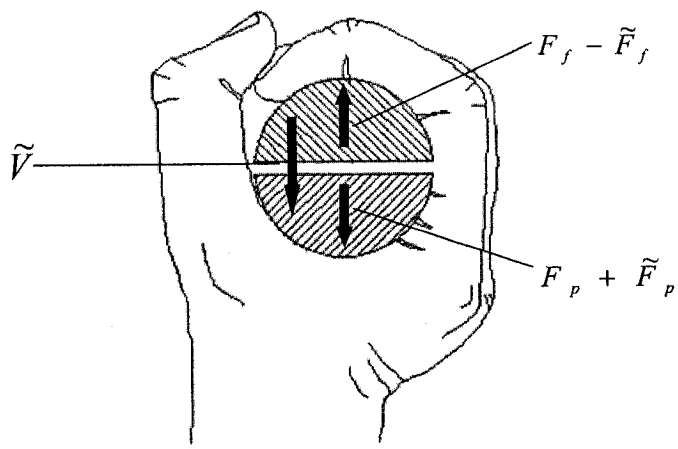

Figure 3.1: Driving-point forces and velocity at the interfaces between fingers and handle, and between palm and handle.

Where $\tilde{F}_p$ and $\tilde{F}_f$ are dynamic components of the palm and fingers forces acting on the palm and the fingers, respectively, and (F_p - F_f) is the net static force applied by palm and the fingers on the handle. A few studies have shown considerably effects of these static forces on the measured impedance response of the hand-arm system. Owing to the highly nonlinear effect of static forces, these are usually considered as controlled variables in the experiments. The static force components, however, are not considered for analysis of mechanical impedance, as it is evident from Eq.(2.5). The total dynamic

force, $\widetilde{F}$, is thus required for analysis of overall impedance and biodynamic force, which can be expressed as:

$$\widetilde{F} = \widetilde{F}_p + \widetilde{F}_f \tag{3.6}$$

Where dynamic forces distributed at the fingers and palm can be computed from:

$$\widetilde{F}_f = (k_4 + j\omega c_4)[X_2(j\omega) - Y(j\omega)] - m_4\omega^2 Y(j\omega)$$

$$\widetilde{F}_p = (k_3 + j\omega c_3)[X_1(j\omega) - Y(j\omega)] - m_3\omega^2 Y(j\omega) \tag{3.7}$$

The biodynamic forces acting on different substructure masses can also be derived in a similar manner. These forces are considered as the forces developed by particular visco-elastic coupling substructure mass. As shown in Figure 3.2, the elements k_0 and c_0 are considered to generate a biodynamic force F_0 for the supporting structure.

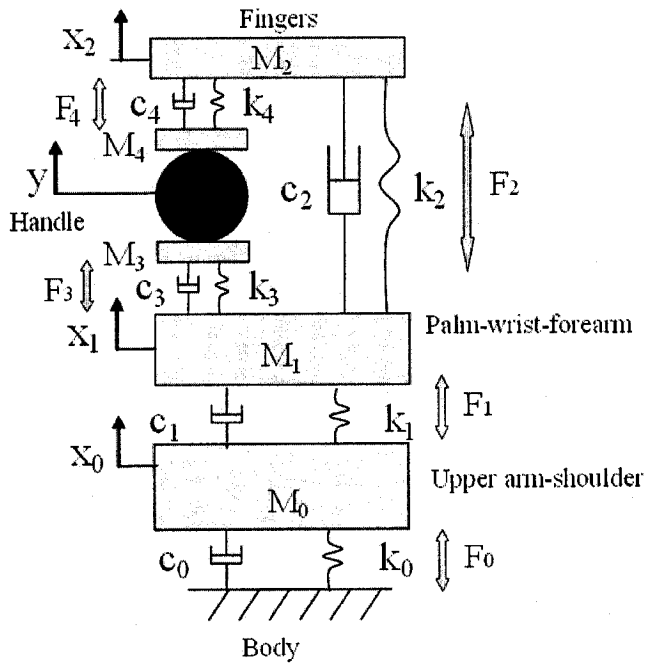

Figure 3.2: Distributed biodynamic forces on different substructure masses

Similarly, elements (k_0, c_0) and (k_1, c_1) are considered to develop biodynamic force F_1 acting on the upper-arm mass m_0, force F_3 acting on palm-wrist-forearm mass m1, and force F_4 acting on fingers mass m_2, respectively. The visco-elastic properties of the carpals, metacarpals and metacarpo-phalangeal joints (k_2, c_2) are considered to develop biodynamic force (F_2) that would act on the masses of the fingers, and palm-wrist-forearm substructures. These forces are derived from:

$$F_0(j\omega) = (k_0 + j\omega c_0)X_0(j\omega)$$

$$F_1(j\omega) = (k_1 + j\omega c_1)[X_0(j\omega) - X_1(j\omega)]$$

$$F_2(j\omega) = (k_2 + j\omega c_2)[X_1(j\omega) - X_2(j\omega)]$$

$$F_3(j\omega) = (k_3 + j\omega c_3)[X_1(j\omega) - Y(j\omega)]$$

$$F_4(j\omega) = (k_4 + j\omega c_4)[Y(j\omega) - X_2(j\omega)] \quad (3.8)$$

3.2.3 Vibration power absorption

It has been well-known that the tissues, especially the soft tissues of the hand-arm system, exhibit significant damping characteristics. The cyclic stress and tissue deformation caused by HTV yield absorption or dissipation of vibration energy/power within the system. The power absorption may thus be considered as a result of the stress and strain stimulations. A number of studies have suggested that the absorbed power can serve as a better measure of HTV exposure than the frequency-weighted acceleration and can provide significant insight into vibration injuries. Biodynamic response of the hand-arm has thus also been expressed in terms of the energy absorbed by the hand and arm. The power (P), amount of energy absorbed per unit time, is computed from force and velocity at the driving-point, such that:

$$P(t) = \tilde{F}(t) \cdot v(t) \tag{3.9}$$

where $\tilde{F}(t)$ is driving force and $v(t)$ is the corresponding driving velocity. The power can also be estimated, in the frequency domain from cross-spectrum density of the force and velocity (Bendat and Piersol, 1992; Burstom, 1994; Aldien et al, 1994). The cross-spectrum density of force and velocity is generally expressed as:

$$P(j\omega) = C_{vF}(\omega) - jQ_{vF}(\omega) \tag{3.10}$$

In the above equation, $P(j\omega)$ is complex rate of vibration energy, $C_{vF}(\omega)$ is coincident spectral density function, or the co-spectrum, and $Q_{vF}(\omega)$ is quadrature spectral density function, or the quad-spectrum. The real component of the power relates to energy absorption associated with tissues deformations and internal friction, which is transformed into heat. The imaginary component determines the energy stored within the biological system. Unlike the other two biodynamic functions, $TR(j\omega)$ and $Z(j\omega)$, the absorbed power can be used to measure a vibration 'dose', as it increases with vibration magnitude and duration.

Since the absorbed power relates to driving force and velocity, similar to the driving-point mechanical impedance, the power flowing into the passive system can also be estimated from MI (Reynolds et al., 1982; Burstrom and lundstrom, 1994). The vibration power absorbed into the hand-arm system can be directly related to $Z(j\omega)$ and $V(\omega)$ in the following manner:

$$P(\omega) = \mathrm{Re}[Z(j\omega)]V^2(\omega) \tag{3.11}$$

Where V is rms velocity corresponding to excitation frequency ω

The total power absorbed into the hand arm system can be derived from sum of power values corresponding to individual frequency band, such that:

$$\overline{P} = \sum_{i=1}^{n} P(\omega_i) \tag{3.12}$$

Where $\overline{P}$ is total power absorbed, $P(\omega_i)$ is the absorbed power in the ith third-octave frequency band with center frequency ω_i and n is total number of frequency band considered

The power absorbed into the hand-arm system is evaluated from the biodynamic response of the model in terms of mechanical impedance. Owing to strong dependence of absorbed power on the excitation magnitude, the analyses are performed under a constant acceleration spectra ($A=10$ m/s^2). The model results are further analyzed to derive energy absorbed within individual substructures by considering the energy dissipated by respective viscous elements. As an example, the energy dissipated within the fingers substructure, P_f, may be computed from energy dissipated by c_2 and c_4, given by:

$$P_2 = c_2 |\dot{Q}_2(j\omega)|^2; \qquad P_4 = c_4 |\dot{Q}_4(j\omega)|^2 \tag{3.13}$$

Where P_2 and P_4, define the energy dissipated by c_2 and c_4, respectively, and $\dot{Q}_2(j\omega) = \dot{X}_2(j\omega) - \dot{Y}(j\omega)$, and $\dot{Q}_4(j\omega) = \dot{X}_2(j\omega) - \dot{X}_1(j\omega)$

The energy absorbed into the fingers is attributed to P_2 and in-part to P_4. The energy absorbed within the finger tissues Pf is thus estimated from the finger impedance, using Eq.(3.11). In a similar manner, the energy dissipated by dissipative elements c_0, c_1 and c_3 could be related to vibration power absorbed within the shoulder and whole body

(P_0), upper-arm (P_1), palm-wrist-forearm (P_3), and carpals and metacarpals tissues (P_2), respectively.

3.3 Distributed Biodynamic Responses

The equations of motion of the proposed model are solved in conjunction with biodynamic for the equations expressed in Chapter 2 to determine the distributed biodynamic responses of the hand-arm model. The responses are evaluated in terms of magnitudes of vibration transmissibility, biodynamic forces, and absorbed power, from Eqs.(3.3), (3.7), (3.8), (3.11) and (3.13).

Figure 3.3 to 3.6 illustrate the distributed and total biodynamic response characteristics derived from the hand-arm system model as functions of excitation frequency. The results are attained under a constant-velocity excitation of 10 m/s^2 rms and three different hand actions, involving combined grip/push forces of 15/35, 30/45 and 50/50 N. The responses of the finger, palm, forearm and upper arm masses are obtained at twenty-one discrete excitation frequencies, which are selected as center frequencies of 1/3-octave bands in the 10-1000 Hz range. Each figure illustrates: (a) vibration transmissibility of fingers (m_2), palm-wrist-forearm (m_1) and upper arm (m_0) masses; (b) biodynamic force of fingers (m_2), palm-wrist-forearm (m_1) and upper arm (m_0) masses; (c) power absorbed into fingers and palm, as determined from driving-point forces, and power absorbed into total hand-arm system, and (d) absorbed power distributed in the hand arm system, as determined from energy dissipated by individual viscous elements.

Figure 3.3 (a) illustrates vibration transmissibility magnitude of the fingers, palm-wrist-forearm and upper-arm masses under the combined action of 30 N grip and 45 N

push forces. The magnitude responses appear to be similar of a dynamic system, while the peak magnitudes suggest different natural frequencies. The palm response suggests resonance frequency near 16 Hz, attributed to interactions of the soft tissue with the handle, while the finger resonance occurs at a frequency near 100 Hz. The magnitude response of the upper arm does not show a peak, which is due to higher damping and lower resonance frequency, as also shown in Table 2.4 (Aatola, 1989; Thomas and Beauchamp, 1998; Gurram et al., 1994b). The fingers mode resonance near 100 Hz and is also consistent with the resonance observed by Aatola (1989) and Thomas and Beauchamp (1998).

The results further show that vibration transmissibility of the palm is higher than that of the fingers and the upper-arm at lower frequencies (<25 Hz). Above 25 Hz, the vibration transmissibility of fingers is significantly higher than those of the palm-wrist-forearm and upper-arm. The responses show that majority of the vibration above 100 Hz is concentrated on the fingers mass, which has also been observed in many experimental studies.

As shown in figure 3.3 (b), at low frequencies (≤100 Hz), the force of palm (F_3) and fore-arm (F_1) and upper-arm (F_0) have their peak values, and they are the dominant force in this frequency range. At high frequencies (≥100 Hz), the force of palm (F_3) and fingers (F_4) become the dominant force. The force of palm (F_3) decreased with the frequency increasing, and the magnitude values of palm and fingers get close to around 10.3 N from 400 Hz to 1,000 Hz. Moreover, at high frequencies (≥100 Hz) the forces of fore-arm (F_1) and upper-arm (F_0) decreased with the frequency increasing, and their

magnitude values are gradually reduced closely to zero. The majority of force F_2 concentrated in the frequency range (20 Hz-200 Hz).

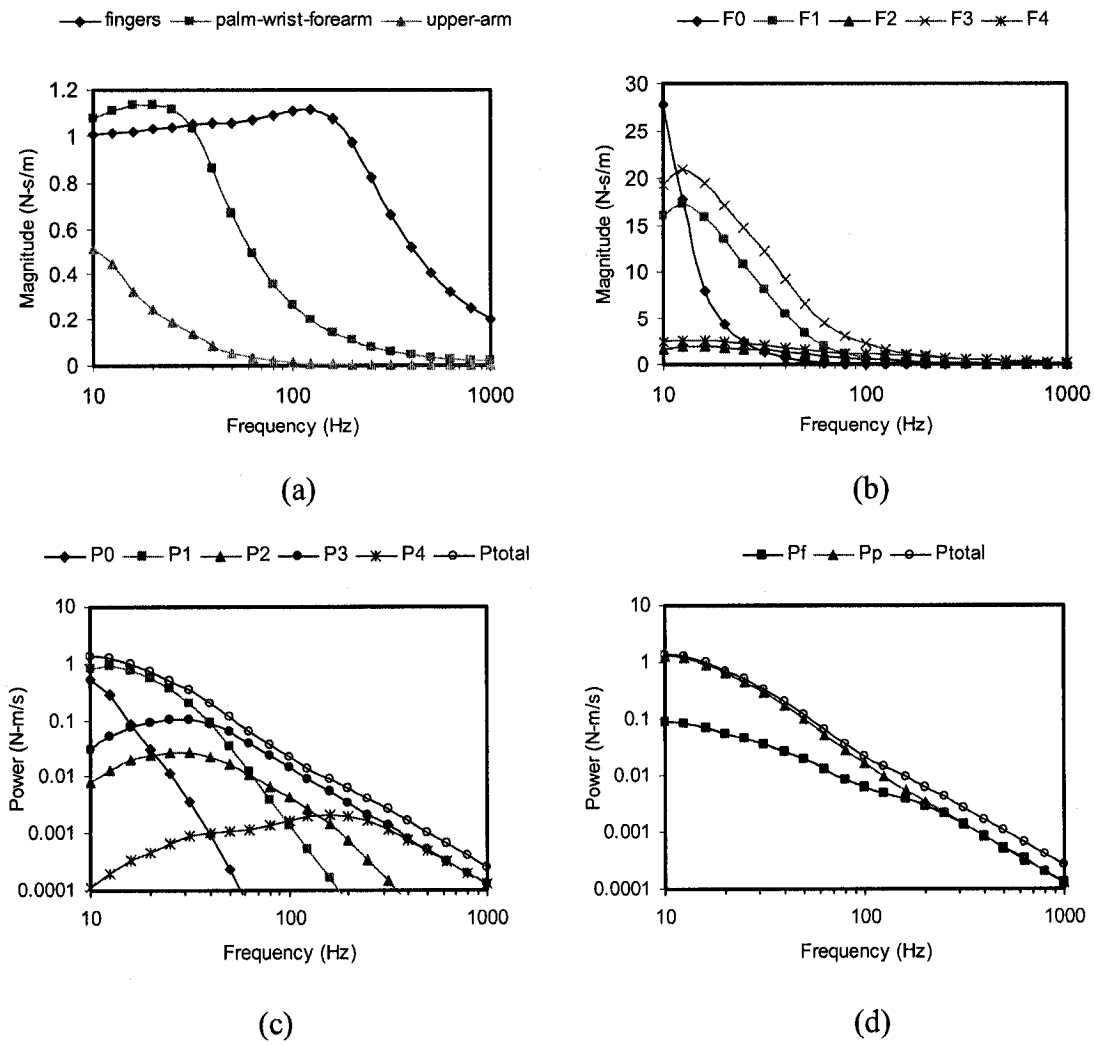

Figure 3.3: Distributed biodynamic response characteristics of the hand-arm vibration model under 30 N grip and 45 N push forces: (a) vibration transmissibility; (b) biodynamic forces; (c) vibration power absorbed in fingers, palm and total hand-arm; and (d) distributed vibration power absorption

Figure 3.3 (c) illustrates the absorbed power distributed on the fingers and palm-wrist-forearm and each damping element of the hand-arm system under 30 N grip and 45 N push forces. As it is shown, the power absorption subjected to a constant-acceleration power spectral density (A=10 m/s^2 rms) is generally a function of frequency. On the

basis of the proposed model structure, the energy dissipated in viscous element c_0 may be used to represent the power absorption P_0 within the shoulder and the upper body beyond the shoulder. In a similar manner, the energies dissipated in c_1, c_3 and c_4 could represent the powers absorbed within the substructures comprising upper arm and a portion of the forearm (P_1), palm-wrist and a portion of the forearm (P_3), and the finger tissues (P_4)contacting the handle, respectively. The power absorbed in fingers (c_4) generally reveals two peaks: one in the hand-arm resonance frequency range and the other one in the finger resonance frequency range. The finger power absorption between the two resonance frequencies also remains at a fairly high level. The energy dissipated in c_2 could characterize the power absorption P_2 in the remaining tissues coupling the fingers with the hand structure.

From the vibration spectra, it can be seen that predominant vibration occurs in the low frequency range (10-30 Hz). Such low frequency vibration is effectively transmitted to the arms, shoulder, neck, and head. The VPA is thus mostly distributed in these substructures, as clearly reflected in results shown in Figure 3. On the other hand, the vibration predominates at frequencies greater than 31.5 Hz and its corresponding VPA is mostly concentrated in fingers and the hand. The resulting VPA that transmits vibration in both the low (20 to 31.5 Hz) and high (>100 Hz) frequency ranges thus occurs in both the fingers and the remaining hand-arm substructures.

Figure 3.4 to 3.6 showed the biodynamic response characteristics of the hand-arm system on the other three hand actions. As it can be seen, their curves trends are generally similar respectively. And the resonance frequencies generally increase with the applied

hand forces increasing. Increasing the force also increases the magnitudes of the responses at all frequencies.

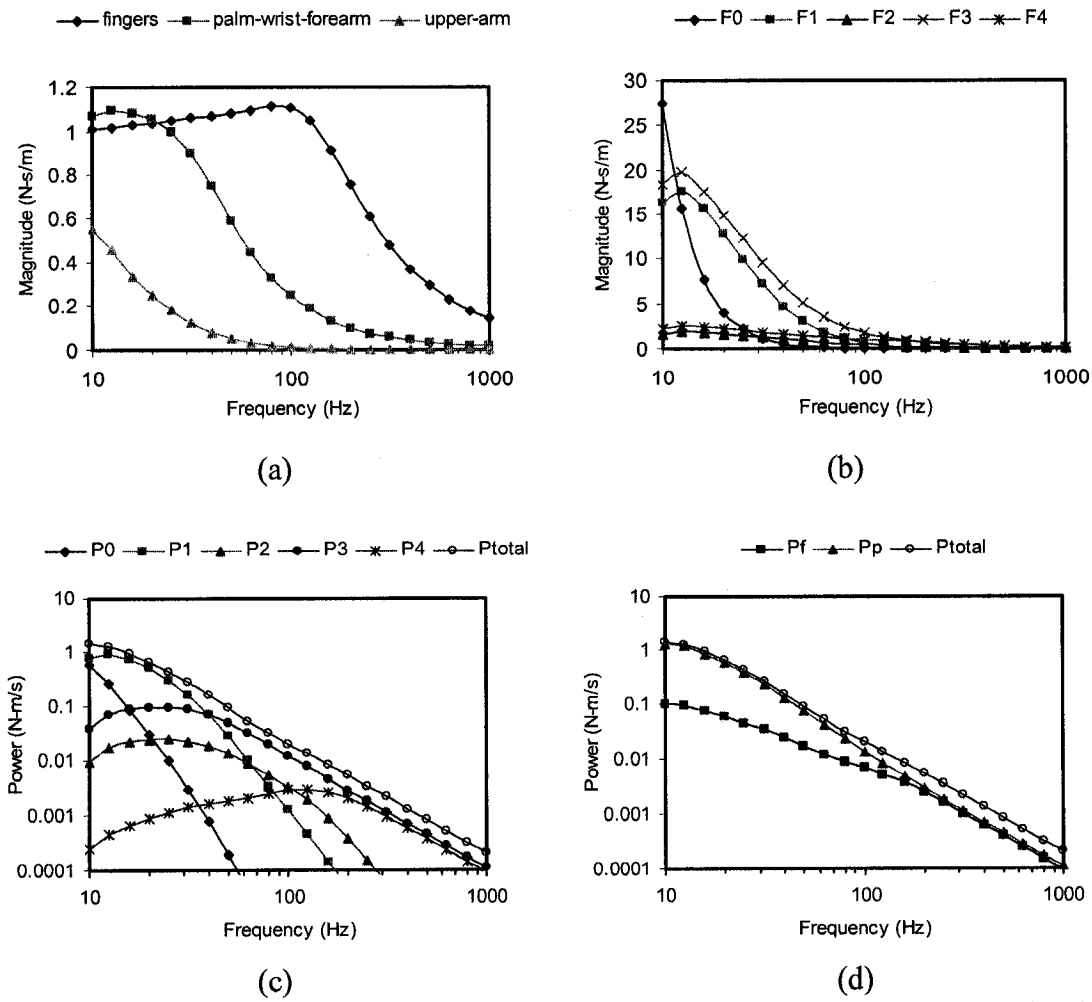

Figure 3.4: Distributed biodynamic response characteristics of the hand-arm vibration model under 15 N grip and 35 N push forces: (a) vibration transmissibility; (b) biodynamic forces; (c) vibration power absorbed in fingers, palm and total hand-arm; and (d) distributed vibration power absorption

Increasing the push force, the force F_2 increased in the high frequency range (100-1,000 Hz), and the peak value of the force F_3 also increased. The total power increased with the hand force increasing. For the grip only action, the energy distributed on damping c_3 and palm in the high frequency range (200-1,000 Hz) is obviously less than which under the other combined hand actions.

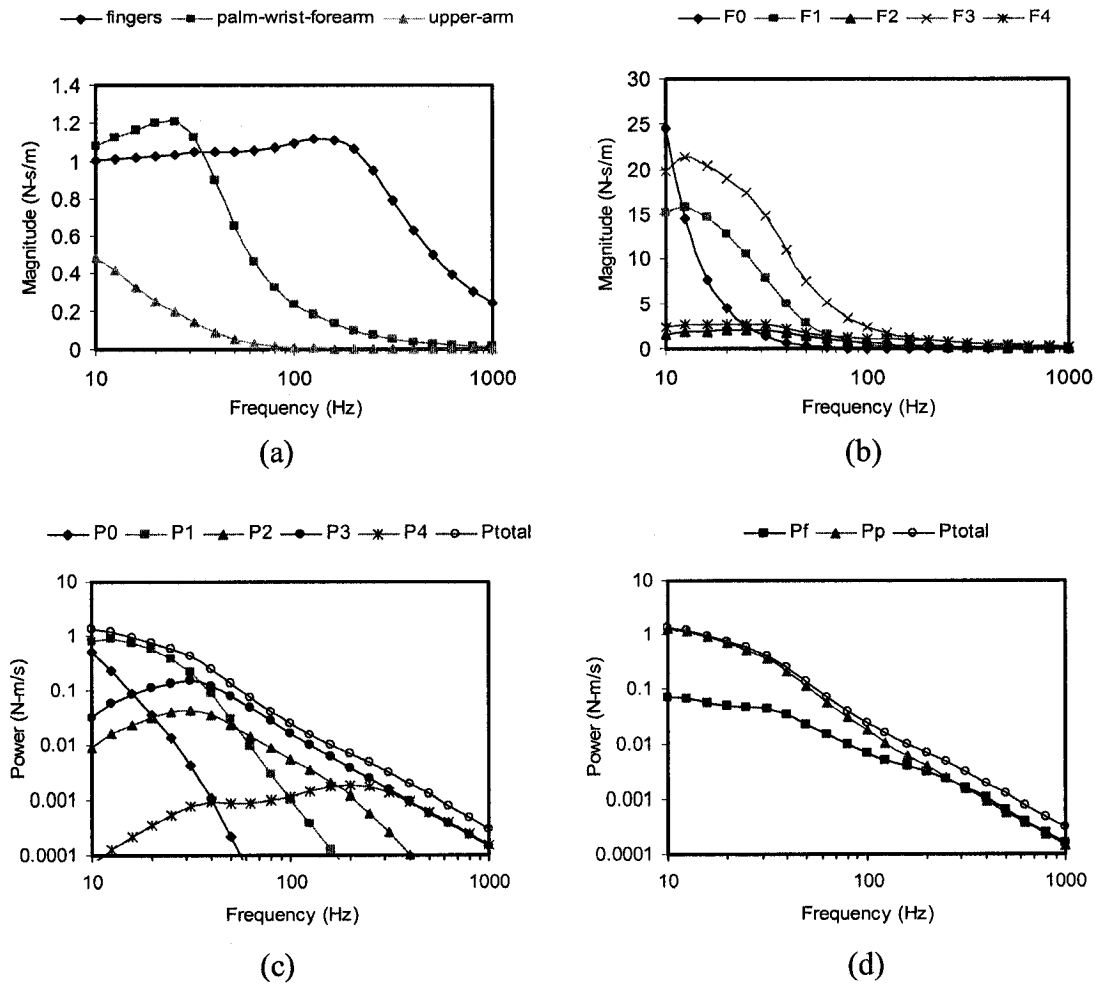

Figure 3. 5: Distributed biodynamic response characteristics of the hand-arm vibration model under 50 N grip and 50 N push forces: (a) vibration transmissibility; (b) biodynamic forces; (c) vibration power absorbed in fingers, palm and total hand-arm; and (d) distributed vibration power absorption

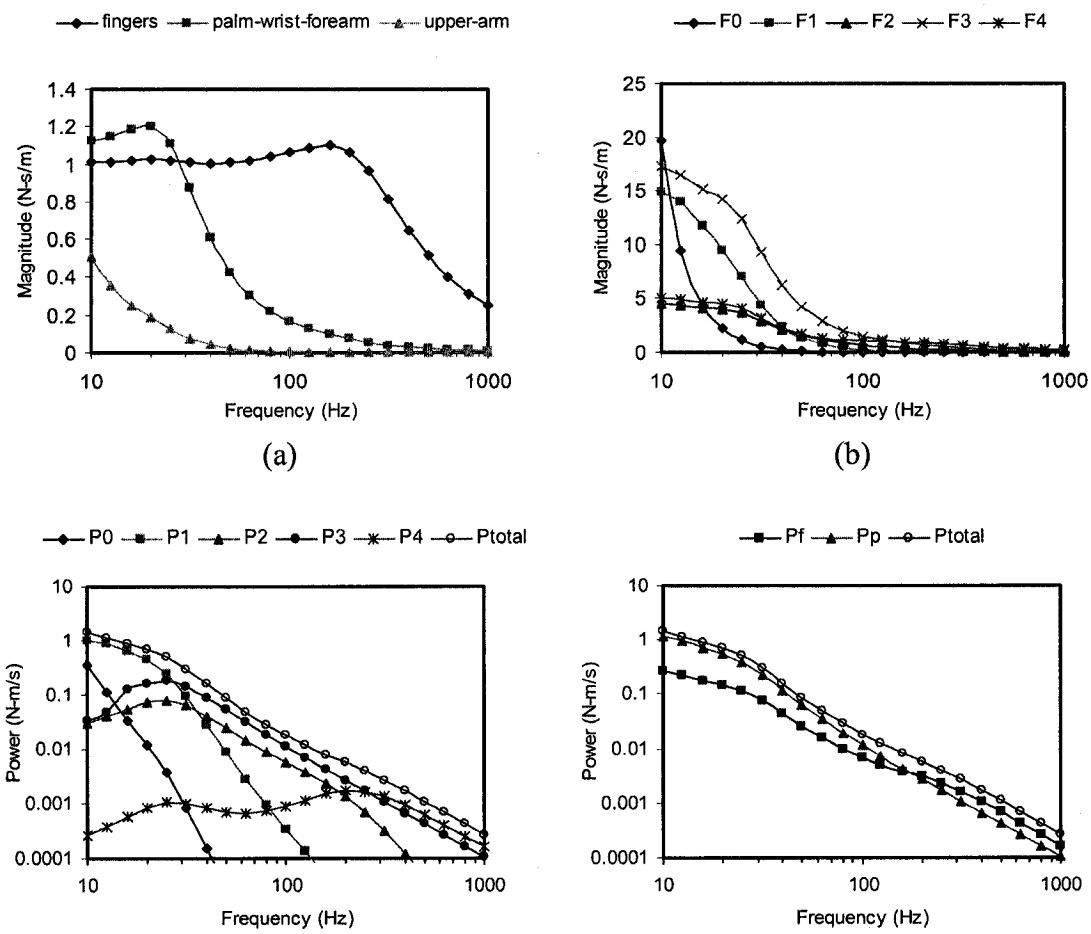

Figure 3.6: Distributed biodynamic response characteristics of the hand-arm vibration model under 50 N grip only forces: (a) vibration transmissibility; (b) biodynamic forces; (c) vibration power absorbed in fingers, palm and total hand-arm; and (d) distributed vibration power absorption

3.4 Discussions on Distributed Biodynamic Responses

3.4.1 Vibration transmissibility

The vibration transmissibility of the hand-arm segments presented in Figures 3.3 (a) to 3.6 (a) suggest that the individual segments behave similar to a single-DOF dynamical system. The magnitudes of vibration transmitted to the hand, forearm and elbow, derived from the model are also compared to measured data reported in published study to examine the validity of the model. Figure 3.7 illustrates comparison of finger

transmissibility magnitude, derived from the model with the measured data, reported by Kihlberg (1995) and Reynolds (1997). The model results exhibit trends that are comparable with the measured data. Both, the measured and model results suggest fingers mode resonance in 125-250 Hz range, and that the finger acts like a rigid body at frequencies above 250 Hz.

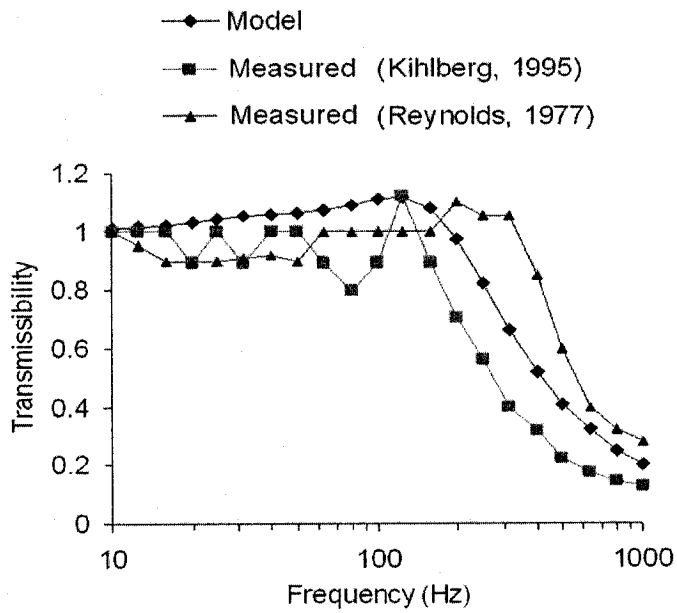

Figure 3.7: Comparison of finger vibration transmissibility response of the model with reported measured data near the finger under the 30 N grip and 45 N push forces

The magnitude of vibration transmissibility of the palm-wrist-forearm substructure, derived from the model, is also compared with the measured near the wrist by Cherian et al. (1996). The comparison again suggests reasonably good agreement on palm-wrist-forearm vibration response of the model with the measured data. Both, the model and model results exhibit considerable attenuation of vibration transmitted to wrist at frequency above 50 Hz. At excitation frequencies above 100 Hz, the transmissibility magnitude is observed to be below 0.2 in both cases. The measured and model response

characteristics clearly illustrate that the vibration transmitted beyond the hand at frequencies above 100 Hz is most significantly attenuated.

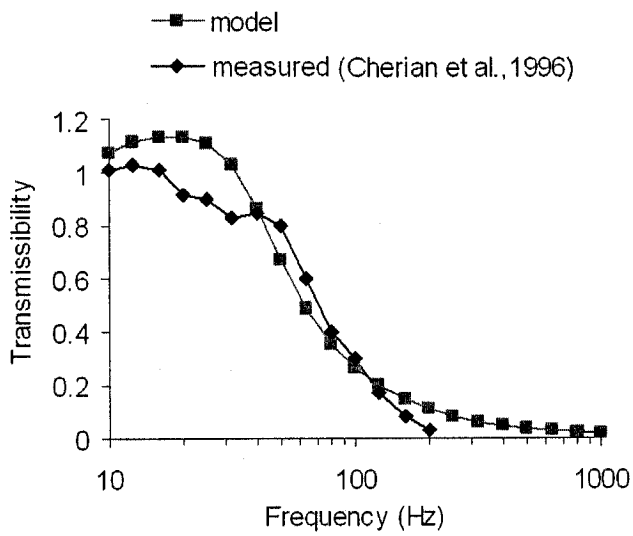

Figure 3.8: Comparison of wrist-forearm vibration transmissibility magnitude response of the model with the measured forearm vibration data under the 30 N grip and 45 N push forces Biodynamic force distribution

3.4.2 Biodynamic force distribution

The biodynamic forces acting on various substructure masses considered in the model shown in Figures 3.3 (b) to 3.6 (b), suggest that large magnitudes of dynamic forces occurs at low frequencies (≤100Hz), with the exception of the force acting on fingers (F_f). This again suggests that vibration at lower frequencies is directly transmitted to the forearm, upper-arm and whole body structures. At frequencies above100 Hz, location of vibration within the hand causes larger biodynamic force acting on the fingers F_4 and the palm force F_3. The forces transmitted to fore-arm (F_1) and upper-arm (F_0) approach nearly negligible magnitudes at higher frequencies, since the majority of vibration is absorbed within the fingers.

3.4.3 Vibration power distribution

As shown in Figure 3.3 (c) to 3.6 (c), the majority of the vibration power absorption in the palm-wrist-forearm structures, attributed to energy dissipated by damping elements c_1 and c_3 occurs at low frequencies (≤100 Hz). The energy absorbed by the upper arm structure in relatively small at these frequencies, although the low frequency vibration is directly transmitted to the upper arm structure. This is attributed to relatively lower damping c_0 and lower vibration magnitude of the upper arm. At low frequencies, the energy flow into the fingers may not be exactly what is actually absorbed in the fingers. At very low frequencies (<20 Hz), however, the majority of the power is absorbed in the upper arm and shoulder structures. The power absorbed in these parts is unlikely to be associated with the finger disorders attributed to HTV. This may explain why vibration-induced white finger (VWF) disorders could be hardly found among the operators of the low frequency ramming tools (Tominaga, 1993). This also explains why these operators complained discomforts in the upper arm, shoulder, neck, and head. Moreover, the shape of energy absorption curve for the finger contact tissues is similar to that of the temporal perception threshold shift measured at 125 Hz (Harada and Griffin).

The results of this study also indicate that the majority of the vibration power distributed in the fingers and palm as determined from energy dissipated by viscous damping elements c_4 and c_3, occurs at frequencies above 200 Hz. This again confirms that the majority of the vibration power at higher frequencies is transmitted to the fingers, and is unlikely to be transmitted to other parts of hand-arm structures. The power absorption thus mostly occurs in the finger tissues. This is consistent with the observations made in previously reported studies on vibration transmission and vibration

power absorption. The palm tissues also exhibit considerable vibration power absorption, since the high-frequency vibration is effectively transmitted to local soft tissues of the palm. High frequency contents of HTV remain limited to local hand tissues. The operations of tools with relatively high frequency vibration are thus unlikely to cause injuries or disorders in the upper-arm and shoulder structures. The weighting defined in the current standard (ISO-5749, 2001) assumes equal effect of vibration velocity at frequencies above 16 Hz. From the results, it can be deduced that the current standard would underestimates the effects of high frequency vibration in terms of risks of vibration-induced fingers and hand disorders. The power absorption in the fingers, palm and wrist substructures (determined from damping elements c_2 and c_3) also suggests that risk imposed by vibration in the 20 to 50 Hz frequency could be relatively high for hand tissues. Grinder users could develop VWF because grinders could generate high magnitudes of vibration, and their high frequency (about 100 Hz) features make the power absorption be concentrated in the hand or fingers. These observations suggest that it is inappropriate to use the total VPA to assess the risk of VWF. They also suggest that the distributed power absorptions may be used as alternative vibration measures for assessing various risks of the hand-transmitted vibration exposure.

The results also show that increasing the push force in the combined actions increases the palm contact stiffness and increases the vibration power transmission to the palm. However, the increased palm contact stiffness reduces the relative motion between the hand and the handle at low frequencies. Hence, the reduced relative displacement reduces the dynamic force acting on the fingers, which further reduces the vibration power transmission to the fingers. The model parameters show that the damping ratio of

the palm decreased with the push force increasing, but this doesn't mean increase the vibration power.

3.5 Summary

This study investigated the basic characteristics of the distributed biodynamic responses based on the response of the entire hand-arm system. The results can be used to predict the distribution of the mechanical impedance, biodynamic force, vibration transmissibility, power absorption on the hand-arm system. At low frequencies, the power is mainly absorbed in the upper arm, shoulder, and those beyond the shoulder. The power absorbed in these parts is unlikely to be closely associated with the finger disorders. However, high frequency features make the power absorption be concentrated in the hand or fingers. These observations suggest that it is inappropriate to use the total VPA to assess the risk of VWF. They also suggest that the distributed power absorptions may be used as alternative vibration measures for assessing various risks of the hand-transmitted vibration exposure. Therefore, this study is useful in the further study of transmitted vibration, vibration-induced injuries or disorders of the hand-arm system, vibration isolation, and tool design.

CHAPTER 4

PREDICTION OF DISTRIBUTED BIODYNAMIC RESPONSES FROM THE TOTAL DRIVING-POINT REPONSE

4.1 Introduction

As stated earlier, the biodynamic responses of the hand-arm system have been invariably reported considering a single driving-point. The resulting data thus describe the biodynamic response of the entire hand-arm system measured at the hand-handle interface. Such a response cannot provide the nature of localized responses for assessment of risks of HTV to a particular substructure. A model derived on the basis of total biodynamic response, however, could be applied to determine the distributed responses, which can provide considerable into localized energy absorption and biodynamic forces and thereby a potential risk assessment method. The clamp-like model structure of the hand, proposed in this study, could be derived using the total hand-arm impedance response, using the curve fitting technique described in Chapter 2. The resulting model, when validated, can then be applied to predict the distributed responses. In this chapter, the model parameters are identified solely on the basis of total hand-arm system response. The validation of the model for predicting distributed responses is then demonstrated by comparing the model results with the measured responses distributed at the fingers and the palm.

4.2 Determinations of Model Parameters

The five-DOF model structure proposed in Chapter 2 is used to derive the total driving-point impedance of the hand-arm system using Eq.(2.8). The model parameters are identified solely on the basis of total hand-arm impedance. The data acquired by

NIOSH for different hand forces (50 N grip-only, 15 N grip and 35 N push, 30 N grip and 45 N push, 50 N grip and 50 N push) were used as the target values of total hand-arm impedance. The model parameters were identified for each hand action, as described in Chapter 2. For this purpose, three different error functions were formulated. Each error function was formulated using the rms error between the impedance predicted by the model and the measured magnitude corresponding to each third-octave band center frequency, such that:

$$\Delta_1 = \sqrt{\frac{1}{n}\sum_{i=1}^{n}[Z_M(\omega i) - Z_E(\omega i)]^2} \tag{4.1}$$

where Δ_1 is the rms deviation or error function, $Z_M(\omega i)$ and $Z_E(\omega i)$ are the predicted and measured impedance values at the center frequency of ith frequency band, respectively, and n is the number of the one third octave bands considered.

The minimization problems were solved subject to following constrains:

$$M_0, M_1, M_2, M_3, M_4, k_0, k_1, k_2, k_3, k_4, c_0, c_1, c_2, c_3, c_4 > 0$$

$$and \qquad \sum_{i=0}^{4} M_i < 10kg \tag{4.2}$$

The minimization problem subject to parameter constraints defined in Eq.(4.3) was solved to determine the model parameters. The minimization of function Δ_1 resulted in considerable errors in source of the frequency bands. In order to achieve a better convergence of the error function, alternate parameter constraints were defined, which resulted in better fitting of target data:

$$M_0 \geq 5;\ M_2 \geq 0.06;\ M_3 \geq 2M_4;\ k_i \geq 1000,\ k_2 > k_1,\ k_4 > k_3,\ \sum_{i=0}^{4} M_i \leq 10$$
$$\text{and the remaing} \quad M_1, M_4, c_0, c_1, c_2, c_3, c_4 > 0 \tag{4.3}$$

The first error minimization function is formulated by considering rms dentations in real and imaginary components of the total hand-arm system impedance response, such that:

$$\Delta_2 = (\Delta_{H\_\mathrm{Re}} + \Delta_{H\_\mathrm{Im}}) \tag{4.4}$$

where Δ_2 is the error minimization function, and Δ_{H_Re} and Δ_{H_Im} are rms values of real and imaginary error components, respectively, between the model and measured impedance responses of the hand arm system.

In some of the reported studies (e.g., Burstrom and Lundstrom, 1994; Kilberg, 1995), the parameter identifications have been performed by fitting the real part of the impedance or the power absorption. An error function based upon rms error in real part of the total hand impedance is also formulated to identification of model parameters, such that:

$$\Delta_3 = \Delta_{H\_\mathrm{Re}} \tag{4.5}$$

The minimization function, defined in Eq.(4.5) was solved subject constraints expressed in Eq. (4.3), with the exception of M_3 and M_4 values. It was observed that these two parameters only affect the imaginary part of the impedance response, which is not considered in this minimization function. These masses were thus subject to equality

constraints based on the values derived from minimization of Δ_1 and Δ_2. These equality constraints were thus defined as:

$M_3 = 0.028$; and $M_4 = 0.014$

The reported impedance data generally exhibit considerably larger derivations in the phase response (Gurram et al., 1994). This is partly attributed to difficulties associated with accurate measurements of the phase relationship between the force and the velocity (Dong et al., 2006b). An alternate error minimization function is thus also formulated on the basis of rms derivation magnitude of the total hand impedance, such that:

$$\Delta_4 = \Delta_{Hand\_Mag} \tag{4.6}$$

Where Δ_{Hand_Mag} is the rms error between the magnitudes of impedance predicted by the model and the measured data.

A minimization algorithm was developed for each of the error function to identify the model parameters, as described in Chapter 2. In an attempt to achieve a global minimum of the error function, a repeated search was performed using different sets of initial parameters vectors. The solutions were found to be quite repeatable for each error function.

4.3 Results

The model parameters identified through minimization of three error functions were applied to determine the model responses in terms of total impedance magnitude and phase responses. The models were also solved to determine the impedance responses at the fingers and the palm using Eq.(2.6) and Eq.(2.7), respectively.

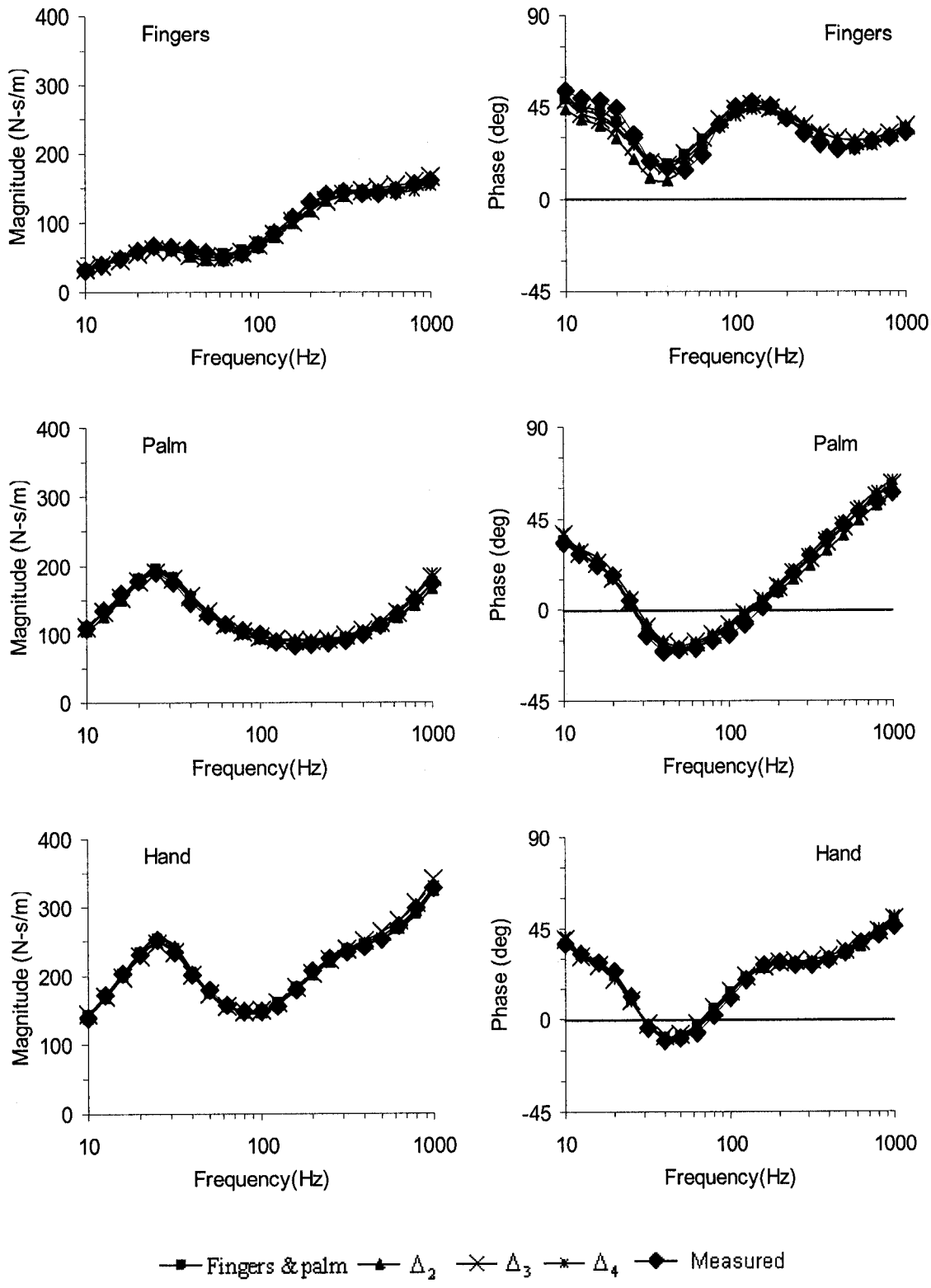

Figure 4.1: Comparisons of model responses attained for parameters identified through solutions of different minimization problems with the measured data (50 N grip).

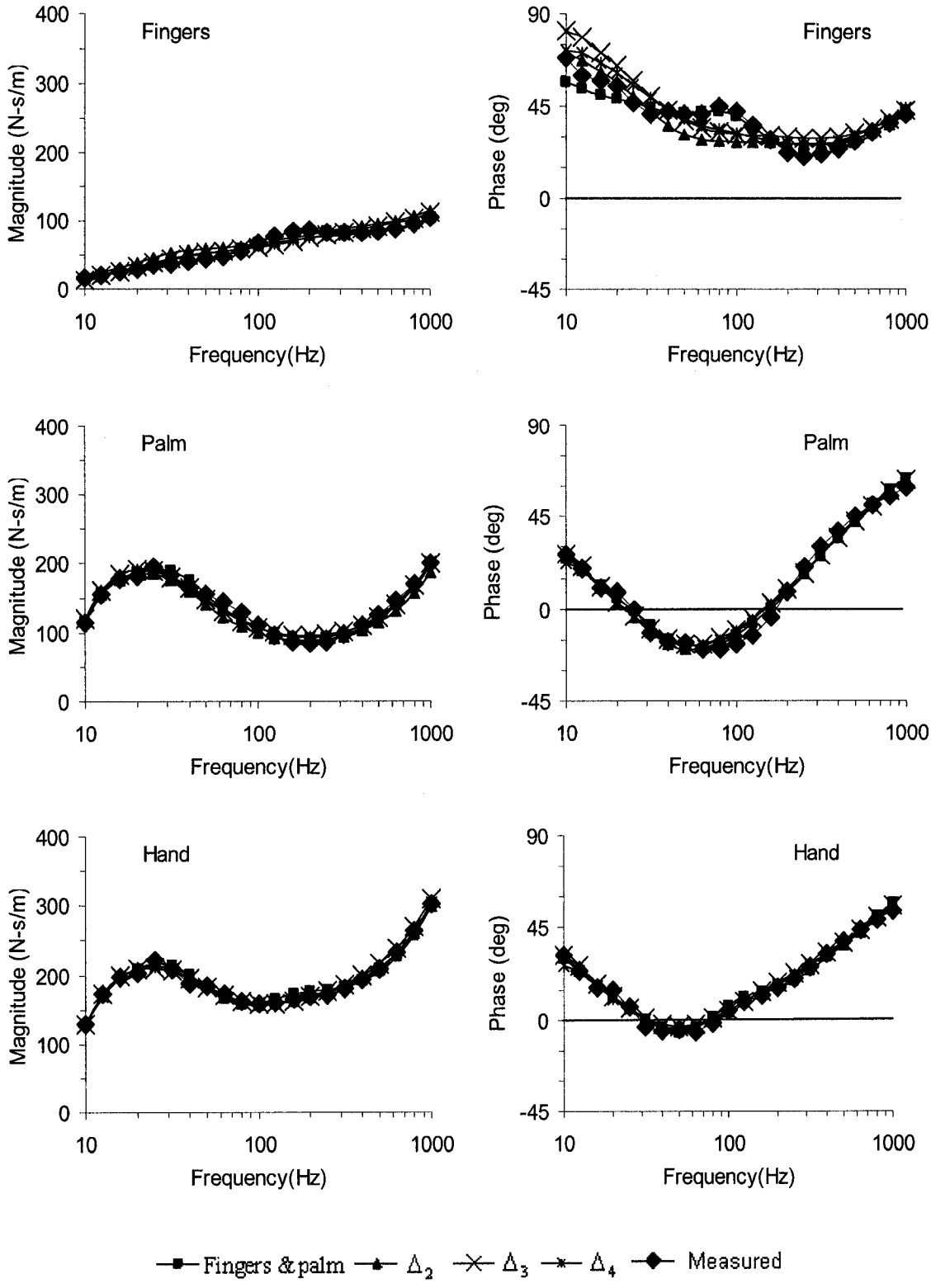

Figure 4.2: Comparisons of model responses attained for parameters identified through solutions of different minimization problems with the measured data (15 N grip and 35 N push).

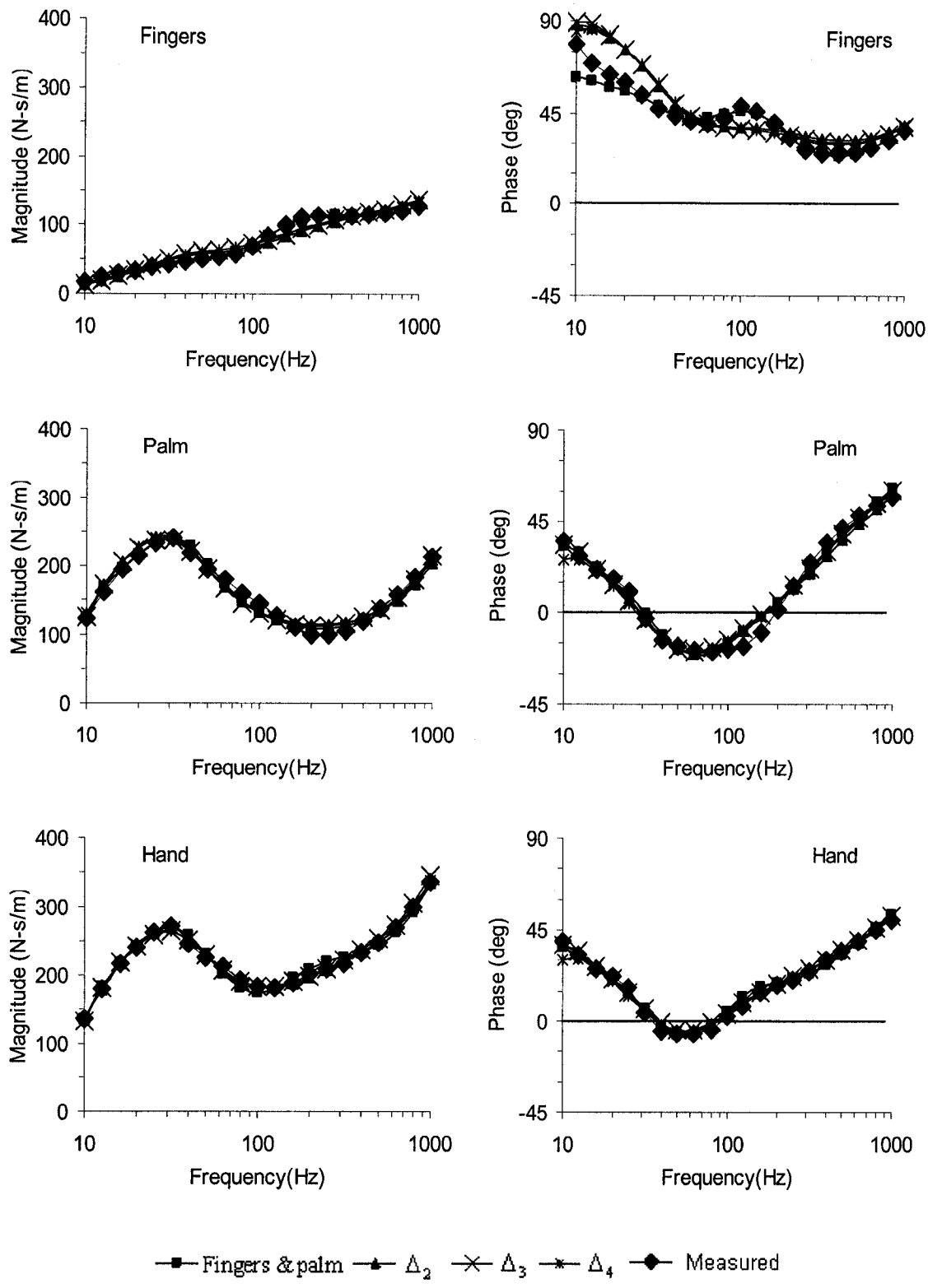

Figure 4.3: Comparisons of model responses attained for parameters identified through solutions of different minimization problems with the measured data (30 N grip and 45 N push).

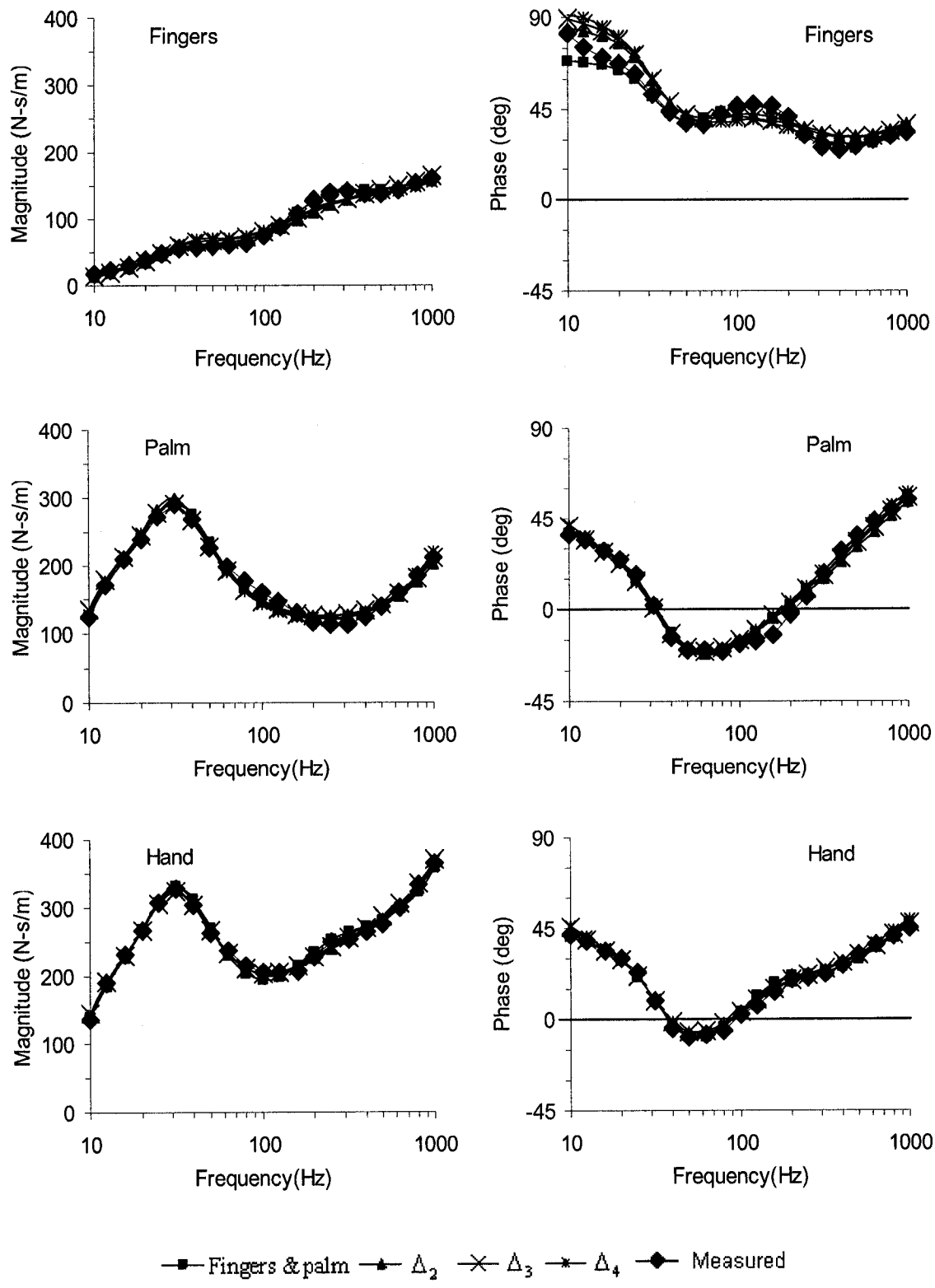

Figure 4.4: Comparisons of model responses attained for parameters identified through solutions of different minimization problems with the measured data (50 N grip and 50 N push).

Figures 4.1 to 4.4 illustrate comparisons of the predicted magnitude and phase responses of the model with the corresponding measured data acquired under four different hand actions. Each figure presents comparisons of the model responses attained for parameters identified through minimization of Δ_2, Δ_3 and Δ_4, with the measured data. The responses attained through minimization of errors in finger and palm impedance in Chapter 2 are also presented.

The results attained through consideration of distributed responses at the fingers and the palm show very good agreements with the measured data in the entire frequency range (10 Hz to 1,000 Hz), as observed in Chapter 2. The results attained for the first error function (Δ_2) involving both the real and imaginary components of the total hand-arm system response also show similar degrees of agreements with the experimental data, irrespective of the hand forces considered. While the predicted finger magnitude responses agree reasonably agree the experimental data, the corresponding phase response show large differences, particularly at frequencies up to 10 Hz.

Although only the real part of the hand response was used in the second error function (Δ_3), the predicted magnitude and phase responses of the hand and those distributed at the palm agree reasonably with the experimental data. The predicted finger responses are similar to those predicted using the first error functions (Δ_2). The model parameters identified through matching the total impedance magnitude (Δ_4) also resulted in similar degree of agreements with the measured data for all the hand forces considered. The results consistently show some deviations in the fingers impedance phase response. The results clearly show that the model derived on the basis of total hand-arm impedance can be effectively applied to predict the responses distributed at the palm and the fingers.

This, however, requires that the model structure include two driving-points representing the finger-handle and palm-handle interfaces. The single-driving-point model, described in ISO-10068 (1998) and in other reported studies (Rakheja et al., 2002), cannot be used to predict the distributed responses.

The model parameters identified through minimization of three error functions are summarized in Table 4.1 to 4.4 for each of the four hand actions considered. The identified parameters are also compared with three presented in Chapter 2 are the basis of minimization of errors in the distributed responses (Table 4.1). The resulting models were further analyzed to determine the natural frequencies of damping ratios of the models, which are also summarized in the Tables. The results show very comparable values of all the parameters, irrespective of the error function considered, although some differences are evident. The derivations model parameters identified through minimization of Δ_2, Δ_3 and Δ_4, and those derived from distributed responses (Chapter 2 and Table 4.1) are generally below 10%. The parameters exceeding those in Table 4.1 by 15% or more are highlighted in Table 4.2 to 4.4. The results suggest that such lower differences occur in the finger contact stiffness (k_4), the finger-hand coupling stiffness (k_2) and damping (c_2), and finger damping ratio (ξ_2) in the three combined grip and push actions. All these parameters are closely related to the finger responses, where notable derivations were observed in the phase response.

Table 4.1: Model parameters identified through minimization of distributed fingers and palm responses of the hand-arm system.

Parameter	Hand actions			
	50 N Grip	15 N Grip 35 N Push	30 N Grip 45 N Push	50 N Grip 50 N Push
M_0 (kg)	5.8543	6.0987	6.5050	5.8626
M_1	1.3242	0.8495	0.9774	1.2482
M_2	0.0828	0.0841	0.0800	0.0825
M_3	0.0247	0.0292	0.0305	0.0287
M_4	0.0131	0.0110	0.0115	0.0132
k_0 (N/m)	13740.3	17272.1	18826.0	16903.3
k_1	2462.0	2416.1	1017.6	1697.9
k_2	6788.1	3445.4	4026.1	4035.4
k_3	26191.7	38684.4	48930.4	52492.0
k_4	157119.0	56152.8	96313.9	143915.8
c_0 (N ·s/m)	107.07	152.87	163.76	169.70
c_1	97.80	159.20	158.94	140.53
c_2	39.03	25.26	28.97	35.47
c_3	81.79	86.53	101.31	114.83
c_4	127.98	74.73	99.87	124.59
f_0 (Hz)	8.3	9.0	8.8	9.0
f_1	25.9	36.4	37.3	34.3
f_2	223.9	134.0	178.2	213.1
ξ_0	0.3528	0.4730	0.4574	0.4813
ξ_1	0.4920	0.6844	0.6236	0.5330
ξ_2	0.7175	0.7079	0.7198	0.7249

Table 4.2: Model parameters identified through minimization of errors in real and imaginary components of the total hand-arm system impedance (Δ_2).

Parameter	Hand actions			
	50 N Grip	15 N Grip 35 N Push	30 N Grip 45 N Push	50 N Grip 50 N Push
M_0 (kg)	5.8870	5.7743	6.1790	6.5868
M_1	1.2823	*1.0005*	1.0961	1.3382
M_2	0.0830	0.0780	0.0728	0.0811
M_3	0.0230	0.0274	0.0283	0.0268
M_4	0.0131	0.0110	0.0115	0.0132
k_0 (N/m)	13675.7	16552.9	17960.9	*20263.4*
k_1	2188.7	2311.7	1034.3	1841.8
k_2	*8283.7*	*2311.7*	*1034.3*	*1841.8*
k_3	25748.7	33460.2	46013.4	51029.2
k_4	*127410.8*	53852.6	68361.7	100422.0
c_0 (N ·s/m)	106.88	163.50	170.14	166.71
c_1	98.88	148.79	147.00	128.64
c_2	*31.70*	*44.69*	*36.45*	38.25
c_3	87.79	83.44	107.42	120.31
c_4	132.55	*88.16*	106.73	130.77
F_0 (Hz)	8.2	9.1	8.8	9.2
F_1	26.6	31.0	33.3	32.2
F_2	203.5	135.0	155.4	*178.7*
ξ_0	0.3549	0.4985	0.4721	*0.3980*
ξ_1	0.4959	0.6924	0.6286	0.5249
ξ_2	0.7748	*1.0054*	*1.0077*	*0.9283*

Table 4.3: Model parameters identified through minimization of errors in real component of the total hand-arm system impedance (Δ_3).

Parameter	Hand actions			
	50 N Grip	15 N Grip 35 N Push	30 N Grip 45 N Push	50 N Grip 50 N Push
M_0 (kg)	5.6852	5.8360	5.7176	6.2521
M_1	1.2848	0.8703	1.0386	1.3138
M_2	0.0841	*0.0684*	0.0749	0.0835
M_3	0.0263	0.0292	0.0305	0.0287
M_4	0.0131	0.0110	0.0115	0.0132
k_0 (N/m)	14342.4	16442.6	16929.0	17721.3
k_1	2457.8	1194.5	1000.0	1595.8
k_2	6940.8	1194.5	1000.0	*1595.8*
k_3	25942.0	37038.1	46974.6	50092.2
k_4	*130353.9*	51207.1	74315.6	*103300.2*
c_0 (N ·s/m)	*88.79*	157.01	160.70	*129.74*
c_1	100.22	159.72	154.34	128.10
c_2	34.85	*39.31*	*39.37*	*41.22*
c_3	86.18	89.73	105.05	118.98
c_4	135.47	83.63	108.94	132.88
F_0 (Hz)	8.6	8.7	8.9	8.8
F_1	26.3	33.9	34.6	32.0
F_2	203.4	139.3	159.6	*178.4*
ξ_0	0.3274	0.5085	0.5018	*0.3817*
ξ_1	0.5063	0.7706	0.6573	0.5393
ξ_2	0.7934	*1.0282*	*0.9881*	*0.9308*

Table 4.4: Model parameters identified through minimization of error in total hand-arm system impedance (Δ_4).

Parameter	Hand actions			
	50 N Grip	15 N Grip 35 N Push	30 N Grip 45 N Push	50 N Grip 50 N Push
M_0 (kg)	5.7037	5.7263	*5.3996*	5.6538
M_1	1.2859	0.8519	1.0089	1.2971
M_2	0.0790	0.0762	0.0721	0.0772
M_3	0.0273	0.0296	0.0297	0.0306
M_4	0.0129	0.0110	0.0115	0.0132
k_0 (N/m)	15116.3	16163.3	*15688.4*	17114.1
k_1	2232.9	*1691.8*	1045.6	1559.4
k_2	7104.9	*1691.8*	*1045.6*	*1559.4*
k_3	26037.9	37767.1	48844.3	51025.5
k_4	156861.9	*45798.6*	*80409.5*	131648.6
c_0 (N ·s/m)	105.54	*185.57*	*224.02*	*134.42*
c_1	102.82	165.49	168.11	130.85
c_2	39.19	*34.92*	*38.96*	*45.04*
c_3	82.38	88.92	104.97	115.00
c_4	123.61	76.14	105.08	123.28
F_0 (Hz)	8.7	8.9	8.9	9.1
F_1	26.3	35.0	35.8	32.5
F_2	229.3	125.6	169.1	209.0
ξ_0	0.3512	*0.5689*	*0.6633*	0.4195
ξ_1	0.5135	0.7607	0.6831	0.5435
ξ_2	0.7160	*0.9247*	*0.9401*	0.8301

4.4 Discussions

This study hypothesized that the proposed clamp-like five-DOF model of the hand-arm system can be used to predict the biodynamic responses distributed at the fingers and the palm of the hand, even though the model is derived on the basis of the total response of the hand-arm system. The results of this study generally support this hypothesis. The results suggest that measured distributed responses should be used, when available, to determine the model parameters. The use of total hand-arm system responses, which are invariably measured, can also yield model parameters that can effectively predict the distributed responses. This is clearly evident from the results shown in Figures 4.1 to 4.4, for the four hand forces considered. The results further suggest that either real or magnitude or real and imaginary components of the measured responses can equally yield a unique set of model parameters.

However, the quality of the prediction seems dependent on the relative values of the responses distributed at the fingers and the palm. As shown in Figures 4.1 to 4.4 and comparisons of the model parameters, all the approaches yield reasonably good predictions of responses distributed at the palm in term of both magnitude and phase. The predicted finger responses, however, generally show errors, particularly in phase. This is because the finger response is much lower than the palm response in the low and intermediate frequencies (<60 Hz) and the relative weighting of the finger response is not comparable with that of the palm response. The error minimization function with relatively larger weighting on errors in finger response thus yields better fitting of the fingers responses. A consideration of the total hand-arm system response, however, does not permit for such weighting.

Although, the minimization functions used in the study yield satisfactory model parameters and responses, the method involving error in real part of the total impedance would require additional information on the skin mass values (M_3 and M_4), which can not be determined directly. However, these two parameters affect only the imaginary part of the response, which may not be important, particularly when only the vibration power absorption is of concern.

4.5 Summary

It is shown that the hand-arm vibration model derived on the basis of total impedance can be effectively applied to determine the distributed biodynamic responses. The resulting model can also be used to predict the distributed vibration power and biodynamic forces. It is further shown that reasonably good model parameters, and distributed and total responses can be predicted using entire real component or magnitude or both real and imaginary components of the total hand-arm system responses.

CHAPTER 5

CONCLUSIONS AND RECOMMENDATIONS

5.1 General

Prolonged exposure to hand transmitted vibration is known to cause several disease among the operators of power tools, The occurrence of vibration white finger (VWF) disease and rate of degeneration can be attributed to several physical and biodynamic factors such as acceleration, frequency, direction of vibration, duration of exposure, pattern of exposure, hand forces and posture. Various epidemiological studies have reported high prevalence rates of VWF symptoms among operators of hand-held power tools. These high prevalence rates have prompted several clinical studies to establish the cause-effect relationships, and engineering studies to improve work place vibration environment. These studies have primarily focused on dynamic response characterization of the hand-arm and development of mathematical models. The characterization of the biodynamic responses of the human hand-arm system to HTV forms an essential basis to effectively evaluate vibration exposures, vibration response of the coupled hand-tool system and to investigate the potential injury mechanisms.

In view of the complex nature of the hand-arm system, the influence of numerous intrinsic and extrinsic parameters, on the hand-arm vibration response characteristics is not yet fully understood. The primary focus of the thesis research was formulated to study various aspects of hand-arm vibration, which included: (i) Develop a new model that mimics the basic structures of the hand-arm system based on the selected experimental data using a curving fitting method, and to evaluate its validity; (ii) Characterize biodynamic response through driving point mechanical impedance

measurement and analysis; (iii) Investigate the distributions of the biodynamic responses expressed in mechanical impedance, biodynamic force, vibration transmissibility, power absorption using the developed model; and (iv) explore the predictions of the distributed biodynamic responses based on the response of the entire hand-arm system.

5.2 Highlights of the Study

The major highlights and contributions of this dissertation research are summarized in the following subsections.

5.2.1 Distributed Biodynamic Responses of the Hand-arm Model

Biodynamic models of human hand-arm system have been proposed to characterize the vibration amplitude and power flow in the coupled hand, tool and work piece system. The applications of mechanical equivalent biodynamic models of the human hand-arm offer considerable potential to carry out assessments through both analytical and experimental analyses, where the involvement of human subjects could be considerably reduced. However, none of the existing models of the hand-arm system can be used to simulate the responses distributed at the fingers and the palm of the hand. The single-point hand-handle coupling relationship invariably assumed in these models is no longer valid for such a simulation. To achieve the goal, it is essential to develop a new model structure based on reliable experimental data. Although a recent study has experimentally investigated the distributed biodynamic responses, the responses have not been simulated and theoretically analyzed. It is unknown whether the model established based on the experimental data can be used to interpret the behaviors of the hand and arm structures, and whether the effects of the hand forces can be reflected in the changes of the model parameters. The proposed new model can be effectively used to conduct

theoretical investigations on the distributed vibration transmission, energy absorption, and vibration isolation concepts. The outputs from this model may also be used as inputs to a finite element biomechanical model for estimating the dynamic stresses and strains in the fingers and the palm-wrist-arm structures under hand-transmitted vibration and different types of hand-handle interactions. While the model revealed almost equally good predictions of the distributed and total responses, and it is judged to be relatively simpler for constructing a hand-arm simulator for studies on power tools vibration and vibration isolation devices.

5.2.2 Biodynamic Characterizations of the Hand-arm System

In the present study, the biodynamic response (BR) of human hand-arm system subjected to a random vibration distributed at the fingers and palm and arm was investigated. The related vibration power absorption (VPA) to each part of the hand-arm was also examined. The distributed BR and VPA can provide useful information for a more comprehensive understanding of the dynamic characteristics of the human hand-arm system and help study the mechanisms of vibration-induced injuries or disorders. They can also be applied to develop more effective prevention strategies and anti-vibration devices for finger protection.

5.2.3 Predictions of Distributed Biodynamic Responses

Many of the reported experimental data of the total biodynamic response of the entire hand-arm system can be used to estimate the distributed responses using the model, which can help understand the influencing factors. The modelling approach may also be used to evaluate the validity of the reported data, which is required for further development of ISO 10068 (1997). The proposed model correlated well with the

experimental data under different hand forces. It is shown that the model derived on the basis of total impedance can effectively predict the distributed responses.

5.3 Major Conclusions

From the results of the study, the following major conclusions are drawn:

- The model with some anatomical representation of the hand-arm system can provide vibration transmissibility of the fingers and the wrist, and distributed biodynamic forces, and power absorptions in the fingers, hand, palm, and arm. The results suggest that the distributed power absorptions may be used as alternative vibration measures for assessing various risks of the hand-transmitted vibration exposure. The vibration power in the low frequency range is mostly absorbed in the arm, shoulder, and upper body. However, high frequency features make the power absorption be concentrated in the hand or fingers.

- The hand-handle interaction is more appropriately represented by two driving-points formed by fingers-handle and palm-handle interfaces. A clamp-like model structure thus accurately describes the power grip condition.

- The biodynamic responses and the model parameters are strongly dependent upon the hand forces imparted on the handle, which suggests nonlinear biodynamic behavior of the hand-arm system.

- The model parameters and deflections of the model masses are reasonable for developing a hand-arm simulator for evaluating effectiveness of anti-vibration devices, such as anti-vibration gloves and anti-vibration handles, and for studies on coupled hand-tool system dynamics.

- From analyses of distributed vibration power, it is concluded that the vibration power at frequencies below 25 Hz is mainly absorbed in the upper arm, shoulder, and those beyond the shoulder. The uses of tools that generate such low frequency vibration are more likely to cause fatigue in the upper arm and shoulder structures.

- The major resonances of the hand-arm system are reflected in the vibration power absorption (VPA) distributed in the fingers. The finger VPA also suggests that exposure to vibration in the mid-frequency range (16 to 500 Hz) would potentially impose a greater risk of developing fingers disorders than that caused by exposure in the other frequency ranges.

- At frequencies higher than 250 Hz, the vibration power is mainly absorbed in the tissues close to the hand-tool contact area, particularly the fingers. The use of tools with high frequency vibration thus poses greater risk of VWF.

- The model parameters can be effectively derived using the total hand-arm system response, while the resulting model can be applied to predict the distributed responses.

5.4 Recommendations for Future Research Work

Characterization of human responses to vibration and understanding of the injury mechanisms would require extensive further efforts at the fundamentals levels. The future direction in this field may include some of the following tasks:

- The model should be further verified when further experimental data are available on the vibration transmitted to various substructures.
- Similar efforts are desirable to predict the biodynamic responses under different working postures that are known to influence the biodynamic responses significantly.
- Further studies are required to determine the effects of various influencing factors on the model parameters. These factors include a widen range of hand forces, arm and body postures, and subject anthropometry, and nature of vibration (sine, impact, and real tool spectrum).
- The proposed model configuration may also be applicable to develop models of the hand-arm system in the other two exposure directions. This may be another opportunity for further studies.

REFERENCE

Aatola, S. (1989). Transmission of vibration to the wrist and comparison of frequency response function estimators, Journal of Sound and Vibration 131(3): 497-507.

Abrams, C.F. and Suggs, C.W. (1969). Chain saw vibration, isolation and transmission through the human arm, Trans. Am. Soc. of Agric. Eng.: 423-425.

Abrams C.F. and Suggs, C.W. (1997). Development of a simulator for use in the measurement of chain saw vibration, App. Ergonomics.; 8:130-134.

Aldien Y., Marcotte P., Rakheja S., Boileau P.-E. (2005). Mechanical impedance and absorbed power of hand-arm under x_h-axis vibration and role of hand forces and posture. Industrial Health 43: 495-508.

ANSI S2.70 (2006). Guide for the measurement and evaluation of human exposure to vibration transmitted to the hand. American National Standard, Acoustical Society of America, Melville, New York, USA.

ANSI S3.40 (1989). Guide for the measurement and evaluation of gloves which are used to reduce exposure to vibration transmitted to the hand. American National Standards Institute (ANSI), New York.

Anttonen, H., Virokannas, H. (1992). Hand vibration among snowmobile drivers and prediction of VWF by vibration standard. In: Dupuis H, et al., (editors). Proceedings of the 6th international conference on hand-arm vibration: 875-883.

Boileau P.-E and Boutin J. (2001). Investigating the relationship in vibration transmissibility characteristics of resilient materials and gloves using standardized test methods. Proceeding of the 9th International Conference on Hand-Arm Vibration, Nancy, France: 397-405.

Bovenzi, M. (1998). Exposure-response relationship in the hand-arm vibration syndrome: an overview of current epidemiology research. Int Arch Occup Environ Health 71: 509-519.

Bovenzi, M., Fiorito, A., Volpe, C. (1987). Bone and joint disorders in the upper extremities of chipping and grinding operators. Int Arch Occup Environ Health 59(2):189-98.

Bovenzi, M., Franzinelli, A., Strambi, F. (1988). Prevalence of vibration-induced white finger and assessment of vibration exposure among travertine workers in Italy. Int Arch Occup Environ Health 61(1-2):25-34.

Bovenzi, M., Lindsell, C.J., Griffin, M.J. (2000). Acute vascular responses to the frequency of vibration transmitted to the hand. Occup Environ Med 57 (6): 422-430.

Bovenzi, M., Lindsell, C.J., Griffin, M.J. (2001). Response of finger circulation to energy equivalent combinations of magnitude and exposure duration. Occup Environ Med 58 (3): 185-193.

Bovenzi, M., Petronio, L. and DiMarino, F., (1980). Epidemiological survey of shipyard workers exposed to hand-arm vibration, Int. Arch. of Occ. & Environ. Health; 46: 251-66.

Brammer, A. (1984). Exposure of the Hand to Vibration in industry, National Research Council Canada, Publication No. NRCC 22845.

Brubaker, R., Mackenzie, C.J.G. and Hutton, S. (1986). Vibration-induced white finger among selected underground rock drillers in British Columbia, Scand. J. of Work, Environ. & Health: 296-300.

Burstrom L. (1990). Absorption of vibration energy in the human hand and arm. Doctorial thesis, Lulea University of Technology.

Burström L. (1997). The influence of biodynamic factors on the mechanical impedance of the hand and arm. Int Arch Occup Environ Health 69 (6): 437-446 Jun 1997

Burström L. and Lundström R. (1994). Absorption of vibration energy in the human hand and arm. Ergonomics 37:879-890.

Burström L., Sorenssön A. (1999). The influence of shock-type vibrations on the absorption of mechanical energy in the hand and arm. Int J Ind Ergonom 23 (5-6): 585-594 Mar 20

Burström, L., Bylund, S.H. (2000). Relationship between vibration dose and the absorption of mechanical power in the hand. Scand J Work Environ Health 26(1):32-36.

Bylund, S.H., Burström, L. (2003). Power absorption in women and men exposed to hand-arm vibration. Int Arch Occup Environ Health 76:313-317.

Byström, B-O., Nilsson, A. and Olsson, E. (1982). Development of artificial hands for use in chain saw vibration measurement, J of Sound & Vib; 82:11-117.

Cherian, T., Rakheja, S. and Bhat, R.B. (1996). An analytical investigation of an energy flow divider to attenuate hand-transmitted vibration, Int. J. of Ind. Ergo.17: 455-467.

Cundiff JS. (1976). Energy dissipation in human hand-arm exposed to random vibration. J Acous Soc Am 59: 212-214.

Cronjager L. and Hesse M. (1990). Hand-arm system's response to stochastic excitation. Proc. of the 5th International Conference on Hand-Arm Vibration, Kanazawa, Japan, 1990, 39-40.

Dandanell, R., Engstrom, K. (1986). Vibration from riveting tools in the frequency range 6 Hz-10 MHz and Raynaud's phenomenon. Scand J Work Environ Health 12:338-342.

Dandekar K., Raju BI., and Srinivasan MA. (2003). 3-D finite-element models of human and monkey fingertips to investigate the mechanics of tactile sense. J Biomech Eng 125(5): 682-91.

Dong RG, McDowell TW, Welcome DE, Smutz PW, Schopper AW. (2005a). The correlation between biodynamic characteristics of human hand-arm system and the isolation effectiveness of anti-vibration gloves. International Journal of Industrial Ergonomics 35: 205-216.

Dong RG, McDowell TW, Welcome DE, Wu JZ. (2004a). Biodynamic Response of Human Fingers in a Power Grip Subjected to a Random Vibration. Journal of Biomechanical Engineering (Transactions of the ASME), 126: 446-456.

Dong RG, Rakheja S, McDowell TW, Welcome DE, Wu JZ, Warren C, Barkley J, Washington B, Schopper AW. (2005b). A method for determining the transmissibility of antivibration gloves using biodynamic responses of hand-arm system. J. of Sound and Vibration, 282 (3-5): 1101-1118.

Dong RG, Rakheja S, Schopper AW, Han B, and Smutz WP. (2001). Hand-transmitted vibration and biodynamic response of the human hand-arm: a critical review. Critical Reviews™ in Biomedical Engineering 29(4): 391-441.

Dong RG, Rakheja S, Smutz WP, Schopper AW, and Wu JZ. (2002). Evaluating anti-vibration performance of a glove using total effective transmissibility. International Journal of Industrial Ergonomics 30: 33-48.

Dong RG, Schopper AW, McDowell TW, Welcome DE, Wu JZ, Smutz WP, Warren C, Rakheja S. (2004b). Vibration Energy Absorption (VEA) in Human Fingers-Hand-Arm System. Medical Engineering & Physics 26(7): 483-492.

Dong RG, TW McDowell, DE Welcome, WP Smutz, AW Schopper, C Warren, JZ Wu, S Rakheja. (2003). On-the-Hand Measurement Methods for Assessing Effectiveness of Anti-Vibration Gloves. International Journal of Industrial Ergonomics 32: 283-298.

Dong RG, Welcome DE, and Wu JZ. (2005c). Frequency weightings based on biodynamics of fingers-hand-arm system. Industrial Health 43: 485-494.

Dong RG, Welcome DE, and Wu JZ. (2005d). Estimation of the biodynamic force acting at the interface between hand and vibrating surface. Industrial Health 43: 516-526.

Dong RG, Welcome DE, McDowell TW, Wu JZ, Schopper AW. (in press. available on-line since September 4, 2005). Frequency weighting derived from power absorption of fingers-hand-arm system under z_h-axis. Journal of Biomechanics.

Dong RG, Welcome DE, McDowell TW. (2005e). Biodynamic Response at the Palm of the Human Hand Subjected to a Random Vibration. Industrial Health 43 (1): 241-255.

Dong RG, Welcome DE, Thomas W. McDowell, Wu JZ. (2006). Measurement of biodynamic response of human hand-arm system. J. of Sound and Vibration 294(4-5): 807-827.

Dong RG, Wu JZ, and Welcome DE. (2005f). Recent advances in biodynamics of hand-arm system. Industrial Health 43: 449-471.

Dong RG, Wu JZ, McDowell TW, Welcome DE, Schopper AW. (2005g). Distribution of mechanical impedance at the fingers and the palm of human hand. Journal of Biomechanics 38(5): 1165-1175.

Dong RG, Wu JZ, Welcome DE, McDowell TW. (2005h). Estimation of vibration power absorption density in human fingers. Journal of Biomechanical Engineering 127: 849-856.

Dong RG, Welcome DE, Wu JZ. (2005i). A novel method for quantifying finger vibration exposure. Proc. of the 13th Japan Group Meeting on Human Responses to Vibration, Osaka, Japan: 185-195.

Engström, K. and Dandanell, R. (1986). Exposure conditions and Raynaud's phenomenon among riveters in the aircraft industry, Scand. J. of Work, Environ. & Health,; 293-295.

European Parliament and the Council of the European Union Directive 2002/44/EC (EU Directive) on the minimum health and safety requirements regarding the exposure of workers to the risks arsing from physical agents (vibration). Official Journal of the European Communities, OJ L177, 6.7.2002.

Fritz M. (1991). An improved biomechanical model for simulating the strain of the hand-arm system under vibration stress. Journal of Biomechanics 24, 1165-1171.

Gemne, G. and Taylor W., Foreword. (1983). Hand-arm vibration and the central autonomic nervous system, J. of Low Freq. Noise and Vib.; Special Volume: 1-12.

Gemne, G., and Saraste, H. (1987). Bone and joint pathology in workers using hand-held vibration tools. Scand J Work Environ Health 13:290-300.

Griffin M, Bovenzi M, Nelson CM. (2003). Dose-response patterns for vibration-induced white finger. Occup Environ Med 60:16-26.

Griffin MJ. (1994). Foundations of hand-transmitted vibration standards, Nagoya J. of Med. Sci., Suppl. 57: 147-164.

Griffin MJ. (1998). Evaluating the effectiveness of gloves in reducing hazards hand-transmitted vibration. Occupational and Environment Medicine (55): 340-348.

Griffin, M.J. (1990). Handbook of human vibration. London: Academic Press.

Gurram R, Rakheja S, and Brammer AJ. (1995a). Driving-point mechanical impedance of the human hand-arm system: Synthesis and model development. Journal of Sound and Vibration 180: 437-458.

Gurram R, Rakheja S, Gouw GJ. (1994a). Biodynamic response of the human hand-arm system subject to sinusoidal and stochastic excitations. In Advances in Industrial Ergonomics and Safety VI. Taylor & Francis: London: 239-246.

Gurram R, Rakheja S, Gouw GJ. (1995b). Mechanical Impedance of the human hand-arm system subject to sinusoidal and stochastic excitations. Int J Ind Ergonom 16 (2): 135-145.

Gurram R., Rakheja S, Gouw GJ. (1994b). Vibration transmission characteristics of the huan hand-arm system and gloves. Int J Ind Ergonom 13 (3): 217-234.

Harada, N., Griffin, M.J. (1991). Factors influencing vibration sense thresholds used to assess occupational exposure to hand-transmitted vibration. British Journal of Industrial Medicine 48: 185-192.

Hempstock, T.I. and O'Connor, D.E. (1989). Measurement of impedance of hand arm system, Proc. Inst. of Acoustics 11(9): 483-490.

Hewitt S. (2002). Round robin testing of anti-vibration gloves towards a revision of ISO 10819:1996. Proceeding of the 37th UK Conference on Human Responses to Vibration, Dept. of Human Sciences, Loughborough University, UK: 118-129.

ISO 10068, (1998). Mechanical vibration and shock -- free, mechanical impedance of the human hand-arm system at the driving point. International Organization for Standardization, Geneva, Switzerland.

ISO 10819, (1996). Mechanical vibration and shock -- Hand-arm vibration -- Method for the measurement and evaluation of the vibration transmissibility of gloves at the palm of the hand. Geneva, Switzerland, International Organization for Standardization.

ISO 13753, (1999). Mechanical vibration and shock -- hand-arm vibration -- method for measuring the vibration transmissibility of resilient materials when loaded by the hand-arm system. International Organization for Standardization, Geneva, Switzerland.

ISO 5349, (1986). Mechanical vibration-Guidelines for the measurement and the assessment of human exposure to hand-transmitted vibration, International Standards Organization, Geneva, Switzerland.

ISO 5349-1, (2001). Mechanical vibration -- measurement and evaluation of human exposure to hand-transmitted vibration -- part 1: General requirements. Geneva, Switzerland: International Organization for Standardization.

ISO 5349-2, (2001). Mechanical vibration -- measurement and evaluation of human exposure to hand-transmitted vibration -- part 2: Practical guidance for measurement in the workplace. Geneva, Switzerland: International Organization for Standardization.

ISO 8727, (1997). Mechanical vibration and shock – Human exposure – Biodynamic coordinate systems, International Standard Organization, Geneva, Switzerland.

ISO 8662, (1-14) (1988-1999). Hand-held portable power tools – Measurement of vibration at the handle. Part 1 –Part 14. International Standard Organization, Geneva, Switzerland.

Jahn R., Hesse M. (1986). Applications of hand-arm models in the investigation of the interaction between man and machine. Scandinavian Journal of Work, Environment & Health 12, 343-346.

Jandak Z. (1989). Energy transfer to the hand-arm system at exposure to vibration. in Hand-arm vibration. Okada, A., Taylor, W., and Dupuis, H., (Eds.), Kanazawa, Japan: Kyoei Press Co.: 49-52.

Kattel, Bheem P. and Fernandez, Jeffery E. (1999). The effects of rivet gun on hand-arm vibration, Int. J. Ind. Ergo.; 23:595-608.

Kihlberg S. (1995). Biodynamic response of the hand-arm system to vibration from an impact hammer and a grinder. International Journal of Industrial Ergonomics 16: 1-8.

Ksiazek MA, Tarnowski J. (2002). Measurements and modeling of hand-handle system. Proceeding of the 37th UK Conference on Human Responses to Vibration, Dept. of Human Science, Loughborough University, UK: 370-381.

Lidström IM. (1973). Measurement of energy dissipation by the body when using a vibrating tool. Nordisk Hygenisk Tidskrift 2: 41-45.

Lidström IM. (1977). Vibration injury in rock drillers, chiselers, and grinders. Some views on the relationship between the quantity of energy absorbed and the risk of occurrence of vibration injury. Proceeding of the 2nd International Conference on Hand-Arm Vibration, Cincinnati, OH, USA: 77-83.

Louda, L., Hartlova, D., Muff, V., Smolikova, L., and Svoboda, L. (1994). Impulsive vibration and exposure limit. Nagoya J. Med. Sci. (57); 165-172.

Lundström R. (1984). Local vibration – Mechanical impedance of the human hand's glabrous skin, Journal of Biomechanics 17:137-144.

Malchaire J, Piette A, Cock N. (2001). Associations between hand-wrist musculoskeletal and sensorineural complaints and biomechanical and vibration work constraints. Ann Occ Hyg 45(6): 479-491.

Marcotte P, Aldien Y, Boileau PE, Rakheja S, Boutin J. (2005). Effect of handle size and hand-handle contact force on the biodynamic response of the hand-arm system under zh-axis vibration. Journal of Sound and Vibration 283(3-5): 1071-1091.

McConnell K.G. (1995). Vibration testing: Theory and practice. New York: John Wiley & Sons.

Mishoe J.W, and C. W. Suggs. (1977). Hand-arm vibration. Part 1: Analytical model of the vibration response characteristics of the hand. Journal of Sound and Vibration 51, 237-253.

Miwa, T. (1964). Studies on hand protectors for portable vibration tools. Industrial Health 2: 95-105.

Miwa, T. (1968). Evaluation methods for vibration effect: Part 6. Measurements of unpleasant and tolerance limit levels for sinusoidal vibrations, Ind. Health 6: 18-27.

Musson, Y., Burdorf, A. and van Drimmelen, D. (1989). Exposure to shock and vibration and symptoms in workers using impact power tools, Annals of Occup. Hygiene,; 33:85-96.

Nilsson, A. and Olsson, E., Test rig for vibration control on chain saws. (1978). Development and design of a test rig with two artificial hands, Technical report: 49T, University Lulea, 1978.

Nilsson T., Burström L., Hagberg M. (1989). Risk assessment of vibration exposure and white fingers among platers. Int Arch Occup Environ Health; 61:473-481.

NIOSH (1989). Criteria for a recommended standard: Occupational exposure to hand-arm vibration. Cincinnati, OH: U.S. Department of Health and Human Services, National Institute for Occupational Safety and Health; NIOSH Publication #89-106.

NIOSH (1997). Musculoskeletal disorders and workplace factors: a critical review of epidemiological evidence for work-related musculoskeletal disorders of the neck, upper extremity, and low back. U.S. Department of Health and Human Services. DHHS (NIOSH) Publication No. 97-141. Cincinnati, OH, USA.

Paddan GS, and Griffin MJ. (2001). Measurement of glove and hand dynamics using knuckle vibration. Proceedings of the 9th international conference on hand-arm vibration, Section 15(6). Nancy, France.

Pelmear PL, and Wasserman DE. (1998). Hand-Arm Vibration: A Comprehensive Guide for Occupational Health Professionals. OEM Press, Beverly Farms, MA, USA.

Pelmear, P.L., Leong, D., Taylor, W. (1989). Nagalingam M, Fung D. Measurement of vibration of hand-held tools: Weighted or unweighted? J Occup Med 31(11):902-8.

Pope, M., Magnusson, M. and Hansson, T. (1997). The upper extremity attenuates intermediate frequency vibrations, Journal of Biomechanics; 103-108.

Pradko F, Lee RA, Greene JD. (1965). Human vibration-response theory. Paper No. 65-WA/HUF-19. Am Soc Mech Eng.

Pyykkö I, Färkkilä M, Toivanen J, Korhonen O and Hyvärinen J. (1976). Transmission of vibration in the hand-arm system with special reference to changes in compression force and acceleration. Scand. J. of Work, Environ. & Health 2: 87-95.

Rakheja S, Dong R, Welcome D, and Schopper AW. (2002b). Estimation of tool-specific isolation performance of anti-vibration gloves. International Journal of Industrial Ergonomics 30: 71-87.

Rakheja S, Wu JZ, Dong RG, and Schopper AW. (2002a). A comparison of biodynamic models of the human hand-arm system for applications to the hand-held power tools. Journal of Sound and Vibration 249(1): 55-82.

Reynolds DD. (1977). Hand-arm vibration: A review of 3 years research. Proceeding of the 2nd International Conference on Hand-Arm Vibration, Cincinnati, OH, USA: 99-128.

Reynolds DD and Falkenberg RJ. (1984). A study of hand vibration on chipping and grinding operators, part II: Four-degree-of-freedom lumped parameter model of the vibration response of the human hand. Journal of Sound and Vibration 95(1984), 499-514.

Reynolds DD, Standlee KG, and Angevine EN. (1977). Hand-arm vibration. Part III: Subjective response characteristics of individuals to hand-induced vibration. Journal of Sound Vibration 51: 267-282.

Reynolds, D. and Angevine EN. (1977). Hand-arm vibration, part II: Vibration transmission characteristics of the hand and arm. Journal of Sound Vibration 51:255-265.

Sakakibara, H. (1998). Pathophysiology and pathogenesis of circulatory, neurological, and musculoskeletal disturbances in hand-arm vibration syndrome. In: Pelmear PL and Wasserman DE, editors, Hand-arm vibration: a comprehensive guide for occupational health professionals. Beverly Farms, Massachusetts: OEM Press.

Sakakibara, H., Kondo, T., Miyao, M., Yamada, S., Nakagawa, T., Kobayahsi, F. and Ono, Y. (1986). Transmission of hand-arm vibration to the head, Scand. J. of Work, Environ. & Health: 359-361.

Seppalainen, A.M., Starck, J. and Harkonen, H. (1986). High-frequency vibration and sensory nerves. Scandinavian J. of Work, Environment and Health (12); 420-422.

Sörensson A and Lundström R. (1992). Transmission of vibration to the hand. Journal of Low Frequency Noise and Vibration 11: 14-22.

Sörensson A and Burström L. (1996). Energy absorption of vibration in the hand for higher frequencies. Journal of Low Frequency Noise and Vibration 15 (2): 71-79.

Sörensson A and Burström L. (1997). Transmission of vibration energy to different parts of the human hand-arm system the hand, Int. Arch. Occup. Environ Health 70: 199-204.

Srinivasan M. (1989). Surface deflection of primate fingertip under line load. Journal of Biomechanics 22(4): 343-9.

Srinivasan M and Dandekar K. (1996). An investigation of the mechanics of tactile sense using two-dimensional models of the primate fingertip. J Biomech Eng 118(1): 48-55.

Starck, J. and Pyykko, I., (1986). Impulsiveness of vibration as an additional factor in the hazards associated with hand-arm vibration, Scand. J. of Work, Environ. & Health,; 323-326.

Starck, J., Pekkarinen, J., Pyykko, I. (1990). Physical characteristics of vibration in relation to vibration-induced white finger. Am. Ind. Hyg. Assoc. J. (51); 179-184.

Stoyneva Z, Lyapina M, Tzvetkov D, Vodenicharov E. (2003). Current pathophysiological views on vibration-induced Raynaud's phenomenon. Cardiovascular Research 57 (3): 615-624.

Tasker, E. G. (1986). Assessment of vibration levels associated with hand-held roadbreakers, Scand. J. of Work, Environ. & Health,; 407-412.

Thomas M and Beauchamp Y. (1998). Development of a new frequency weighting filter for the assessment of grinder exposure to wrist transmitted vibration. Computers & Industrial Engineering 35 (3-4): 651-654.

Tominaga Y. (1993). The relationship between vibration exposure and symptoms of vibration syndrome. Journal of Science of Labor: 1-14.

Tominaga, Y. (2005). New frequency weighting of hand-arm vibration. Industrial Health 43: 509-515.

Walker, D., Jones, B. and Ogston, S. (1986). Occurrence of white finger in the gas industry, Scand. J. of Work, Environ. & Health, 301-303.

Wasserman J, Logston D, and Wasserman D. (2005). The use of a resistive pressure sensor to assess glove effects on tool transmitted vibration. Proceeding of the 10th International Conference on Hand-Arm Vibration, Las Vegas, USA.

Wasserman, D.E. (1987). Human Aspects of Occupational Vibraiton, Elsevier Science Publishers.

Welcome D.E., Dong R.G. (June 2006). Instrumented handles for studying hand-transmitted vibration exposure. Proceedings of the 1st American Conference on Human Vibration, Morgantown, WV.

Wu JZ, Dong RG , Welcome DE. (2006a). Analysis of the Point Mechanical Impedance of Fingerpad in Vibration. Medical Engineering & Physics.

Wu JZ, Dong RG, Rakheja S, Schopper AW. (2002). Simulation of Mechanical Responses of Fingertip to Dynamic Loading. Medical Engineering Physics 24: 253-264.

Wu JZ, Dong RG, Schopper AW, Smutz WP. (2003a). Analysis of skin deformation profiles during sinusoidal vibration fingerpad. Annals of Biomedical Engineering 31(7):867-878.

Wu JZ, Dong RG, Smutz WP, Rakheja S. (2003b). Dynamic interaction between a fingerpad and a flat surface: experiments and analysis. Med. Eng. Phys. 25(5): 397-406.

Wu JZ, Dong RG, Smutz WP, Schopper AW. (2003c). Modeling of time-dependent force response of fingertip to dynamic loading. Journal of Biomechanics 36(3): 383-392.

Wu JZ, Dong RG, Welcome DE. (2006b). Three-dimensional finite element simulations of the mechanical response of the fingertip to static and dynamic compressions. Computer Methods in Biomechanics and Biomedical Engineering.